AD_____

Award Number: W81XWH-04-1-0208

TITLE: Novel Gbeta Mimic Kelch Proteins Gpb1 and Gpb2 Connect G-Protein Signaling to Ras via Yeast Neurofibromin Homologs Ira 1 and Ira 2: A Model for Human NF1

PRINCIPAL INVESTIGATOR: Joseph Heitman, M.D., Ph.D.

CONTRACTING ORGANIZATION: Duke University
Durham, NC 27710

REPORT DATE: March 2006

TYPE OF REPORT: Annual

PREPARED FOR: U.S. Army Medical Research and Materiel Command
Fort Detrick, Maryland 21702-5012

REPORT DOCUMENTATION PAGE

Form Approved
OMB No. 0704-0188

1. REPORT DATE *(DD-MM-YYYY)*	**2. REPORT TYPE**	**3. DATES COVERED** *(From - To)*
01-03-2006	Annual	1 Mar 2005 - 28 Feb 2006

4. TITLE AND SUBTITLE
Novel Gbeta Mimic Kelch Proteins Gpb1 and Gpb2 Connect G-Protein Signaling to Ras via Yeast Neurofibromin Homologs Ira 1 and Ira 2: A Model for Human NF1

5a. CONTRACT NUMBER

5b. GRANT NUMBER
W81XWH-04-1-0208

5c. PROGRAM ELEMENT NUMBER

6. AUTHOR(S)
Joseph Heitman, M.D., Ph.D.

E-Mail: rebecca.casey@duke.edu

5d. PROJECT NUMBER

5e. TASK NUMBER

5f. WORK UNIT NUMBER

7. PERFORMING ORGANIZATION NAME(S) AND ADDRESS(ES)

Duke University Medical Center
Durham, NC 27710

8. PERFORMING ORGANIZATION REPORT NUMBER

9. SPONSORING / MONITORING AGENCY NAME(S) AND ADDRESS(ES)
U.S. Army Medical Research and Materiel Command
Fort Detrick, Maryland 21702-5012

10. SPONSOR/MONITOR'S ACRONYM(S)

11. SPONSOR/MONITOR'S REPORT NUMBER(S)

12. DISTRIBUTION / AVAILABILITY STATEMENT
Approved for Public Release; Distribution Unlimited

13. SUPPLEMENTARY NOTES-Original contains colored plates: ALL DTIC reproductions will be in black and white.

14. ABSTRACT:

The Neurofibromatosis type 1 (NF1) gene encodes a large tumor suppressor protein, neurofibromin, which is a Ras GTPase-activating protein (RasGAP) activity. Although the NF1 gene was identified over a decade ago, the biological roles of neurofibromin in cellular processes remain unclear. Therefore it is crucial for therapy and developing new drugs for NF1 patients to elucidate how the RasGAP activity of neurofibromin is controlled. To achieve this goal, it is also important to identify regulatory elements for neurofibromin. We are investigating the molecular mechanisms by which the Ras GAP activity of the yeast neurofibromin homologs Ira1/2 is regulated as a model to understand human NF1. We have found that the kelch Gb subunit mimics Gpb1/2 interact with Ira1/2 and control the Ras GAP activity of Ira1/2. Here, we found that the Gpb1/2 proteins are localized to the cell membrane in a Gpa2 dependent manner and function at the cell membrane. Gpb1/2 bind to the C-terminus of Ira1/2 and stabilize the Ira1/2 proteins. Moreover we also identified a Gpb1/2 binding domain near the C-terminus of Ira1/2 (GBD) that is significantly conserved in neurofibromin homologs, including a human counterpart. Therefore, similar regulatory mechanisms might be conserved in evolution.

15. SUBJECT TERMS
GTPase Activating Protein (GAP); Ras: Yeast; Signal Transduction; Adenylyl Cyclase; Protein Kinase A

16. SECURITY CLASSIFICATION OF:			**17. LIMITATION OF ABSTRACT**	**18. NUMBER OF PAGES**	**19a. NAME OF RESPONSIBLE PERSON**
a. REPORT	**b. ABSTRACT**	**c. THIS PAGE**			USAMRMC
U	U	U	UU	115	**19b. TELEPHONE NUMBER** *(include area code)*

Table of Contents

Introduction

Neurofibromatosis type 1 (NF1) is one of the most common genetic disorders in humans and the Ras GTPase-activating protein (RasGAP) neurofibromin is intimately associated with NF1 (For reviews, see Dasgupta and Gutmann, 2003; Parada, 2000; Zhu and Parada, 2002). It is therefore critical to elucidate the molecular mechanisms by which the RasGAP activity of neurofibromin are regulated, as well as the biological roles of neurofibromin, which are as yet incompletely understood. We employ the budding yeast *Saccharomyces cerevisiae* as a model to understand how the GAP activity of the yeast neurofibromin homologs, Ira1 and Ira2, is governed. The biochemical and biological roles of these yeast homologs are well conserved in evolution (Ballester et al., 1990; Ballester et al., 1989; Buchberg et al., 1990; Martin et al., 1990; Tanaka et al., 1991; Tanaka et al., 1989; Tanaka et al., 1990a; Tanaka et al., 1990b; Xu et al., 1990a; Xu et al., 1990b).

Recently, we identified the kelch Gβ mimic proteins Gpb1 and Gpb2, which are structurally and functionally related to Gβ subunits yet share no primary sequence identity with known Gβ subunits (Harashima and Heitman, 2002). We discovered that Gpb1/2 bind to Ira1/2 in vivo and regulate cAMP signaling by inhibiting the Gα subunit Gpa2 and concomitantly activating the Ira1/2 RasGAPs. In the approved Statement Of Work (See appendices), we proposed to elucidate the roles of the Gβ mimic kelch proteins Gpb1/2 in regulating the yeast neurofibromin homologs Ira1/2 for the first years of this project. We have found that Gpb1/2 are localized to the cell membrane in a Gpa2-dependent manner (Harashima and Heitman, 2005) and function at the cell membrane where Gpb1/2 bind to the C-terminus of Ira1/2 and stabilize the Ira1/2 proteins.

We have expended the past six months finalizing in considerable detail our studies on the Gpb1/2 interactions and impact on Ira1/2 function in response to a favorable yet detailed review of our manuscript submitted to *Molecular Cell*. The manuscript was submitted originally to Molecular Cell on August 6, 2005 and reviewer comments were received on September 1, 2006. An extensively revised manuscript (see attached pdf) was resubmitted to *Molecular Cell* on March 20, 2006, and is currently under review. These findings set the stage for the progression of the studies then to examine NF1 and possible mammalian kelch protein homologs of Gpb1/2. We summarize here our findings, and focus on our progress and studies since our last updated report was submitted six months ago on September 13, 2005.

Body

A carboxy terminal domain of Ira1 spanning from amino acids 2715 to 2925 was identified as the Gpb1/2 binding domain (GBD). To understand how Gpb1/2 control Ira1/2 RasGAP activity, the Gpb1/2 binding domain on Ira1/2 was identified. In this study, the Ira1 protein was deleted for N-terminal and C-terminal regions and fused to the 3HA protein tag. Using these deletion constructs and FLAG-Gpb1/2 constructs, physical protein interactions were examined in vivo by FLAG tag based affinity purification methods, and a Gpb1/2 binding domain (GBD) was identified and mapped to a carboxy-terminal segment spanning amino acid residues 2715-2925 (Figures 2 and 5 in Supporting Data). The GBD in the Ira2 protein was also identified in the corresponding region of Ira2 (Supplemental Figure 1 in Supporting Data).

The GBD is significantly conserved in evolution. To examine whether the GBD is conserved in evolution, psi-BLAST searches in the NCBI database were performed using the amino acid sequence of the GBD derived from the yeast Ira1 neurofibromin homolog, revealing identity with neurofibromin homologs including one in Drosophila, mouse, and human. Therefore, the GBD that is the binding target of the Gpb1/2 kelch proteins is conserved in evolution. Importantly many mutations (including nonsense mutations, deletions, and mutations in splice sites) have been identified in the corresponding domain of human neurofibromin from NF1 patients (Ars et al., 2003; De Luca et al., 2003; Fahsold et al., 2000; Origone et al., 2002; Rasmussen and Friedman, 2000; Upadhyaya et al., 1997).

Binding of Gpb1/2 to the GBD stabilizes the Ira1/2 proteins. In parallel with the experiments described above, protein stability of the deletion derivatives was also assessed by western blot using anti-HA antibodies. Remarkably, the deletion of the C-terminus resulted in instability of Ira1/2 (Figure 5 in Supporting Data). Furthermore, the protein levels of Ira1/2 were dramatically reduced in *gpb1,2* double mutant cells compared to wild-type cells (Figure 2 in Supporting Data). RT-PCR analysis of *IRA1*/2 expression revealed comparable transcript levels between *gpb1,2* mutant and wild-type cells. Reintroduction of the *GPB1/2* genes into *gpb1,2* double mutant cells restored Ira1/2 protein levels to the wild-type level (Figure 2 in Supporting Data). Therefore, Gpb1/2 stabilize the Ira1/2 proteins by binding to the GBD.

New studies conducted to finalize publication for *Molecular Cell*. In response to the reviews of our submitted manuscript, we have conducted extensive new studies and have added substantial new information supporting the conclusion that Gpb1/2 bind to the conserved C-terminal domain of Ira1/2 and stabilize Ira1/2 to control their RasGAP activity. These studies shed light on how RasGAP activity of the mammalian counterpart neurofibromin is controlled, which largely remains unknown.

We summarize here the major points. **First**, we have conducted key biochemical experiments that reveal the involvement of Gpb1/2 in stabilizing Ira1/2. As shown in Figures 4C and D, the half-lives of Ira1 (panel C) and Ira2 (panel D) in *gpb1,2* double mutant cells are much shorter than in wild-type cells. In these key experiments, the half lives of the Ira1 and Ira2 proteins were measured by pulse-chase after cycloheximide

addition and IP-Western blot. In contrast to the control protein Fpr1, the half-lives for both Ira proteins were substantially reduced in the absence of Gpb1/2. These findings substantiate and extend the biochemical and genetic data shown in Figures 4A and B, 5, and 6. **Second**, we have constructed a 3HA tagged Gpb1/2 binding domain (GBD) of Ira1 that spans amino acids 2715-2925 and the corresponding Ira2 GBD to test for protein-protein interactions with Gpb1/2. **Third**, we show that the 3HA tagged GBDs from Ira1 and Ira2 indeed bind to Gpb1/2, as shown in Figure 5D and Supplemental Figure 1D. **Fourth**, we have substantially improved Figures 4A and B by repeating experiments and including new data. We have measured Ras2-GTP levels in *ira2* single and *ira1,2* double mutant cells expressing wild-type Ras2. We show in Figure 4A that the Ras2-GTP level in *ira2* mutant cells is almost equivalent to that in *ira1* single and *gpb1,2* double mutant cells that express the wild-type Ras2 protein, and the Ras2-GTP level in *ira1,2* mutant cells is largely equivalent to that in wild-type and *gpb1,2* single mutant cells expressing a dominant form of Ras2 ($Ras2^{G19V}$). We have measured Ras2-GTP levels in *ira2* single and *ira1,2* double mutant cells. *ira2* mutant cells expressing the wild-type Ras2 protein exhibited a 5-fold increase in Ras2-GTP, similar to *ira1* single mutant cells. On the other hand, an approximately 25-fold increase was observed in *ira1,2* mutant cells that express the wild-type Ras2 protein, which is comparable to wild-type cells expressing the dominant active $Ras2^{G19V}$ protein (Figure 4A). These results are consistent with previous findings by Tanaka *et al*. (Cell, 1990). Therefore, Ira1 and Ira2 are largely functionally redundant.

We addressed the issue as to why there is a difference between *gpb1,2* double mutant cells expressing the wild-type Ras2 protein (5-fold increase) and those expressing

the dominant active Ras2^{G19V} protein (25-fold increase) with respect to the Ras2-GTP level. Our biochemical data provide evidence that the Ira1/2 RasGAP proteins are both still present in *gpb1,2* mutant cells, although their levels are significantly decreased. Furthermore, Ira1 and Ira2 are functionally redundant. Therefore, the reduced but not abolished level of Ira1/2 contributes to the observed difference in Ras2-GTP.

We also measured the Ras2-GTP levels when Gpb1/2 were overexpressed in wild-type cells. Our data provide evidence that Gpb1/2 overexpression elicits little if any effect on Ras2-GTP level in wild-type cells (data not shown). This is consistent with the finding that Gpb1/2 overexpression is unable to inhibit pseudohyphal differentiation in wild-type cells.

We have conducted additional co-immunoprecipitation studies (see Figure 5 and Supplemental Figure 1) to further support the conclusion that the Gpb1/2 binding domain (GBD) is present in the conserved C-terminal region in Ira1/2. Furthermore, the GBD (2715~2925 aa) in Ira1 was deleted and tested for an impact on stability, and we found that this Ira1 deletion variant was destabilized (Figure 5). This observation supports the hypothesis that Gpb1/2 stabilize Ira1/2 by binding to the GBD. We also expressed the Ira1/2 isolated GBD to test for association with Gpb1/2. As shown in Figure 5D and Supplemental Figure 1D, the GBD from Ira1/2 binds to Gpb1/2, further assigning the GBD to the conserved C-terminal region.

We examined whether Gpb1/2 could affect a protein-protein interaction between Ira1 and adenylyl cyclase. Because a physical interaction between Ira1 and Cyr1 has not been demonstrated directly, we constructed a functionally FLAG tagged Cyr1 protein and tested for interaction with the 3HA tagged Ira1 in vivo. We were unable to detect

interaction between the FLAG tagged Cyr1 protein and the Ira1-3HA fusion protein under our standard conditions (data not shown). This result raises the possibility that Cyr1 is indirectly associated with Ira1. This is consistent with our hypothesis that Cyr1 regulatory elements including Gpr1, Gpa2, Gpb1/2, Ras, Cdc25, and Ira1/2 form a supramolecular complex and control Cyr1 activity in response to extracellular stimuli (Figure 7 and Discussion). Further studies will be required to understand in detail these aspects of the mechanisms by which cAMP is produced and signals.

We have tested whether Ras is required for the observed interaction of Gpb1/2 with Ira1/2 and whether Gpa2 might compete with Ira1/2 for binding to Gpb1/2. To answer these questions, Gpb2-Ira1 interactions were examined in the presence and absence of Ras2 or Gpa2. We found that Ras2 is dispensable for this interaction, and the data are presented in Figure 2D. We also found that loss of Gpa2 elicits little effect on Gpb2-Ira1 interaction, if any (data not shown). This finding indicates that there is no competition between Gpa2 and Ira1/2 for Gbp1/2 interaction.

Invasive growth, nitrogen starvation sensitivity, glycogen accumulation, and cAMP levels have been examined as independent corroboration of our findings and model (Figure 7) and are included as panels in Figures 2 and 6.

Key Research accomplishments for years one and two.

1. The kelch Gβ mimic Gpb1/2 proteins are recruited to the plasma membrane in a Gα Gpa2 dependent manner.
2. Gpb1/2 function at the cell membrane.
3. The yeast neurofibromin homologs Ira1 and Ira2 were identified as physical binding partners for the kelch proteins Gpb1/2.
4. Genetic and physical data support Ira1/2 as physiological targets of Gpb1/2.
5. The amino acids 2715-2925 in Ira1 and the corresponding region in Ira2 were identified as the GBD (Gpb1/2 binding domain) that is conserved in evolution.
6. Pulse-chase studies were conducted to establish unequivocally that Gpb1/2 bind to and stabilize the yeast neurofibromin homologs Ira1/2 via the GBD.

Reportable outcomes

1. A senior research associate in my laboratory who is working on this project was awarded the Young Investigator Award from the Children's Tumor Foundation (formerly the National Neurofibromatosis Foundation) in 2004.
2. Our study entitled: "Gα subunit Gpa2 recruits kelch repeat subunits that inhibit receptor-G protein coupling during cAMP induced dimorphic transitions in *Saccharomyces cerevisiae*" was published in *Molecular Biology of the Cell* in 2005 (See Appendices).
3. Our study entitled: "The kelch proteins Gpb1 and Gpb2 inhibit Ras activity via association with the *Saccharomyces cerevisiae* RasGAP neurofibromin homologs Ira1 and Ira2" has been extensively revised in response to reviewers' comments and was resubmitted to *Molecular Cell* on March 20, 2006.

Conclusions

In our studies, we have identified the Gpb1/2 binding domain (GBD) near the C-terminus of the neurofibromin homologs Ira1/2. Furthermore we found that Gpb1/2 stabilize Ira1/2 by binding to the GBD. This conclusion has now been documented by pulse-chase analysis, establishing this conclusion unequivocally occurs at the protein level. Therefore loss of Gpb1/2 results in a decrease in the RasGAP Ira1/2 proteins and consequently to an increase in the GTP bound form of Ras, which is the active form of Ras and ultimately associated with NF1. Importantly the GBD is significantly conserved in neurofibromin homologs, including the human counterpart, and mutations that lead to loss of the GBD have been identified from NF1 patients. Therefore the same regulatory mechanisms may be conserved in evolution, and this study could provide information as to how the RasGAP activity of neurofibromin is regulated and ultimately provide therapeutic clues for NF1 patients and possible avenues for novel drug development.

References

Ars, E., Kruyer, H., Morell, M., Pros, E., Serra, E., Ravella, A., Estivill, X., and Lázaro, C. (2003). Recurrent mutations in the *NF1* gene are common among neurofibromatosis type 1 patients. J Med Genet *40*, e82.

Ballester, R., Marchuk, D., Boguski, M., Saulino, A., Letcher, R., Wigler, M., and Collins, F. (1990). The *NF1* locus encodes a protein functionally related to mammalian GAP and yeast *IRA* proteins. Cell *63*, 851-859.

Ballester, R., Michaeli, T., Ferguson, K., Xu, H. P., McCormick, F., and Wigler, M. (1989). Genetic analysis of mammalian GAP expressed in yeast. Cell *59*, 681-686.

Buchberg, A. M., Cleveland, L. S., Jenkins, N. A., and Copeland, N. G. (1990). Sequence homology shared by neurofibromatosis type-1 gene and *IRA-1* and *IRA-2* negative regulators of the *RAS* cyclic AMP pathway. Nature *347*, 291-294.

Dasgupta, B., and Gutmann, D. H. (2003). Neurofibromatosis 1: closing the GAP between mice and men. Curr Opin Genet Dev *13*, 20-27.

De Luca, A., Buccino, A., Gianni, D., Mangino, M., Giustini, S., Richetta, A., Divona, L., Calvieri, S., Mingarelli, R., and Dallapiccola, B. (2003). NF1 gene analysis based on DHPLC. Hum Mutat *21*, 171-172.

Fahsold, R., Hoffmeyer, S., Mischung, C., Gille, C., Ehlers, C., Kücükceylan, N., Abdel-Nour, M., Gewies, A., Peters, H., Kaufmann, D., *et al.* (2000). Minor lesion mutational spectrum of the entire *NF1* gene does not explain its high mutability but points to a functional domain upstream of the GAP-related domain. Am J Hum Genet *66*, 790-818.

Harashima, T., and Heitman, J. (2002). The Gα protein Gpa2 controls yeast differentiation by interacting with kelch repeat proteins that mimic Gβ subunits. Mol Cell *10*, 163-173.

Harashima, T., and Heitman, J. (2005). Gα subunit Gpa2 recruits kelch repeat subunits that inhibit receptor-G protein coupling during cAMP induced dimorphic transitions in *Saccharomyces cerevisiae*. Mol Biol Cell *16*, 4557-4571.

Martin, G. A., Viskochil, D., Bollag, G., McCabe, P. C., Crosier, W. J., Haubruck, H., Conroy, L., Clark, R., O'Connell, P., Cawthon, R. M., and et al. (1990). The GAP-related domain of the neurofibromatosis type 1 gene product interacts with *ras* p21. Cell *63*, 843-849.

Origone, P., De Luca, A., Bellini, C., Buccino, A., Mingarelli, R., Costabel, S., La Rosa, C., Garrè, C., Coviello, D. A., Ajmar, F., *et al.* (2002). Ten novel mutations in the human neurofibromatosis type 1 (NF1) gene in Italian patients. Hum Mutat *20*, 74-75.

Parada, L. F. (2000). Neurofibromatosis type 1. Biochim Biophys Acta *1471*, M13-19.

Rasmussen, S. A., and Friedman, J. M. (2000). *NF1* gene and neurofibromatosis 1. Am J Epidemiol *151*, 33-40.

Tanaka, K., Lin, B. K., Wood, D. R., and Tamanoi, F. (1991). *IRA2*, an upstream negative regulator of RAS in yeast, is a RAS GTPase-activating protein. Proc Natl Acad Sci U S A *88*, 468-472.

Tanaka, K., Matsumoto, K., and Toh-e, A. (1989). *IRA1*, an inhibitory regulator of the *RAS*-cyclic AMP pathway in *Saccharomyces cerevisiae*. Mol Cell Biol *9*, 757-768.

Tanaka, K., Nakafuku, M., Satoh, T., Marshall, M. S., Gibbs, J. B., Matsumoto, K., Kaziro, Y., and Toh-e, A. (1990a). *S. cerevisiae* genes *IRA1* and *IRA2* encode proteins that may be functionally equivalent to mammalian *ras* GTPase activating protein. Cell *60*, 803-807.

Tanaka, K., Nakafuku, M., Tamanoi, F., Kaziro, Y., Matsumoto, K., and Toh-e, A. (1990b). *IRA2*, a second gene of *Saccharomyces cerevisiae* that encodes a protein with a domain homologous to mammalian *ras* GTPase-activating protein. Mol Cell Biol *10*, 4303-4313.

Upadhyaya, M., Osborn, M. J., Maynard, J., Kim, M. R., Tamanoi, F., and Cooper, D. N. (1997). Mutational and functional analysis of the neurofibromatosis type 1 (*NF1*) gene. Hum Genet *99*, 88-92.

Xu, G. F., Lin, B., Tanaka, K., Dunn, D., Wood, D., Gesteland, R., White, R., Weiss, R., and Tamanoi, F. (1990a). The catalytic domain of the neurofibromatosis type 1 gene product stimulates *ras* GTPase and complements *ira* mutants of *S. cerevisiae*. Cell *63*, 835-841.

Xu, G. F., O'Connell, P., Viskochil, D., Cawthon, R., Robertson, M., Culver, M., Dunn, D., Stevens, J., Gesteland, R., White, R., and et al. (1990b). The neurofibromatosis type 1 gene encodes a protein related to GAP. Cell *62*, 599-608.

Zhu, Y., and Parada, L. F. (2002). The molecular and genetic basis of neurological tumours. Nat Rev Cancer *2*, 616-626.

Appendices

Statement of Work

Task 1. To characterize the roles of the Gβ mimic kelch proteins Gpb1 and Gpb2 in regulating the yeast neurofibromin homologs Ira1 and Ira2 (Months 1-12):

a. Determine the role of Gpb1/2 on Ira1/2 (Months 1-4.5)
    I. Construct and develop materials required for GAP assay of Ira1/2 (Months 1-3).
    II. Perform GAP assay to examine the roles of Gpb1/2 on Ira1/2 RasGAP activity (Months 3-4.5).
b. Identify the Gpb1/2-binding domain on Ira1/2 (Months 1-6):
    I. Construct Ira1/2 derivatives carrying various deletions in the N-terminal, central, and C-terminal regions (Months 1-4.5).
    II. Test protein-protein interactions and identify the Gpb1/2-binding domain (Months 4.5-6).
c. Identify amino acid residues in Ira1/2 required for protein-protein interactions with Gpb1/2 (Months 6-12):
    I. Mutagenize the Gpb1/2-interacting domain in Ira1/2 and clone into the yeast two-hybrid vector (Months 6-7).
    II. Test protein-protein interactions and identify amino acids required for physical interactions with Gpb1/2 (Months 7-9).

III. Introduce mutations in the *IRA1/2* genes that abolish physical interactions with Gpb1/2 in vivo (Months 9-11).

IV. Test for pseudohyphal differentiation to characterize the role of the mutated amino acids in vivo (Months 11-12).

Task 2. To identify amino acid residues important for function of neurofibromin and Ira1/2 (Months 12-24):

a. Construct and express the *NF1* gene in yeast *ira1,2* mutants to examine whether the full length neurofibromin is functional when heterologously expressed in yeast cells (Months 12-13).

b. To identify putative Gpb1/2 binding sites in neurofibromin (Months 13-24):

   I. Introduce mutations in those ones of neurofibromin and clone these novel *NF1* alleles into yeast and mammalian expression vectors (Months 13-17).

   II. Express these *NF1* alleles in the yeast *ira1,2* mutant and mouse $NF1^{-/-}$ cells and characterize the roles of the mutated amino acids in vivo (Months 17-24).

c. To characterize the roles of the consensus PKA phosphorylation sites in neurofibromin and Ira1/2 (Months 13-24):

   I. Introduce mutations in candidate PKA phosphorylation sites in neurofibromin and Ira1/2 (Months 13-17).

II. Express these *NF1* mutant alleles in the yeast *ira1,2* mutant and mouse *NF1*$^{-/-}$ cells and the *IRA1/2* mutant alleles in the *ira1,2* mutant cells and test for phenotypes to examine the roles of those putative PKA phosphorylation sites (Months 17-24).

Task 3. To identify a human Gpb1/2 counterpart (Months 24-36):

a. To examine whether yeast Gpb1/2 interact with neurofibromin (Months 24-27):
    I. Construct FLAG-Gpb1/2 to be expressed and transfected into murine cells (Months 24-25).
    II. Examine protein-protein interactions by FLAG tag based immunopurification methods and western blots using anti-neurofibromin and anti-FLAG antibodies (Months 25-27).
b. To isolate a human Gpb1/2 counterpart (Months 27-36):
    I. Perform psi-BLAST searches against human sequence databases (Month 27).
    II. Make constructs for analysis in the yeast two-hybrid system and test protein-protein interactions between neurofibromin and putative Gpb1/2 counterparts (Months 27-31).

III. Also generate yeast two-hybrid constructs of the candidate Gpb1/2 binding domain in neurofibromin and screen human two-hybrid libraries to identify putative Gpb1/2 counterparts (Months 31-36).

Supporting Data

Figure legends

Figure 1. Genetic interactions between *gpb1,2* and *ras2* mutations. (A) *gpb1,2* mutations are unable to suppress the synthetic growth defect of *gpa2 ras2* mutant cells. Diploid *gpa2::G418/gpa2::hph ras2::nat/RAS2* (left, THY388a/α) and *gpb1,2::loxP/gpb1,2::loxP gpa2::loxP-G418/GPA2 ras2::nat/ras2::nat* (right, see "Materials and Discussion") cells were sporulated and dissected. Progeny genotypes were determined based on segregation of the dominant drug resistant markers (*G418*, *hph*, and *nat*). (B-F) *ras2* mutations alleviate increased PKA phenotypes associated with *gpb1,2* mutations, including enhanced pseudohyphal growth (B), hyperinvasive growth (C), increased *FLO11* expression (D), sensitivity to nitrogen starvation (E), and reduced glycogen accumulation (F). Diploid strains, MLY61a/α (WT), THY170a/α (*gpa2*), XPY5a/α (*tpk2*), MLY187a/α (*ras2*), THY212a/α (*gpb1,2*), THY242a/α (*gpb1,2 gpa2*), THY245a/α (*gpb1,2 tpk2*), and THY247a/α (*gpb1,2 ras2*) were employed to assay pseudohyphal growth, and isogenic haploid strains, MLY40α (WT), THY170α, XPY5α, MLY187α, THY212α, THY242α, THY245α, and THY247α to study invasive growth, *FLO11* expression, sensitivity to nitrogen starvation, and glycogen accumulation. (G) Glucose-induced cAMP production in WT (MLY40α), *ras2* (MLY187α), *gpb1,2* (THY212α), and *gpb1,2 ras2* (THY247α) mutant cells. Glucose was added to glucose starved cells, and at the indicated time points, cells were collected and cAMP levels were determined. The values shown are the mean of two independent experiments.

Figure 2. Kelch Gβ mimic subunits interact with RasGAP Ira1/2. (A and B) Ira1 (A) and Ira2 (B) physically bind to Gpb1/2 in vivo. The N-terminally FLAG-tagged Gpb1 (pTH111) and Gpb2 (pTH88) proteins were expressed in yeast cells that also express C-terminally 3HA tagged Ira1 (THY355a, panel A) or Ira2 (THY356a, panel B). (C) Gpb2 requires both the unique N-terminal and the C-terminal kelch domains to interact with Ira1. The N-terminally FLAG tagged Gpb2 N-terminal region (FLAG-Gpb2N, pTH190), C-terminal kelch domains (FLAG-Gpb2C, pTH188), or full length Gpb2 (FLAG-Gpb2, pTH88) were co-expressed with the Ira1-3HA protein in vivo (THY381a). Positions of molecular marker (128, 85, 41.7, and 32.1 k) are indicated to the right of the panel. (D) Ras2 is dispensable for the Gpb2-Ira1 interaction. Protein-protein interactions between Gpb2 and Ira1 were examined in the presence (THY355a) and absence (THY479α) of Ras2 using cells that express the FLAG tagged Gpb2 (pTH88). Crude cell extracts were prepared from exponentially growing cells and subjected to immunoprecipitations using anti-FLAG affinity gel. To verify expression levels of the 3HA tagged Ira1/2 proteins and because of low expression levels of Ira1/2, the Ira1/2-3HA proteins were immunoprecipitated using anti-HA agarose beads, eluted, and then analyzed by western analysis and indicated as "Input". Cells expressing both Ira1-3HA and Trp1-FLAG fusion proteins (THY450a) served as the control. Fpr1 was used as the loading control.

Figure 3. Genetic interactions between *gpb1,2* and *ira1,2* mutations. (A) Wild-type (MLY61a/α), *gpb1,2* (THY212a/α), *ira1,2* (THY345a/α), *ira1* (THY337a/α), *ira2* (THY336a/α), and *gpb1,2 ira1,2* (THY346a/α) mutant strains were assayed

for pseudohyphal growth. (B) The dominant active *GPA2*^{Q300L} (pTH48) and *RAS2*^{G19V} (pMW2) alleles were introduced into wild-type (MLY61a/α) and *gpb1,2* mutant cells (THY212a/α) and tested for effects on filamentous growth. (C) The *IRA2* gene (pKF56) suppressed the increased filamentous phenotype of *gpb1,2* mutant cells (THY212a/α). pTH27 (*GPB2*) and an empty vector pTH19 were introduced into wild-type (MLY61a/α) or *gpb1,2* mutant cells (THY212a/α) as controls. Cells were grown on SLAD agar medium at 30ºC for 5 days and photographed in panels A, B, and C. Haploid cells indicated were tested for invasive growth (D), nitrogen starvation sensitivity (E), glycogen accumulation (F), and glucose-induced cAMP production (G). (D) Cells were grown on YPD at 30ºC for 5 days and photographed after weak (W), mild (M) or strong (S) washing. (E) Cells were grown on YPD at 30ºC for 2 days, replica-plated onto nitrogen replete (+NH_4) and no nitrogen (-NH_4) media. After 6 (left panel) or 10 (right panel) days at 30 ºC, cells were replica-plated onto YPD again and incubated under the same conditions. (F) Glycogen levels of cells grown on YPD at 30ºC for 2 days were determined using iodine vapor. (G) cAMP levels were determined in response to glucose readdition as described in the legend of Figure 1.

Figure 4. Kelch subunits Gpb1/2 stabilize the RasGAP proteins Ira1/2. (A) The relative increase in Ras2-GTP was examined in isogenic wild-type (MLY41a) and *ras2* (MLY187α), *ira1* (THY337a), *ira2* (THY336a), *ira1,2* (THY345a), and *gpb1,2* (THY212a) mutant cells, expressing the wild-type (pMW1) or dominant active (G19V, pMW2) *RAS2* gene. Representative data are shown in the upper panel.

Note that purified Ras2-GTP from *ira1,2* double mutant cells expressing the wild-type Ras2 protein and wild-type and *gpb1,2* mutant cells that express the dominant active Ras2 ($Ras2^{G19V}$) protein was 5-fold diluted prior to western analysis, as the levels of Ras2-GTP in these cells were higher than those in the other cells. This permitted accurate measurement of the levels of Ras2-GTP by densitometry. After detection of levels of the GTP bound Ras2 and total cellular Ras protein ("Input") by western blot, signals were densitometrically quantified. Levels of Ras2-GTP were normalized to "Input" Ras2 levels and shown as a relative level to Ras2-GTP in wild-type cells in the lower panel. The values shown in the lower panel are the means of two or three independent experiments with the standard error of the mean. (B) The *GPB1* (pTH26) and *GPB2* (pTH114) genes were introduced into wild-type strains THY427a (*IRA1-3HA*) and THY428a *(IRA2-3HA*) and *gpb1,2* double mutant strains THY425a (*gpb1,2 IRA1-3HA*) and THY426a (*gpb1,2 IRA2-3HA*) to examine protein stability of Ira1/2 and the interactions between Ras2 and Ira1/2. The Ira1/2-Ras2 protein complex was co-immunoprecipitated using anti-HA conjugated agarose gels and eluted by the addition of HA peptide (shown as "Co-IP (HA)" in upper panel). A yeast strain THY475 (Trp1-3HA) carrying the empty vector pTH19 was employed as a control. Fpr1 served as a loading control. "NT" indicates the non-tagged, wild-type Ira1 or Ira2 protein. Based on densitometric analysis the steady state protein levels of Ira1 and Ira2 were reduced in *gpb1,2* double mutant cells by at least 2- to 10-fold compared to wild-type cells. Cells expressing a 3HA tagged Trp1 fusion protein served as a control. Note that the Ira1/2 proteins were undetectable in western blot using crude extracts because of low expression levels. (C and D) Gpb1/2 stabilize Ira1/2. Protein stability of Ira1 (C) and Ira2

(D) was investigated by cycloheximide-chase assay in the presence and absence of Gpb1/2. Cycloheximide (CHX) was added to exponentially growing cells at a final concentration of 50 μg/ml. At the indicated time points after CHX addition, cells expressing the 3HA tagged Ira1 protein (THY425 and THY427, panel C) or the 3HA tagged Ira2 protein (THY426 and THY428, panel D) were collected, washed, and cell extracts were prepared. The 3HA tagged Ira1/2 proteins were analyzed as above. After western blot (upper panel), signals were densitometorically quantified, and % protein abundance of Ira1 and Fpr1 at "Time 0" is shown in the lower panel.

Figure 5. Kelch Gpb1/2 subunits bind to the C-terminus of Ira1. The FLAG-Gpb1 (pTH111) and FLAG-Gpb2 (pTH88) fusion proteins were expressed in yeast cells that also express the 3HA tagged wild type Ira1 or Ira1 deletion variants, and protein complexes were immunoprecipitated. (A) Schematic of Ira1 deletion proteins created and summary of results obtained from assays of protein abundance (western blots) and Gpb1/2 binding (immunoprecipitation) as below. Positions of deletions created in Ira1 are shown and numbered. A conserved region between Ira1/2 and the human neurofibromin protein is shaded in grey. The RasGAP related domain (GRD) and the Gpb1/2 binding domain (GBD) are shown as a hatched and dark grey rectangle, respectively. (B) Protein interactions were investigated using crude cell extracts from cells expressing the 3HA tagged full length Ira1 (1~3092, THY355a) or Ira1 deletion variants (1~2925 (THY424a), 1~2714 (THY402a), 1~2432 (THY401a), and 1~1257 (THY404a)). Positions of full length wild-type Ira1 (1~3092 aa) and deletion variants (1~2925 and 1~1257 aa) are indicated to the left of the panel. Positions at which

molecular weight markers (250, 210, and 148 k) migrated are indicated to the right of the panels. The deletion of 167 amino acids from the Ira1 C-terminus leads to reduced protein levels of Ira1 from 3- to 7 fold in comparison of the full length Ira1 protein level and the further deletion (378 amino acids) results in undetectable levels ("Input" panel). Note that some smaller Ira1-3HA species were also detected via the C-terminal HA tag, indicating that these are proteolysis products lacking N-terminal regions. This further supports the assignment of the GBD to the C-terminal region of Ira1. (C) N-terminal deletion Ira1 variants (2433~3092 aa (THY438a) and 2715~3092 aa (THY440a)) were tested for interaction with Gpb1/2. Positions of the N-terminal deletion Ira1 variants (2432~3092 and 2715~3092 aa) are indicated to the left of the panel. (D) A putative GBD of Ira1 spanning amino acids 2715~2925 (THY468a) was examined for Gpb1/2 interactions. Note that a deletion Ira1 variant that lacks this domain (Ira1 Δ2715~2925 aa variant in panel A) was undetectable because of protein instability, consistent with the role of Gpb1/2 in Ira1 protein stability. Crude extracts were prepared from cells grown to mid-log phase in synthetic dropout medium. Protein complexes were immunoprecipitated using anti-FLAG affinity gel. Because the levels of the full length Ira1 and these Ira1 N- and C-terminal deletion variant proteins in crude extracts were too low to detect by western blot, the full length and deletion Ira1 proteins were immunoprecipitated using anti-HA agarose beads, eluted, subject to western analysis, and examined for protein stability and indicated as "Input" in panels B, C, and D. Yeast strains (THY450a, THY464a, and THY467a) that carry the empty vector pTH19 were used as a control. Fpr1 in crude cell extracts served as loading controls and were also shown as "Input".

Figure 6. The C-terminus of Ira1/2 is necessary for function. (A) Isogenic homozygous diploid cells were tested for filamentous growth: WT (MLY61a/α), *gpb1,2* (THY212a/α), *ira1* (THY337a/α), *IRA1-3HA* (1~3092 aa, THY355a/α), *IRA1-3HA* (1~2925 aa, THY424a/α), *IRA1-3HA* (1~2714 aa, THY402a/α), *IRA1-3HA* (ΔGBD (Δ2715~2925 aa), THY471a/α). Cells were grown at 30°C for 5 days on SLAD medium and photographed. Invasive growth (B), nitrogen starvation sensitivity (C), and glycogen accumulation (D) were examined using isogenic haploid cells. (B) Cells were grown on YPD 30°C for 5 days and washed off under a current of water. (C) After 7 days on nitrogen replete or depleted medium, cells were replica-plated onto YPD. (D) Glycogen accumulation was assessed using iodine vapor. Details were as described in the figure legend to Figure 1.

Figure 7. A dual role of the kelch proteins Gpb1/2 as molecular brakes on cAMP signaling. (A) A schematic of the yeast neurofibromin homolog Ira1 and human neurofibromin proteins. A conserved region including the GRD and the GBD is shown in grey. GRD; hatched rectangle, GBD; bold rectangle. (B) A model for how the kelch Gβ mimic proteins Gpb1/2 control cAMP signaling. See details in the text.

Supplemental Figure 1. The GBD in Ira2 maps to the equivalent C-terminal region of Ira1. (A) The protein structure of the Ira1/2 proteins is depicted schematically. Positions of deletions created in Ira1/2 are shown and numbered. The Gpb1/2 biding domain (GBD) on Ira2 was also determined by assessing

protein interactions between Gpb1/2 and C-terminal (1~2922 aa (THY 456a) and 1~2702 aa (THY 457a), panel B) and N-terminal (2703~3079 aa (THY 466a), panel C) Ira2 deletion variants and an Ira2 C-terminal domain (2703~2922 aa (THY473), panel B). The migration positions of full length wild-type Ira2 (3079 aa) and Ira2 deletion variants (1~2922 aa) are indicated to the left of the panel. Positions at which molecular weight markers (250, 210, and 148 k) migrated are also indicated to the right of the panels in B. Yeast strains (THY451a, THY466a,and THY474a) carrying the empty plasmid pTH19 were employed as a control. Details are essentially as described in the legend to Figure 5, unless otherwise specifically noted.

Figure 1. Harashima et al.

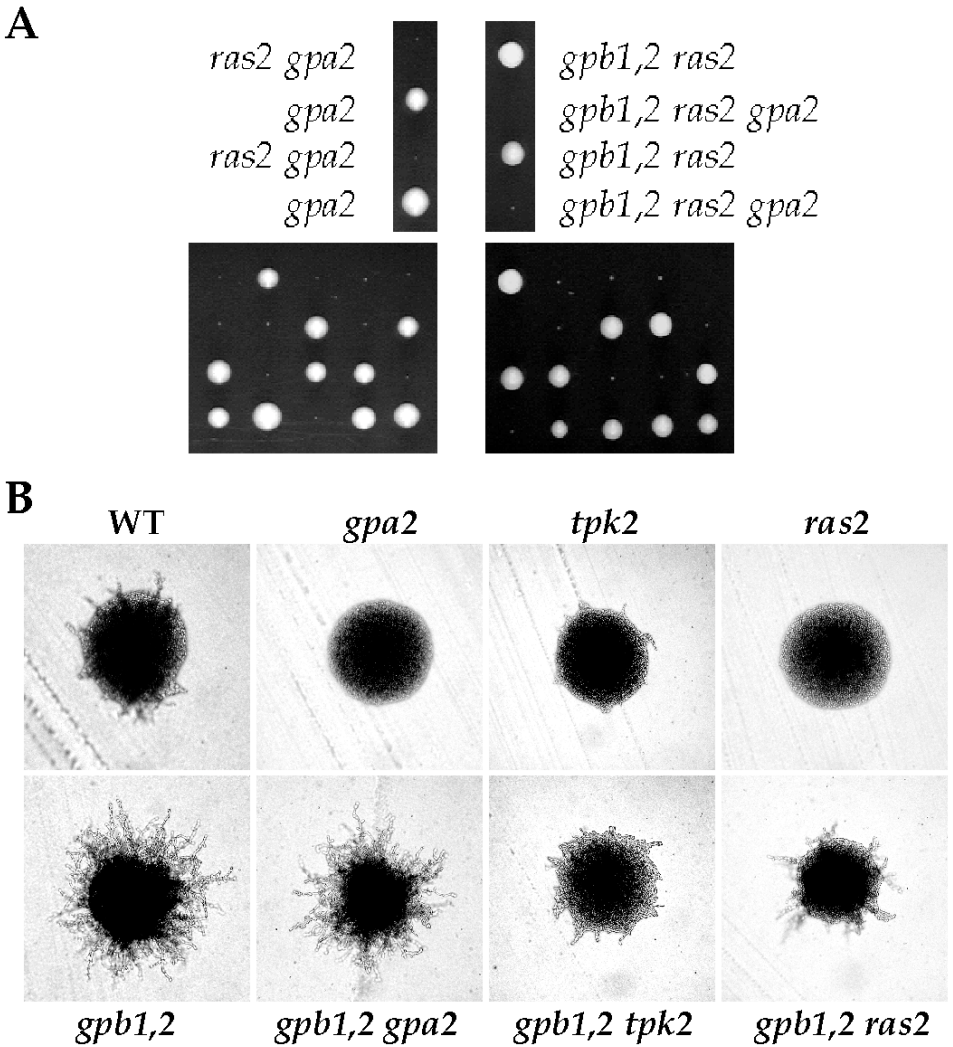

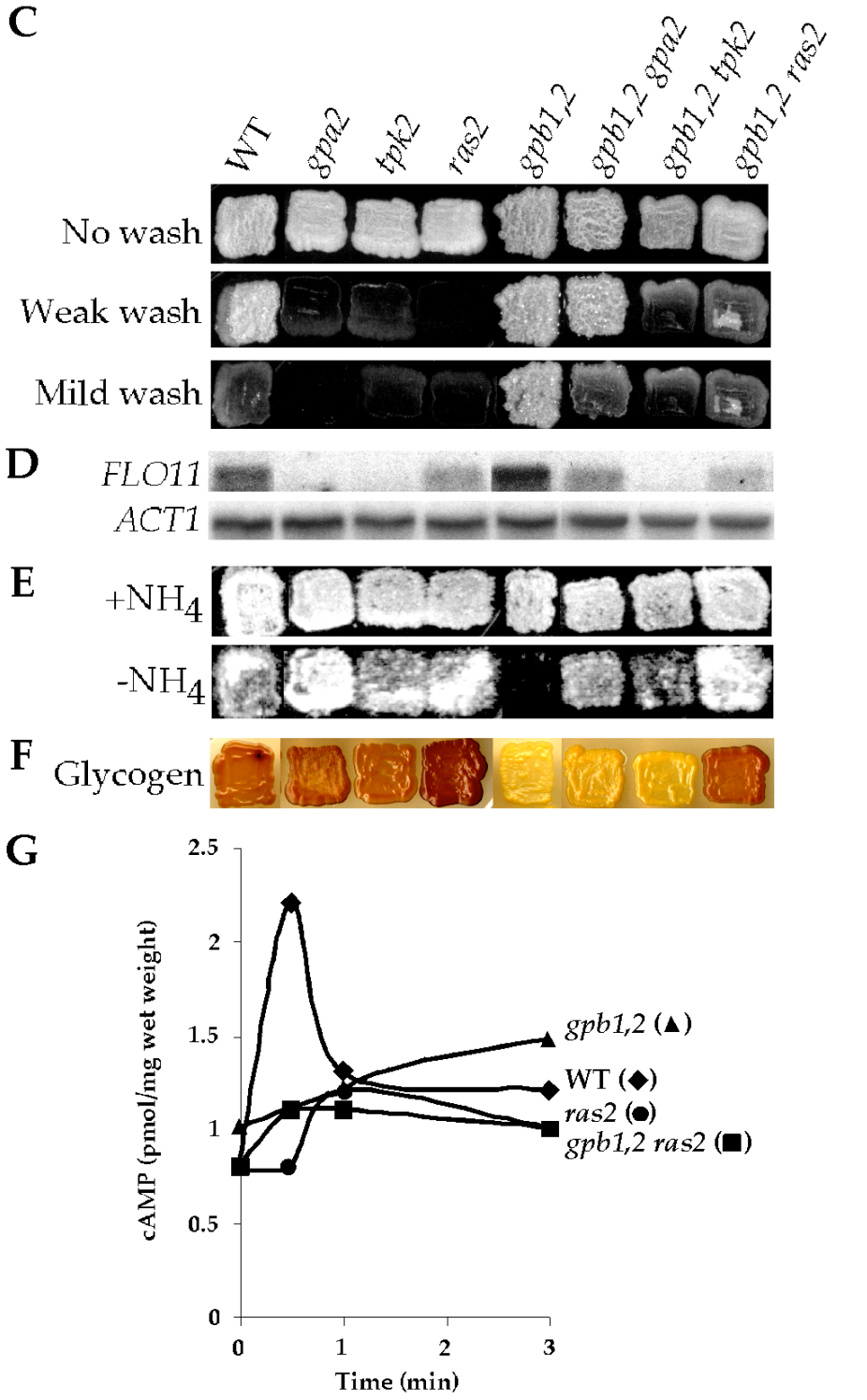

Figure 2. Harashima et al.

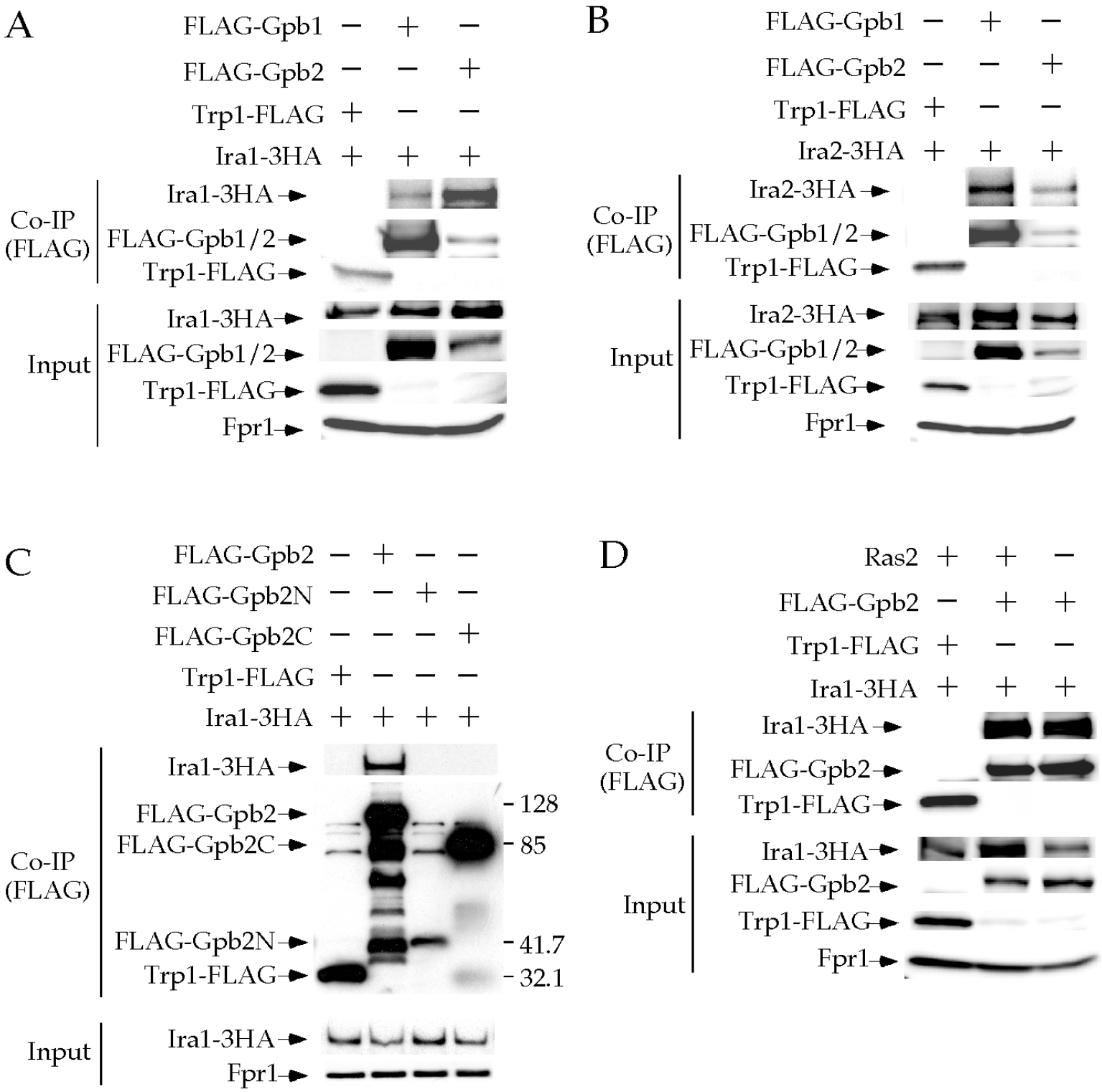

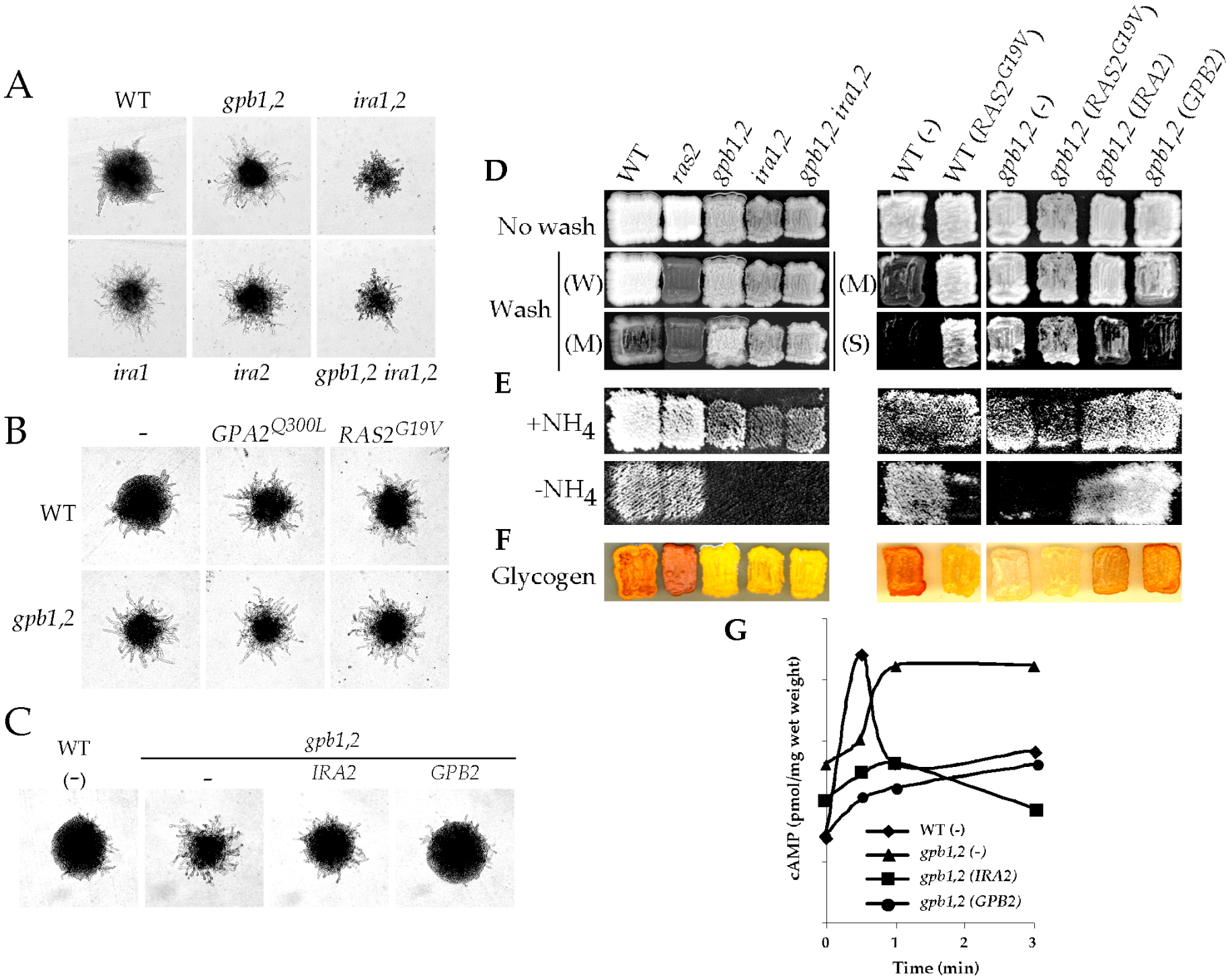
A
WT
gpb1,2
ira1,2
ira1
ira2
gpb1,2 ira1,2
B
-
GPA2Q300L
RAS2G19V
WT
gpb1,2
C
WT
(-)
gpb1,2
-
IRA2
GPB2
D
WT
ras2
gpb1,2
ira1,2
gpb1,2 ira1,2
WT (-)
WT (RAS2G19V)
gpb1,2 (-)
gpb1,2 (RAS2G19V)
gpb1,2 (IRA2)
gpb1,2 (GPB2)
No wash
Wash
(W)
(M)
(M)
(S)
E
+NH4
-NH4
F
Glycogen
G
cAMP (pmol/mg wet weight)
WT (-)
gpb1,2 (-)
gpb1,2 (IRA2)
gpb1,2 (GPB2)
0
1
2
3
Time (min)

Figure 4. Harashima et al.

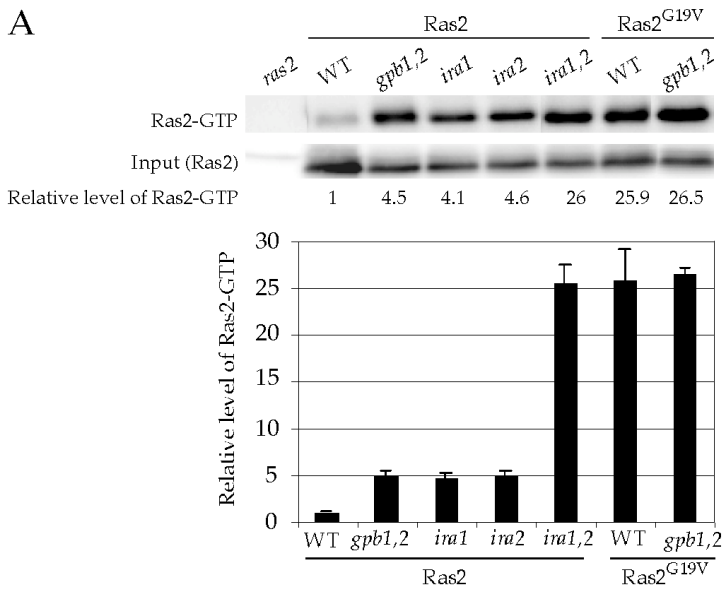

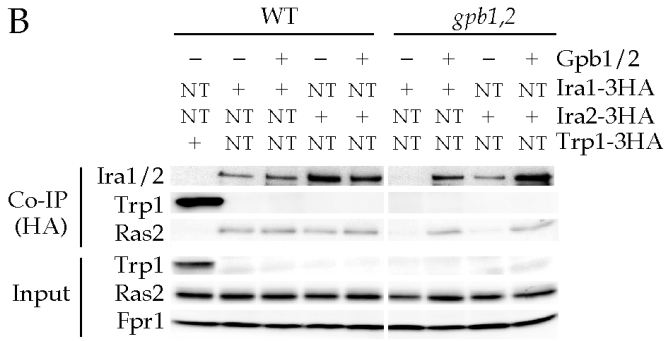

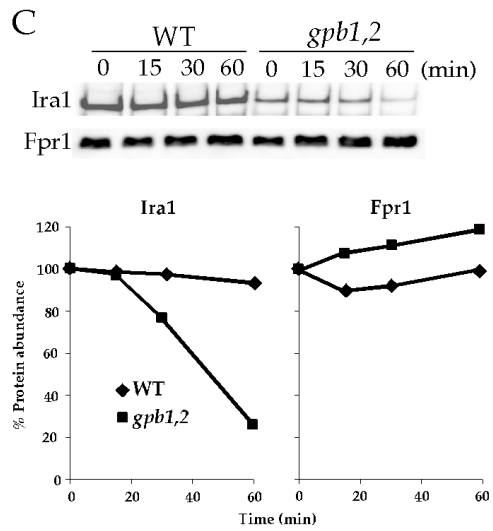

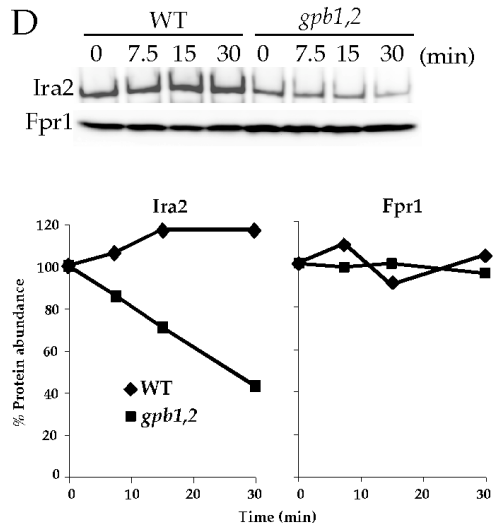

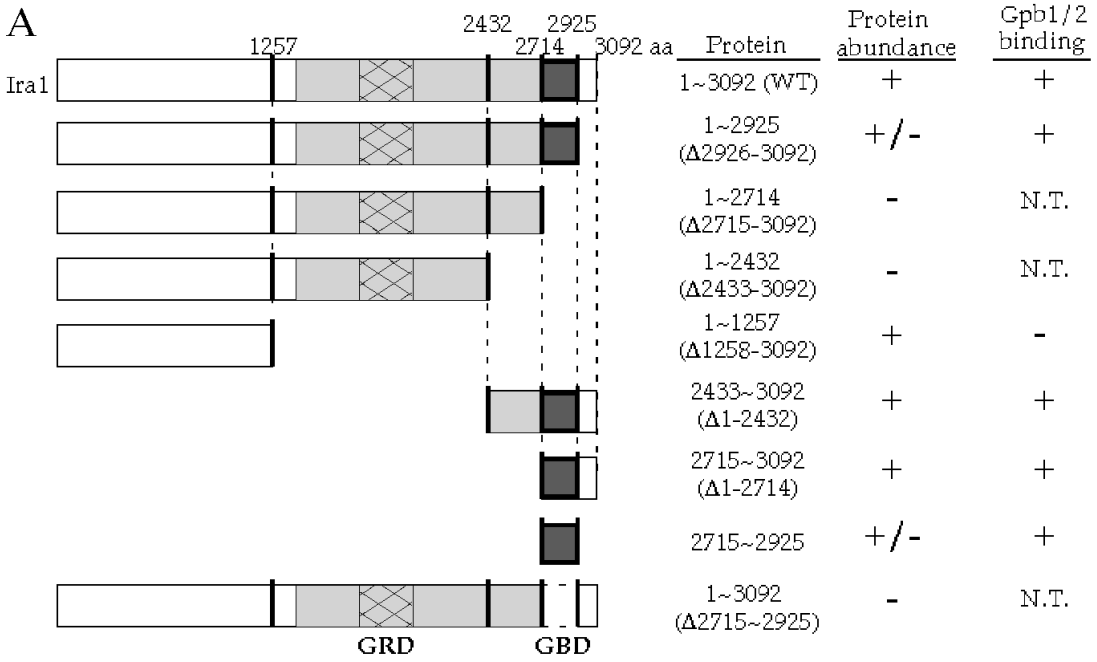
A
1257
2432
2714
2925
3092 aa
Ira1
GRD
GBD
Protein
Protein abundance
Gpb1/2 binding
1~3092 (WT) + +
1~2925 (Δ2926-3092) +/- +
1~2714 (Δ2715-3092) - N.T.
1~2432 (Δ2433-3092) - N.T.
1~1257 (Δ1258-3092) + -
2433~3092 (Δ1-2432) + +
2715~3092 (Δ1-2714) + +
2715~2925 +/- +
1~3092 (Δ2715~2925) - N.T.

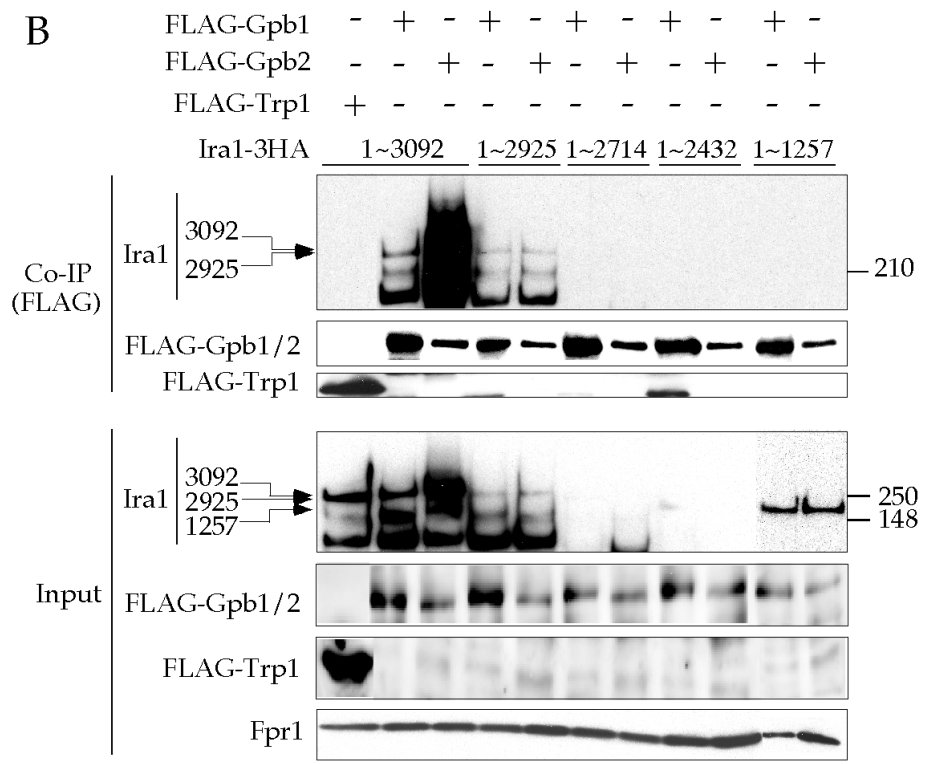
B
FLAG-Gpb1
FLAG-Gpb2
FLAG-Trp1
Ira1-3HA
1~3092
1~2925
1~2714
1~2432
1~1257
Co-IP (FLAG)
Ira1
3092
2925
210
FLAG-Gpb1/2
FLAG-Trp1
Input
Ira1
3092
2925
1257
250
148
FLAG-Gpb1/2
FLAG-Trp1
Fpr1

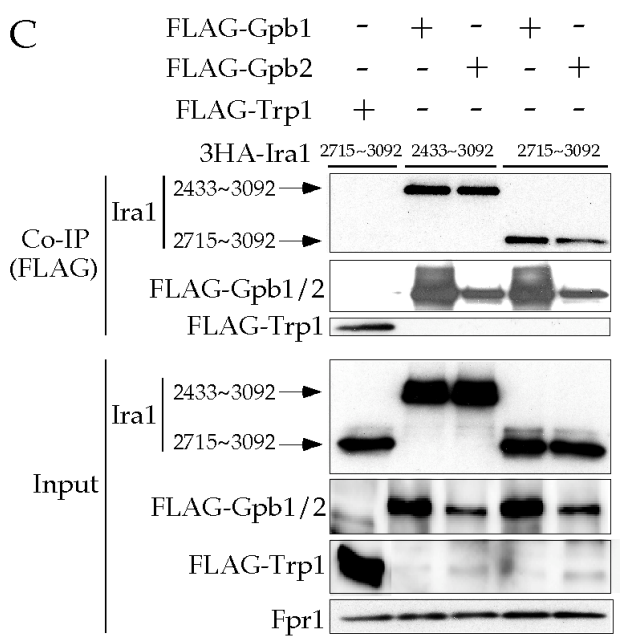
C
FLAG-Gpb1
FLAG-Gpb2
FLAG-Trp1
3HA-Ira1
2715~3092
2433~3092
2715~3092
Co-IP (FLAG)
Ira1
2433~3092
2715~3092
FLAG-Gpb1/2
FLAG-Trp1
Input
Ira1
2433~3092
2715~3092
FLAG-Gpb1/2
FLAG-Trp1
Fpr1

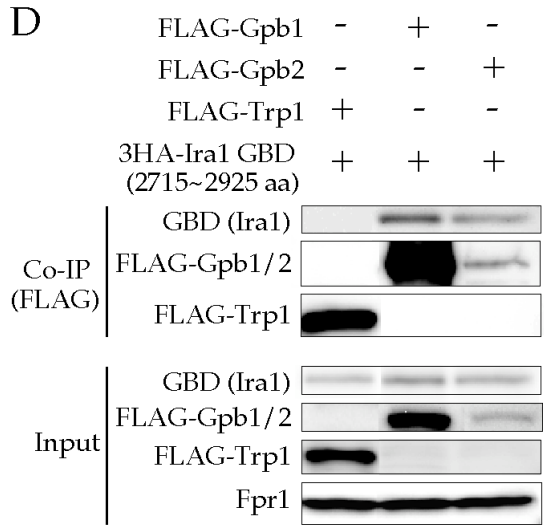
D
FLAG-Gpb1
FLAG-Gpb2
FLAG-Trp1
3HA-Ira1 GBD (2715~2925 aa)
Co-IP (FLAG)
GBD (Ira1)
FLAG-Gpb1/2
FLAG-Trp1
Input
GBD (Ira1)
FLAG-Gpb1/2
FLAG-Trp1
Fpr1

Figure 6. Harashima et al.

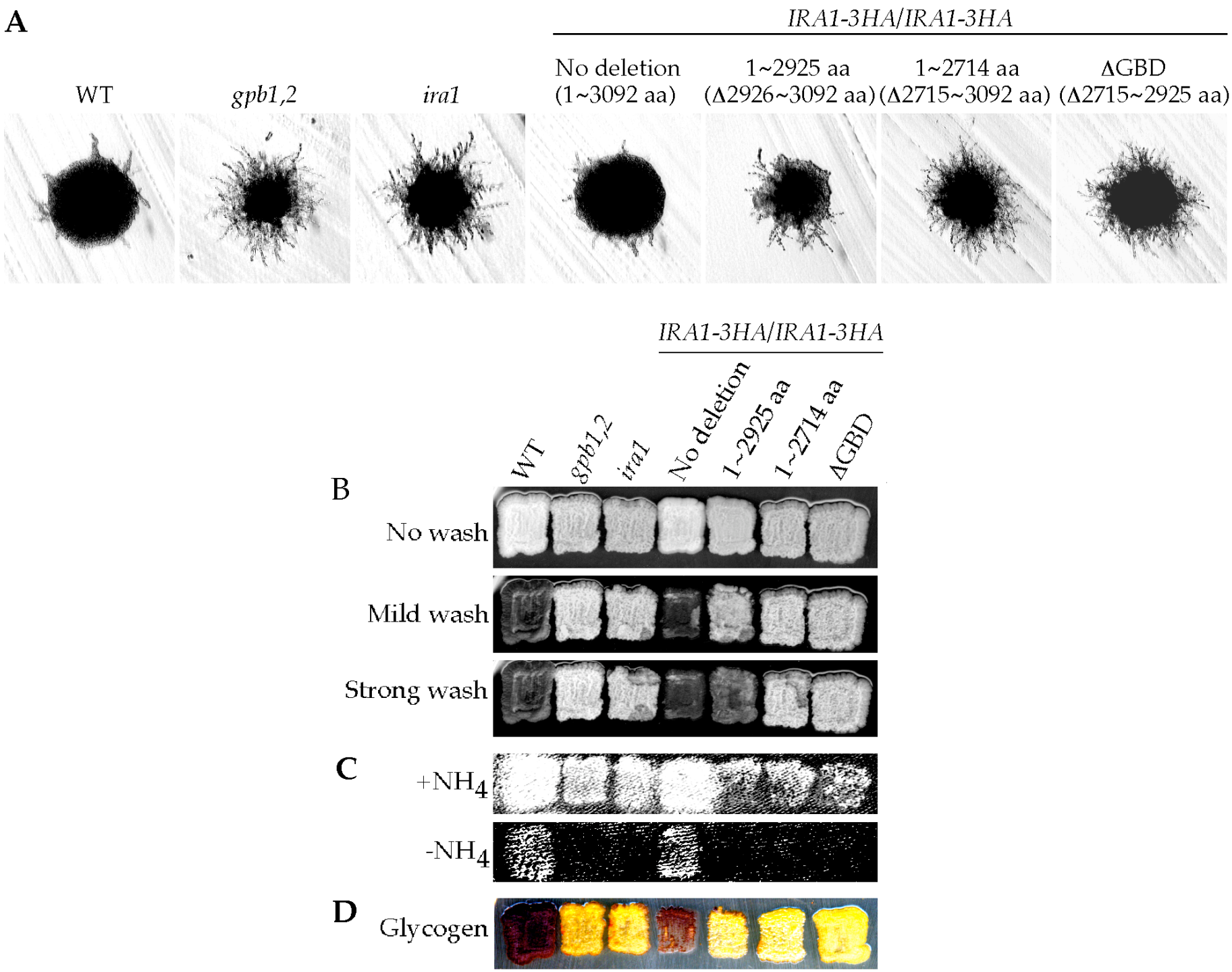

Figure 7. Harashima et al

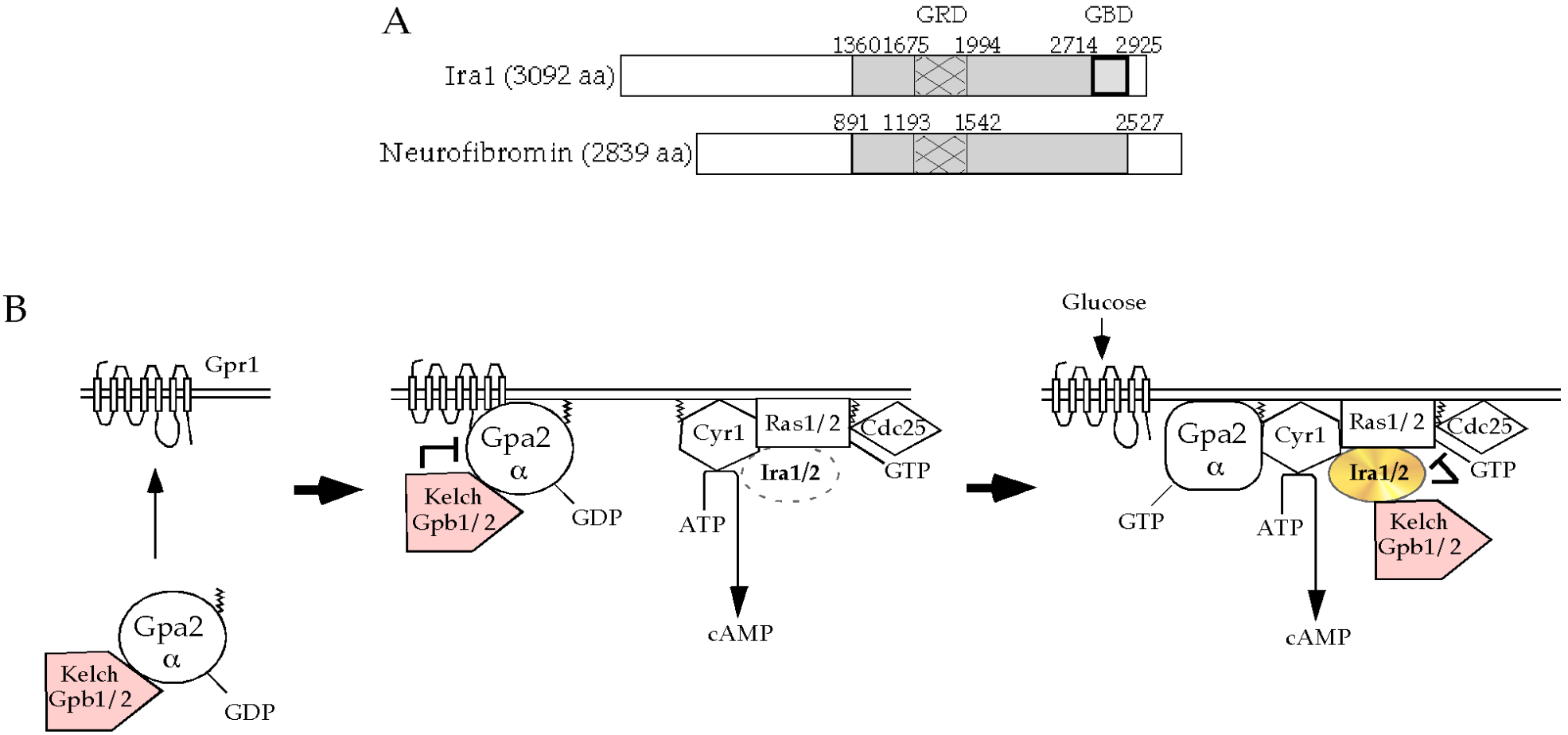

- Gpa2-dependent membrane localization
- Gpb1/2-dependent inhibition of Gpr1-Gpa2 coupling
- Ras-dependent adenylyl cyclase activation
- Gpa2-dependent adenylyl cyclase activation
- Gpb1/2-dependent Ira1/2 stabilization

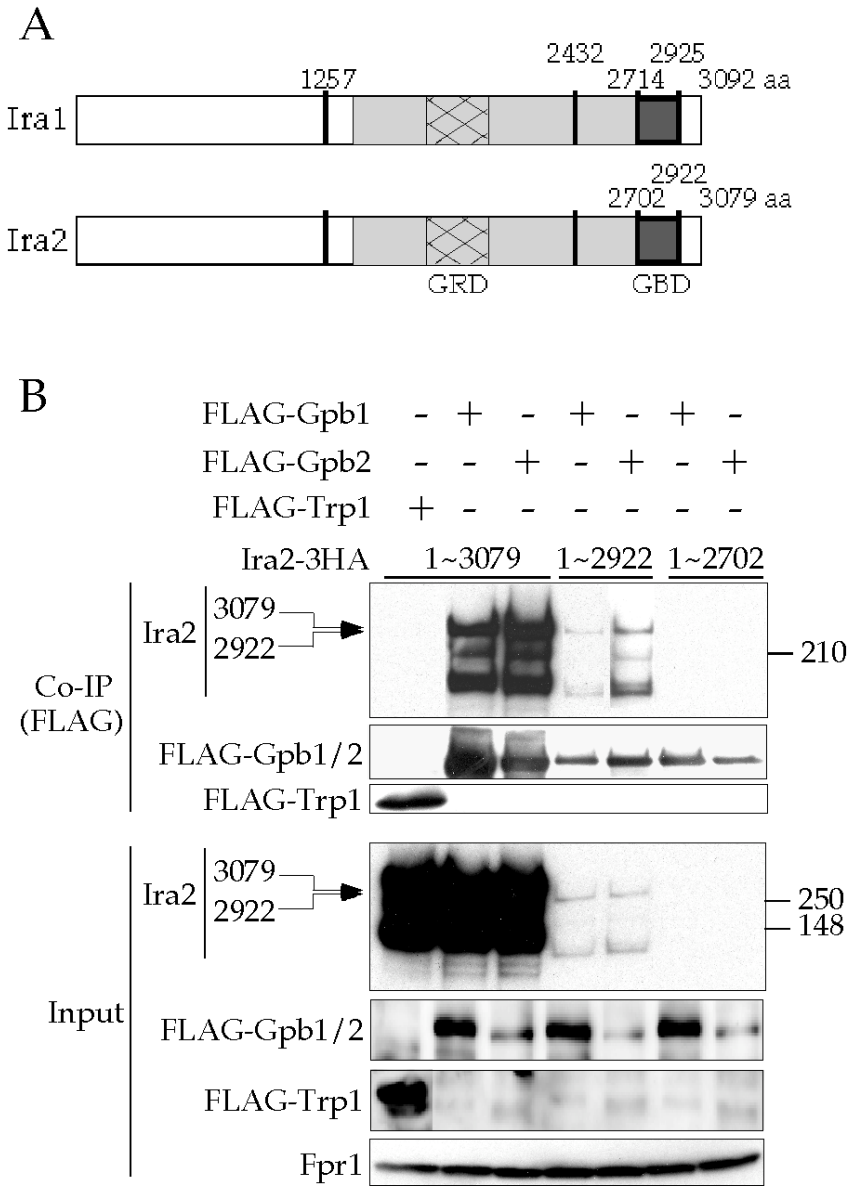
A
Ira1
1257
2432
2925
2714
3092 aa
Ira2
2922
2702
3079 aa
GRD
GBD
B
FLAG-Gpb1 - + - + - + -
FLAG-Gpb2 - - + - + - +
FLAG-Trp1 + - - - - - -
Ira2-3HA 1~3079 1~2922 1~2702
Co-IP (FLAG)
Ira2
3079
2922
210
FLAG-Gpb1/2
FLAG-Trp1
Input
Ira2
3079
2922
250
148
FLAG-Gpb1/2
FLAG-Trp1
Fpr1
C
FLAG-Gpb1 - + -
FLAG-Gpb2 - - +
FLAG-Trp1 + - -
Ira2-3HA 2703~3079
Co-IP (FLAG)
Ira2 (2703~3079)
FLAG-Gpb1/2
FLAG-Trp1
Input
Ira2 (2703~3079)
FLAG-Gpb1/2
FLAG-Trp1
Fpr1
D
FLAG-Gpb1 - + -
FLAG-Gpb2 - - +
FLAG-Trp1 + - -
Ira2-3HA 2703~2922
Co-IP (FLAG)
Ira2 (2703~2922)
FLAG-Gpb1/2
FLAG-Trp1
Input
Ira2 (2703~2922)
FLAG-Gpb1/2
FLAG-Trp1
Fpr1

Molecular Biology of the Cell
Vol. 16, 4557–4571, October 2005

Gα Subunit Gpa2 Recruits Kelch Repeat Subunits That Inhibit Receptor-G Protein Coupling during cAMP-induced Dimorphic Transitions in *Saccharomyces cerevisiae*

Toshiaki Harashima* and Joseph Heitman*†

*Department of Molecular Genetics and Microbiology and †Howard Hughes Medical Institute, Duke University Medical Center, Durham, NC 27710

Submitted May 9, 2005; Revised June 23, 2005; Accepted July 12, 2005
Monitoring Editor: Charles Boone

All eukaryotic cells sense extracellular stimuli and activate intracellular signaling cascades via G protein-coupled receptors (GPCR) and associated heterotrimeric G proteins. The *Saccharomyces cerevisiae* GPCR Gpr1 and associated Gα subunit Gpa2 sense extracellular carbon sources (including glucose) to govern filamentous growth. In contrast to conventional Gα subunits, Gpa2 forms an atypical G protein complex with the kelch repeat Gβ mimic proteins Gpb1 and Gpb2. Gpb1/2 negatively regulate cAMP signaling by inhibiting Gpa2 and an as yet unidentified target. Here we show that Gpa2 requires lipid modifications of its N-terminus for membrane localization but association with the Gpr1 receptor or Gpb1/2 subunits is dispensable for membrane targeting. Instead, Gpa2 promotes membrane localization of its associated Gβ mimic subunit Gpb2. We also show that the Gpa2 N-terminus binds both to Gpb2 and to the C-terminal tail of the Gpr1 receptor and that Gpb1/2 binding interferes with Gpr1 receptor coupling to Gpa2. Our studies invoke novel mechanisms involving GPCR-G protein modules that may be conserved in multicellular eukaryotes.

INTRODUCTION

All eukaryotic cells deploy on their surface signaling modules composed of G protein-coupled receptors (GPCR) and heterotrimeric G proteins to sense extracellular cues. GPCRs are conserved from yeasts to humans and constitute a family of cell surface receptors that contain seven transmembrane domains and sense myriad extracellular ligands including nutrients, odorants, hormones and pheromones, and photons (Gilman, 1987; Strader *et al.*, 1994; Lefkowitz, 2000; Mombaerts, 2004). Heterotrimeric G proteins consist of α, β, and γ subunits, in which the Gα subunits are guanine nucleotide binding proteins and the Gβγ subunits form a membrane-tethered heterodimer (Bourne, 1997; Sprang, 1997; Gautam *et al.*, 1998; Schwindinger and Robishaw, 2001; Cabrera-Vera *et al.*, 2003). Ligand binding triggers conformational changes in the GPCR that stimulate GDP-GTP exchange on Gα and release of the Gβγ dimer. Released Gα-GTP, Gβγ, or both signal downstream effectors. GTP-to-GDP hydrolysis (either intrinsic or RGS protein-stimulated) induces reassociation of the Gα-GDP subunit with Gβγ, extinguishing the signal (De Vries and Gist Farquhar, 1999; Guan and Han, 1999; Ross and Wilkie, 2000).

The yeast *Saccharomyces cerevisiae* expresses 3 GPCRs (Ste2, Ste3, and Gpr1) and 2 Gα subunits (Gpa1 and Gpa2), comprising two signaling modules: one that senses pheromones during mating and the other that senses nutrients and controls filamentous growth (Lengeler *et al.*, 2000; Harashima and Heitman, 2004). *S. cerevisiae* exists in two haploid mating types, **a** and α, which communicate via mating pheromones. **a** haploid cells express **a** pheromone and the GPCR Ste2 to sense extracellular α pheromone. α haploid cells express α pheromone and the GPCR Ste3 that senses **a** pheromone. In both cell types, Ste2 and Ste3 are coupled to the Gα subunit Gpa1, which forms a conventional heterotrimeric G protein with the Gβγ subunits Ste4/18. On pheromone binding to either receptor, GDP-GTP exchange occurs on Gpa1 and the Ste4/18 Gβγ complex dissociates. The liberated Ste4/18 dimer activates the pheromone responsive MAP kinase cascade culminating in mating (for reviews, see Dohlman and Thorner, 2001; Dohlman, 2002; Schwartz and Madhani, 2004).

In contrast to the pheromone GPCRs that are haploid- and mating-type-specific, a distinct GPCR, Gpr1, is expressed in both diploid and haploid cells. The Gpr1 receptor activates cAMP-PKA signaling and governs diploid pseudohyphal differentiation and haploid invasive growth via the coupled Gα subunit Gpa2 (for reviews, see Lengeler *et al.*, 2000; Pan *et al.*, 2000; Gancedo, 2001; Harashima and Heitman 2004). *gpr1* and *gpa2* mutants are defective in both pseudohyphal growth and transient cAMP production in response to glucose (Kübler *et al.*, 1997; Lorenz and Heitman, 1997; Colombo *et al.*, 1998; Yun *et al.*, 1998; Kraakman *et al.*, 1999; Lorenz *et al.*, 2000; Rolland *et al.*, 2000; Tamaki *et al.*, 2000; Lemaire *et al.*, 2004). Recent studies provide evidence that glucose and structurally related sugars serve as ligands for the GPCR Gpr1 (Kraakman *et al.*, 1999; Lorenz *et al.*, 2000; Rolland *et al.*, 2000; Lemaire *et al.*, 2004).

The yeast Gα subunit Gpa2 shares 35–55% identity with other fungal and mammalian Gα subunits, and the predicted secondary structures are highly conserved between Gpa2 and canonical Gα subunits (Harashima and Heitman,

This article was published online ahead of print in *MBC in Press* (http://www.molbiolcell.org/cgi/doi/10.1091/mbc.E05–05–0403) on July 19, 2005.

Address correspondence to: Joseph Heitman (heitm001@duke.edu).

2004). Amino acid residues that confer dominant phenotypes when mutated are also conserved. For instance, a mutation of Gln^{300} to Leu (Q300L) in Gpa2 is analogous to the Giα1 Q204L mutation that abolishes the intrinsic GTPase activity and functions as an activated form of Gpa2 (Harashima and Heitman, 2002). A mutation of Gly^{299} to Ala (Gpa2 G299A) is analogous to Giα1 G203A and Gαs G226A that fail to undergo the GTP-induced conformational change and thereby serves as a dominant negative allele and interacts with Gpb1/2 and Gpr1 more strongly compared with the wild-type Gpa2 (Lorenz and Heitman 1997; Harashima and Heitman, 2002).

Nevertheless, Gpa2 does not form a heterotrimeric complex with the known yeast G$\beta\gamma$ subunits Ste4/18 (Lorenz *et al.,* 2000; Harashima and Heitman, 2002, 2004). Recent studies identified two novel Gpa2 associated proteins, the kelch proteins Gpb1 and Gpb2, which are functionally redundant and share ~35% identity (Harashima and Heitman, 2002; Batlle *et al.,* 2003). The kelch motif is known to mediate protein-protein interactions (Adams *et al.,* 2000). Gpb1 and Gpb2 each contain seven kelch repeats, which share no sequence homology with the seven WD40 repeats of canonical Gβ subunits. The crystal structure of the kelch repeat enzyme galactose oxidase reveals that the seven kelch repeats can adopt a seven-bladed β-propeller structure strikingly similar to Gβ subunits (Ito *et al.,* 1991, 1994; Wall *et al.,* 1995; Lambright *et al.,* 1996; Sondek *et al.,* 1996; Adams *et al.,* 2000; Harashima and Heitman, 2002).

gpb1,2 mutants exhibit enhanced PKA phenotypes, including increased filamentous growth, sensitivity to nitrogen starvation and heat shock, reduced glycogen accumulation, and reduced sporulation (Harashima and Heitman, 2002; Batlle *et al.,* 2003). The *gpb1,2* mutant phenotypes are partially alleviated by *gpa2* mutations and abolished by mutation of the *TPK2* gene that encodes one of the three PKA catalytic subunits. These genetic findings support a model in which the kelch proteins Gpb1/2 negatively regulate the cAMP signaling pathway by inhibiting Gpa2 and an unidentified target that may be an upstream element of the PKA pathway including adenylyl cyclase or its regulator Ras or regulatory proteins of Ras (Harashima and Heitman, 2002).

In contrast to canonical Gα subunits, Gα Gpa2 has an extended N-terminus (Figure 1). This region shares no homology with known Gα subunits, whereas the remainder of Gpa2 shares >60% identity with Gα subunits in closely related yeasts and >40% identity with mammalian Gα subunits. The N-terminal regions of Gα subunits are known to mediate membrane localization and physical interactions with the cognate GPCR and G$\beta\gamma$ dimer (Navon and Fung, 1987; Hamm *et al.,* 1988; Journot *et al.,* 1991; Lambright *et al.,* 1996; Wall *et al.,* 1998; Yamaguchi *et al.,* 2003; Herrmann *et al.,* 2004).

All Gα subunits of heterotrimeric G proteins bear N-terminal lipid modifications (myristoylation and palmitoylation) necessary for membrane targeting (for reviews, see Chen and Manning, 2001; Cabrera-Vera *et al.,* 2003). Myristoylation involves the irreversible cotranslational addition of a 14-carbon myristoyl group on glycine at the second position in the consensus sequence MGXXXS and this occurs via an amide linkage after proteolytic removal of the initiating methionine (Johnson *et al.,* 1994; Ashrafi *et al.,* 1998; Farazi *et al.,* 2001). Palmitoylation occurs on all Gα subunits with the exception of Gαt (transducin) and involves posttranslational attachment of a saturated 16-carbon fatty acid, palmitate, via thioester linkage to cysteine residue(s) near the N-terminus. There is no palmitoylation consensus sequence, and palmitoylation is reversible and may be regulated. Both palmitoylation and myristoylation may play roles in addition to membrane localization (Linder *et al.,* 1991; Gallego *et al.,* 1992; Wedegaertner *et al.,* 1993; Wilson and Bourne, 1995; Wise *et al.,* 1997; Morales *et al.,* 1998; Evanko *et al.,* 2000; Fishburn *et al.,* 2000).

S. cerevisiae serves as a powerful model to study GPCR-G protein signaling (for reviews, see Jeansonne, 1994; Lengeler *et al.,* 2000; Dohlman and Thorner, 2001; Dohlman, 2002; Harashima and Heitman, 2004). The Gα subunit Gpa1 is myristoylated at the Gly^2 residue and palmitoylated at the Cys^3 residue (Song and Dohlman, 1996; Song *et al.,* 1996). Myristoylation is required for Gpa1 membrane targeting and palmitoylation, yet not for interaction with G$\beta\gamma$ (Song *et al.,* 1996). On the other hand, a Gpa1 palmitoylation-site mutant protein ($Gpa1^{C3A}$) is still partially localized to the plasma membrane, partially functional, and bound to G$\beta\gamma$ (Song and Dohlman, 1996). The G$\beta\gamma$ dimer, the associated GPCR Ste2/3, or components of the Gpa1 mediated MAP kinase cascade are not required for Gpa1 membrane localization (Song and Dohlman, 1996), but the Ste4/18 G$\beta\gamma$ dimer does promote receptor-Gpa1 coupling (Blumer and Thorner, 1990).

The distinct Gα subunit Gpa2 forms an unusual protein complex with the atypical binding partner kelch Gβ mimics Gpb1/2 and contains an extended N-terminus. Thus novel regulatory mechanisms may direct Gpa2 to the plasma membrane and enable Gpa2 to function as a molecular switch. Here we show that Gpa2 shares similar characteristics with Gpa1 involving lipid modifications and their function. Gpa2 interacting proteins are dispensable for Gpa2 membrane localization. However, unexpectedly, Gpa2 is required for membrane targeting of the kelch Gβ mimic Gpb2, in striking contrast to conventional heterotrimeric G proteins. Furthermore, the kelch Gβ mimic proteins Gpb1/2 were found to interfere with Gpr1 receptor-Gα Gpa2 coupling.

MATERIALS AND METHODS

Strains, Media, and Plasmids

Media and standard yeast experimental procedures were as described (Sherman, 1991). To express genes heterologously in yeast cells, an attenuated *ADH1* promoter and an *ADH1* terminator from the yeast two-hybrid vector pGBT9 were amplified by fusion PCR using primers, GCTTGCATGCAACTTCTTTT/CGACGGATCCCCGGGAATTCCATCTTTCAGGAGGCTTGCT and AGCAAGCCTCCTGAAAGATGGAATTCCCGGGGATCCGTCG/CGGCATGCCGGTAGAGGTGT, for the 1st round PCR and primers, GCTTGCATGCAACTTCTTTT/CGGCATGCCGGTAGAGGTGT for the second round PCR. The resulting PCR products were blunted with T4 DNA polymerase and cloned into the 2μ plasmid YEplac195 that was digested with *Hin*dIII and *Eco*RI and then blunted with T4 DNA polymerase to create a yeast expression vector pTH19 (*URA3* 2μ). pTH171 (*LEU2* 2μ), pTH172 (*TRP1* 2μ), and pTH173 (*LYS5* 2μ) are pTH19 derivatives. The nuclear localization signal (NLS) derived from the SV40 T antigen (PPKKKRKVA) was used to direct fusion proteins into the nucleus (Arévalo-Rodríguez and Heitman, 2005). pFA6a-GFP(S65T)-kanMX6 was used as the substrate for PCR to amplify GFP (Longtine *et al.,* 1998). Plasmids and yeast strains used in this study are listed in Tables 1 and 2. Details of plasmids and strains are available upon request.

Pseudohyphal and Invasive Growth

Pseudohyphal and invasive growth assays were investigated as described previously (Harashima and Heitman, 2002).

Microscopic Studies

If not specifically described in figure legends, growth conditions were as follows. For protein localization study, cells were grown in synthetic minimal media to stationary phase and examined for protein localization under a fluorescent microscope (Zeiss Axioskop2 plus, Thornwood, NY) or a confocal microscope (Zeiss LSM 410).

Table 1. *S. cerevisiae* strains

Strain	Genotype	Source/Reference
Σ1278b congenic strains		
MLY40α	*MATα ura3-52*	Lorenz and Heitman (1997)
MLY61a/α	*MAT***a**/α *ura3-52/ura3-52*	Lorenz and Heitman (1997)
MLY97a/α	*MAT***a**/α *ura3-52/ura3-52 leu2Δ::hisG/leu2Δ::hisG*	Lorenz and Heitman (1997)
MLY132α	*MATα gpa2Δ::G418 ura3-52*	Lorenz and Heitman (1997)
MLY132a/α	*MAT***a**/α *gpa2Δ::G418/gpa2Δ::G418 ura3-52/ura3-52*	Lorenz and Heitman (1997)
MLY212a/α	*MAT***a**/α *gpa2Δ::G418/gpa2Δ::G418 ura3-52/ura3-52 leu2Δ::hisG/leu2Δ::hisG*	Lorenz and Heitman (1997)
MLY232a/α	*MAT***a**/α *gpr1Δ::G418/gpr1Δ::G418 ura3-52/ura3-52*	Lorenz *et al*. (2000)
MLY277a/α	*MAT***a**/α *gpa2Δ::G418/gpa2Δ::G418 gpr1Δ::G418/gpr1Δ::G418 ura3-52/ura3-52*	Laboratory stock
THY212a/α	*MAT***a**/α *gpb1Δ::hph/gpb1Δ::hph gpb2Δ::G418/gpb2Δ::G418 ura3-52/ura3-52*	Harashima and Heitman (2002)
THY224a/α	*MAT***a**/α *gpg1Δ::hph/gpg1Δ::hph ura3-52/ura3-52*	This study
THY243a/α	*MAT***a**/α *gpb1Δ::hph/gpb1Δ::hph gpb2Δ::G418/gpb2Δ::G418 gpr1Δ::hph/gpr1Δ::hph ura3-52/ura3-52*	Harashima and Heitman (2002)
THY246a/α	*MAT***a**/α *gpb1Δ::hph/gpb1Δ::hph gpb2Δ::G418/gpb2Δ::G418 gpg1Δ::nat/gpg1Δ::nat ura3-52/ura3-52*	Harashima and Heitman (2002)
S288C background strains		
S1338	*MAT***a** *ura3Δ::loxP leu2Δ::loxP trp1Δ::loxP gal2*	Ito-Harashima
THY452	*MAT***a** *ura3Δ::loxP leu2Δ::loxP trp1Δ::loxP lys5Δ::loxP gal2*	This study

Preparation of Crude Cell Extracts and Immunoprecipitation

Total cell extracts from yeast cells that were grown to midlog phase ($OD_{600} \cong 0.8$) in synthetic dropout media were prepared in lysis buffer (50 mM HEPES, pH 7.6, 120 mM NaCl, 0.3% CHAPS, 1 mM EDTA, 20 mM NaF, 20 mM β-glycerophosphate, 0.1 mM Na-orthovanadate, 0.5 mM dithiothreitol, protease inhibitors (Calbiochem, La Jolla, CA; cocktail IV), and 0.5 mM phenylmethylsulfonyl fluoride) using a bead-beater. After centrifugation (25,000 × *g*, 20 min), crude extracts (2 mg) were mixed with anti-FLAG M2 affinity gel (Sigma, St. Louis, MO) to precipitate FLAG tagged proteins.

In Vivo Lipid Modifications

Cells were grown in 10 ml of SD-Ura medium to OD_{600} = 0.6–0.7, collected, and resuspended into 5 ml of fresh SD-Ura medium. After 10 min, cerulenin was added at a final concentration of 2 μg/ml, and cells were incubated for an additional 15 min under the same conditions. Subsequently, [^{3}H]myristic acid or [^{3}H]palmitic acid was added to the cultures at a final concentration of 50 μCi/ml for myristoylation analysis or 500 μCi/ml for palmitoylation analysis. After 3 h, cells were collected and washed once with H_2O and twice with phosphate-buffered saline. Preparation of crude cell extracts and immunoprecipitation of FLAG tagged proteins were performed as above. The bound FLAG tagged proteins were eluted by boiling for 5 min in SDS-PAGE sample buffer in the presence of β-mercaptoethanol for the myristoylation analysis and in the absence of β-mercaptoethanol for the palmitoylation analysis (Song and Dohlman, 1996). After SDS-PAGE, gels were fixed in H_2O/2-propanol/acetic acid (65:25:10 vol/vol/vol) for 30 min and then soaked at room temperature for 18 h either in 1 M hydroxylamine (pH 7.0) to cleave thioester-linked fatty acids or 1 M Tris-HCl (pH 7.0) as a control. The gels were fixed again, treated with Amplify (Amersham, Piscataway, NJ) for 30 min, dried, and then exposed to an x-ray film (BioMax MS film, Eastman Kodak, Rochester, NY) with an intensifying screen (BioMax Transcreen LE, Kodak) at −80°C for 1–2 mo. Expression of the FLAG-tagged proteins was verified by Western blot analysis using anti-FLAG M2 antibody (Sigma).

cAMP Assay

cAMP assay was as described in Lorenz *et al.* (2000) with some modifications. Briefly, at the time points indicated, 0.5 ml of cell suspension was transferred into a microfuge tube containing 0.5 ml of 10% ice-cold trichloroacetic acid and was immediately frozen in liquid nitrogen. To prepare intracellular cAMP, cells were permeabilized by defrosting at 4°C overnight. Cell extracts were neutralized by ether extraction and lyophilized. Intracellular cAMP levels were determined by using a cAMP enzyme immunoassay kit (Amersham).

RESULTS

Gα Subunit Gpa2 Is Myristoylated and Palmitoylated

The Gα protein Gpa2 is coupled to the GPCR Gpr1 and signals to activate the downstream effector adenylyl cyclase in response to glucose. Based on analogy to other GPCR-Gα systems, we hypothesized that Gpa2 would be localized to the cell membrane for function. To address this, Gpa2 was fused to green fluorescent protein (GFP). To avoid perturbing protein localization or receptor coupling sequences typically linked to the amino and carboxy terminal regions of Gα proteins (Figure 1A), GFP was fused between the first 10 amino acids (1–10) of Gpa2 and the remainder of the protein (amino acids 4–449) to produce a Gpa2$^{1-10}$-GFP-Gpa2$^{4-449}$ internal fusion protein. This Gpa2-GFP fusion protein was functional based on its ability to complement the pseudohyphal defect of *gpa2* mutant cells (unpublished data). As shown in Figure 2A, the Gpa2-GFP fusion protein was localized to the cell membrane. A C-terminally GFP tagged Gpa2 protein was nonfunctional (unpublished data), in accord with the known role of the Gα C-terminal domain in receptor coupling (Slessareva *et al.*, 2003; Herrmann *et al.*, 2004).

To establish the minimal Gpa2 domain required for membrane localization, the first 10 (Gpa2$^{1-10}$), 20 (Gpa2$^{1-20}$), or 30 (Gpa2$^{1-30}$) amino acids of Gpa2 were fused to a GFP cassette and expressed in vivo. All three C-terminally tagged Gpa2-GFP proteins were localized to the plasma membrane (Figure 2A). Therefore, as few as the first 10 amino acids of Gpa2 suffice for plasma membrane targeting.

In conventional Gα subunits, lipid modifications of the N-terminus mediate membrane localization (Chen and Manning, 2001). Myristoylation occurs at Gly^2 in the myristoylation consensus sequence G^{2}XXXS^6 (Johnson *et al.*, 1994). Palmitoylation can occur at any cysteine residue near the N-terminus. Gpa2 contains glycine and serine in the second and sixth positions for myristoylation and cysteine at the fourth position from the N-terminus. To examine whether these sites are lipid modified, a Gpa2$^{1-20}$-GFP-FLAG protein in which the first 20 amino acids of Gpa2 were fused to a GFP-FLAG cassette was expressed in yeast cells and assessed for lipid modifications. Gpa2$^{1-20}$-GFP-FLAG variants containing mutations in the potential lipid modification sites (G2A, C4A, or S6Y) were also analyzed.

As a positive control for lipid modification experiments, an equivalent Gpa1$^{1-20}$-GFP-FLAG protein was constructed,

Table 2. Plasmids

Plasmid	Description	Source/Reference
pTH19	P_{ADH1} *URA3* 2μ	This study
pTH26	P_{ADH1}-*GPB1 URA3* 2μ (pTH19)	This study
pTH27	P_{ADH1}-*GPB2 URA3* 2μ (pTH19)	This study
pTH47	P_{ADH1}-*GPA2 URA3* 2μ (pTH19)	This study
pTH48	P_{ADH1}-$GPA2^{Q300L}$ *URA3* 2μ (pTH19)	This study
pTH49	P_{ADH1}-$GPA2^{G299A}$ *URA3* 2μ (pTH19)	This study
pTH62	P_{ADH1}-$GPA2^{G2A}$ *URA3* 2μ (pTH19)	This study
pTH65	P_{ADH1}-$GPA2^{1–30\ aa}$::*GFP URA3* 2μ (pTH19)	This study
pTH68	P_{ADH1}-$GPA2^{C4A}$ *URA3* 2μ (pTH19)	This study
pTH69	P_{ADH1}-$GPA2^{S6Y}$ *URA3* 2μ (pTH19)	This study
pTH71	P_{ADH1}-$GPA2^{1–10\ aa}$::*GFP URA3* 2μ (pTH19)	This study
pTH73	P_{ADH1}-*GFP URA3* 2μ (pTH19)	This study
pTH75	P_{ADH1}-*GFP-GPB2 URA3* 2μ (pTH19)	This study
pTH80	P_{ADH1}-$GPA2^{1–10}$::*GFP*::$GPA2^{4–449}$ *URA3* 2μ (pTH19)	This study
pTH81	P_{ADH1}-$GPA2^{1–20\ aa}$::*GFP-FLAG URA3* 2μ (pTH19)	This study
pTH84	P_{ADH1}-*GFP-GPB2 LEU2* 2μ (pTH171)	This study
pTH91	P_{ADH1}-$GPA2^{1–20\ aa\ G2A}$::*GFP-FLAG URA3* 2μ (pTH19)	This study
pTH92	P_{ADH1}-$GPA2^{1–20\ aa\ C4A}$::*GFP-FLAG URA3* 2μ (pTH19)	This study
pTH93	P_{ADH1}-$GPA2^{1–20\ aa\ S6Y}$::*GFP-FLAG URA3* 2μ (pTH19)	This study
pTH100	P_{ADH1}- *GFP-FLAG URA3* 2μ (pTH19)	This study
pTH103	P_{ADH1}-$GPA1^{1–20\ aa}$::*GFP-FLAG URA3* 2μ (pTH19)	This study
pTH106	P_{ADH1}-*GFP-GPB1 URA3* 2μ (pTH19)	This study
pTH114	P_{ADH1}-*GPB2 LEU2* 2μ (pTH171)	This study
pTH127	P_{ADH1}-$GPA1^{1–10}$-$GPA2^{Δ1–100}$ *URA3* 2μ (pTH19)	This study
pTH128	P_{ADH1}-$GPA1^{1–10}$-$GPA2^{Δ1–100\ G299A}$ *URA3* 2μ (pTH19)	This study
pTH130	P_{ADH1}-$GPA2^{Δα\ (51–57)\ G299A}$ *URA3* 2μ (pTH19)	This study
pTH133	P_{ADH1}-$GPA2^{Δα\ (51–57)}$ *URA3* 2μ (pTH19)	This study
pTH134	P_{ADH1}-$GPA1^{1–10}$-$GPA2^{Δ1–29\ G299A}$ *URA3* 2μ (pTH19)	This study
pTH136	P_{ADH1}-$GPA2^{Δ16–84\ G299A}$ *URA3* 2μ (pTH19)	This study
pTH144	P_{ADH1}-$GPA1^{1–10}$-$GPA2^{Δ1–14\ G299A}$ *URA3* 2μ (pTH19)	This study
pTH145	P_{ADH1}-$GPA2^{Δ46–84\ G299A}$ *URA3* 2μ (pTH19)	This study
pTH149	P_{ADH1}-$GPA2^{G2A}$-*NLS URA3* 2μ (pTH19)	This study
pTH155	P_{ADH1}-$GPA2^{Δ46–100}$ *URA3* 2μ (pTH19)	This study
pTH157	P_{ADH1}-$GPA1^{1–10}$-$GPA2^{Δ1–29}$ *URA3* 2μ (pTH19)	This study
pTH158	P_{ADH1}-$GPA2^{Δ46–84}$ *URA3* 2μ (pTH19)	This study
pTH159	P_{ADH1}-$GPA2^{Δ31–84\ G299A}$ *URA3* 2μ (pTH19)	This study
pTH160	P_{ADH1}-$GPA2^{Δ31–84}$ *URA3* 2μ (pTH19)	This study
pTH161	P_{ADH1}-$GPA2^{Δ16–84}$ *URA3* 2μ (pTH19)	This study
pTH163	P_{ADH1}-*MLS-GFP-GPB2 URA3* 2μ (pTH19)	This study
pTH164	P_{ADH1}-*MLS-GFP-GPB1 URA3* 2μ (pTH19)	This study
pTH166	P_{ADH1}-*NLS-GFP-GPB2 URA3* 2μ (pTH19)	This study
pTH167	P_{ADH1}-*NLS-GFP-GPB1 URA3* 2μ (pTH19)	This study
pTH168	P_{ADH1}-$GPA2^{Δ46–100\ G299A}$ *URA3* 2μ (pTH19)	This study
pTH169	P_{ADH1}-$GPA1^{1–10}$-$GPA2^{Δ1–14}$ *URA3* 2μ (pTH19)	This study
pTH170	P_{ADH1}-*GFP-GPR1C TRP1* 2μ (pTH172)	This study
pTH171	P_{ADH1} *LEU2* 2μ	This study
pTH172	P_{ADH1} *TRP1* 2μ	This study
pTH173	P_{ADH1} *LYS5* 2μ	This study
pTH174	P_{ADH1}-*GPB1 LYS5* 2μ (pTH173)	This study
pTH178	P_{ADH1}-$GPA2^{Δ46–449}$ *URA3* 2μ (pTH19)	This study
pTH191	P_{ADH1}-$GPA1^{1–10}$-$GPA2^{Δ1–44}$ *URA3* 2μ (pTH19)	This study
pTH192	P_{ADH1}-$GPA1^{1–10}$-$GPA2^{Δ1–44\ G299A}$ *URA3* 2μ (pTH19)	This study

which was derived from the Gpa1 Gα subunit coupled to the Ste2/3 pheromone receptors (Figure 2B). Gpa1 is known to be myristoylated at the second position on glycine (Gly^2) and palmitoylated on cysteine in the third position (Cys^3) (Song and Dohlman, 1996; Song *et al.*, 1996). Gpa1 myristoylation is essential for membrane localization and function and required for palmitoylation, and palmitoylation also promotes membrane localization and function. In addition, the first 9 amino acids of Gpa1 suffice for membrane localization of a Gpa1-GST fusion protein (Gillen *et al.*, 1998).

As shown in Figure 2B, the wild-type Gpa2 fusion protein was myristoylated and the myristoylation site and myristoylation consensus sequence mutant proteins, $Gpa2^{G2A}$ and $Gpa2^{S6Y}$, were not, suggesting that Gpa2 is subject to myristoylation at Gly^2. Gpa2 was also palmitoylated and a mutation in the putative palmitoylation site ($Gpa2^{C4A}$) abolished this modification (Figure 2C). Therefore, Gpa2 is also subject to palmitoylation at Cys^4. We note that the $Gpa2^{C4A}$ fusion protein exhibited a decreased level of myristoylation compared with the wild-type protein. Interestingly, reduced myristoylation was also observed with the $Gpa1^{C3S}$ mutant (Song and Dohlman, 1996). These results are indicative of either a sequence preference in the myristoylation consensus sequence (G^2XXXS^6) or a role for palmitoylation in promoting myristoylation or its maintenance.

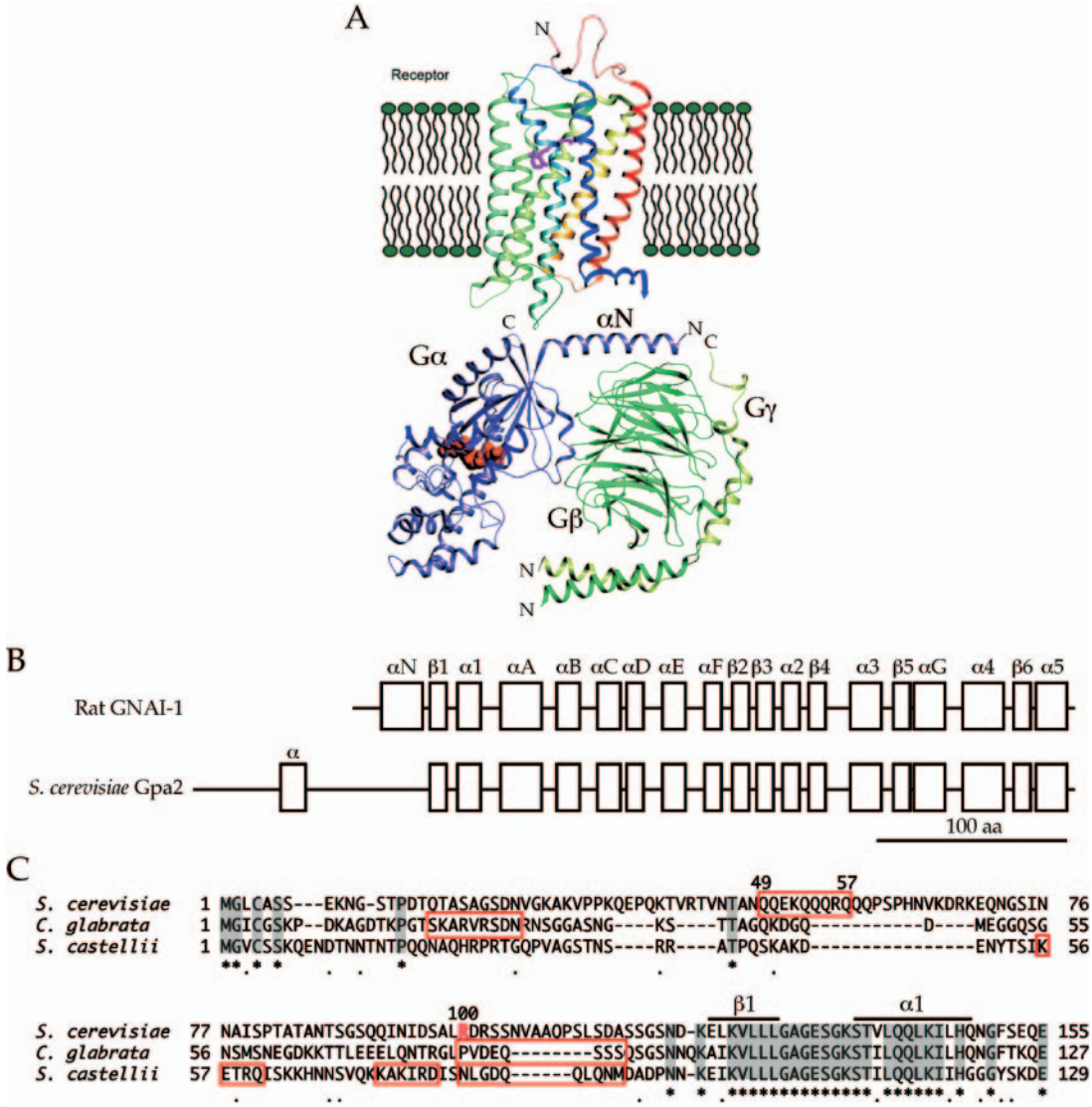

Figure 1. N-terminal alpha helix of Gα subunits (αN domain) is involved in receptor and Gβγ dimer coupling. (A) The αN domain provides one of the binding interfaces between Gα and Gβ and the receptor. This image shows a hypothetical model (PDB file 1BOK) for a GPCR-G protein module (GPCR; Rhodopsin, PDB file 1F88, G protein; PDB file 1GOT). The αN domain of the Gα subunit that is required for Gβ subunit and receptor coupling is shown (modified from Cabrera-Vera *et al.,* 2003). (B) The predicted secondary structures of the conventional rat Gαi subunit and the yeast Gα Gpa2 protein based on PHD (Rost *et al.,* 1993). Gpa2 shares 34% identity with the rat Gαi subunit and the predicted secondary structure is highly conserved between the two, except for the extended Gpa2 N-terminus. Secondary structure assignments were based on those of $G_{\alpha t/\alpha I}$ (Lambright *et al.,* 1996). (C) An alignment of the amino acid sequence of the N-terminus of Gpa2 homologues from *S. cerevisiae* and the related yeasts *C. glabrata* and *S. castellii*. *C. glabrata* and *S. castellii* express homologues of the *S. cerevisiae* GPCR Gpr1 and Gβ mimic Gpb1/2 proteins as well as a Gpa2 homologue, yet the N-termini of their Gpa2 homologues share no significant homology. Amino acids forming a potential alpha helix in the N-termini are indicated by red rectangles. Identical amino acids are marked (*) and shaded in gray, and conserved amino acids are also indicated (●). The 100th amino acid (R) of Gpa2 is shown in red. The β1 and α1 domains assigned in Figure 1B are shown. Alignments were obtained using Clustal W (Thompson *et al.,* 1994).

Similar to Gpa1, Gpa2 requires myristoylation for palmitoylation because the G2A and S6Y mutations, which abolish myristoylation, also blocked palmitoylation. Consistent with these results, the Gpa2-GFP-FLAG proteins bearing the G2A, C4A, or S6Y mutations failed to localize to the plasma membrane, and thus myristoylation and palmitoylation are required for Gpa2 plasma membrane localization (Figure 2A).

To address the physiological roles of these lipid modifications, the G2A, C4A, and S6Y mutations were introduced into the *GPA2* gene and expressed in a Σ1278b *gpa2/gpa2* diploid or *gpa2* haploid mutant strain. As shown in Figure 2, D and E, the $GPA2^{G2A}$ myristoylation site mutant failed to complement either the pseudohyphal or the invasive growth defects. The $GPA2^{S6Y}$ and $GPA2^{C4A}$ myristoylation consensus sequence or palmitoylation site mutants showed severe defects in both assays. Furthermore, introduction of a dominant active mutation (Q300L) that abolishes Gpa2 GTPase activity failed to restore activity of the $GPA2^{G2A}$ mutant protein ($Gpa2^{G2A,\ Q300L}$, unpublished data). Thus, myristoylation and palmitoylation both play critical roles in Gpa2 membrane localization and signaling. Importantly, the unusual Gα subunit Gpa2 shares common features with the

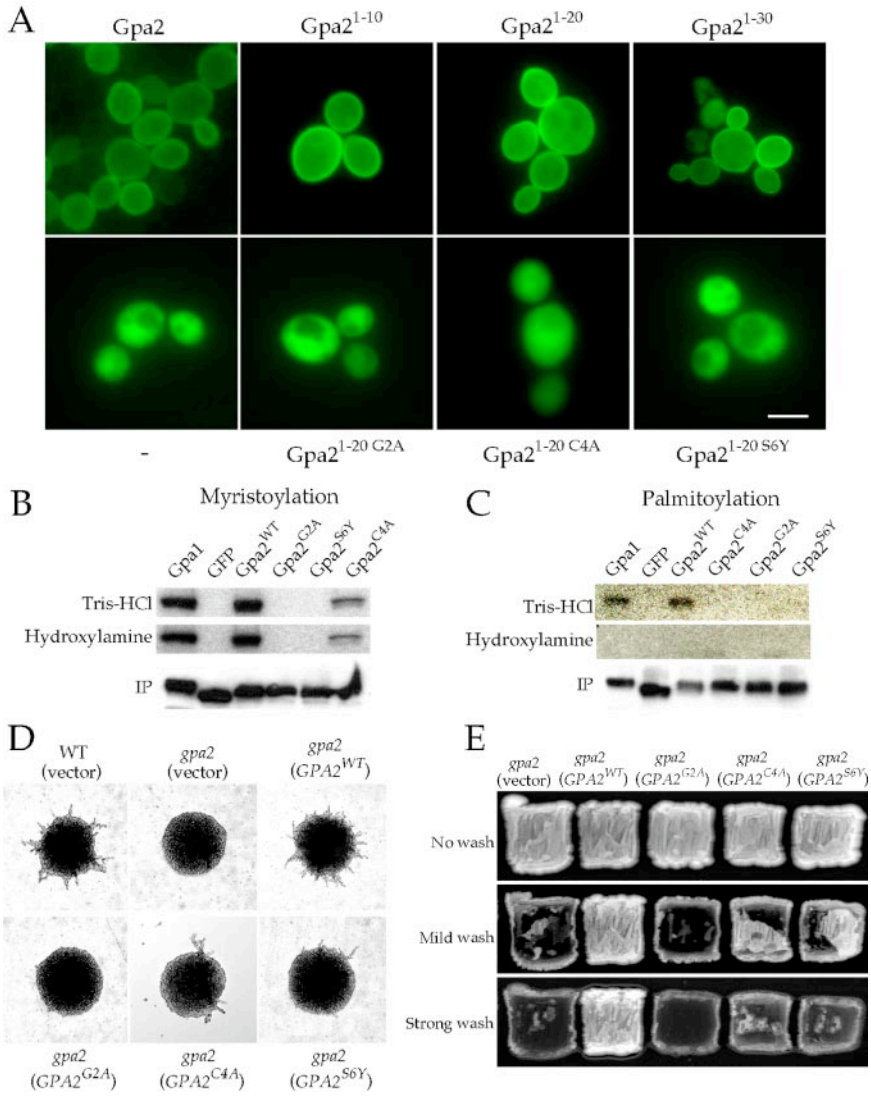

Figure 2. Myristoylation and palmitoylation are required for membrane localization and function of the Gα subunit Gpa2. (A) The first 10 amino acids from Gpa2 are sufficient for membrane localization. A functionally, internally GFP-tagged Gpa2 (Gpa2, pTH80), truncated GFP-tagged Gpa2 proteins, $Gpa2^{1–10}$-GFP ($Gpa2^{1–10}$, pTH71), $Gpa2^{1–20}$-GFP-FLAG ($Gpa2^{1–20}$, pTH81), and $Gpa2^{1–30}$-GFP ($Gpa2^{1–30}$, pTH65), or mutant truncated GFP-tagged Gpa2 proteins, $Gpa2^{1–20\ G2A}$-GFP-FLAG ($Gpa2^{1–20\ G2A}$, pTH91), $Gpa2^{1–20\ C4A}$-GFP-FLAG ($Gpa2^{1–20\ C4A}$, pTH92), and $Gpa2^{1–20\ S6Y}$-GFP-FLAG ($Gpa2^{1–20\ S6Y}$, pTH93), were expressed from a 2μ plasmid in wild-type yeast cells (MLY61a/α) to test for protein localization. The GFP cassette alone (−, pTH73) was also expressed as a control. Scale bar, 5 μm. (B and C) Gpa2 is myristoylated (B) and palmitoylated (C). *gpa2* mutant cells (MLY132a/α) expressing the $Gpa2^{1–20}$-GFP-FLAG ($Gpa2^{WT}$, pTH81), $Gpa2^{1–20\ G2A}$-GFP-FLAG ($Gpa2^{G2A}$, pTH91), $Gpa2^{1–20\ S6Y}$-GFP-FLAG ($Gpa2^{S6Y}$, pTH93), $Gpa2^{1–20\ C4A}$-GFP-FLAG ($Gpa2^{C4A}$, pTH92), GFP-FLAG (GFP, pTH100), or $Gpa1^{1–20}$-GFP-FLAG (Gpa1, pTH103) proteins were metabolically labeled with [^{3}H]myristic acid or [^{3}H]palmitic acid. FLAG-tagged proteins were purified using anti-FLAG affinity gel and subjected to SDS-PAGE. Gels were treated with 1 M Tris-HCl, 1 M hydroxylamine that cleaves the palmitoyl moiety of fatty acids, or subjected to Western blot using an anti-FLAG antibody to verify purified protein levels. Radiolabeled purified proteins were visualized by autoradiography. (D and E) Myristoylation and palmitoylation are required for Gpa2 function. Full-length wild-type ($Gpa2^{WT}$, pTH47) or mutant Gpa2 proteins ($Gpa2^{G2A}$ (pTH62), $Gpa2^{C4A}$ (pTH68), and $Gpa2^{S6Y}$ (pTH69)) were expressed in *gpa2* mutant cells (MLY132a/α or MLY132α) to test for diploid filamentous growth (D) and haploid invasive growth (E). *gpa2* mutant cells containing an empty plasmid (pTH19) served as control.

conventional Gα subunit Gpa1 with respect to lipid modifications and their physiological roles.

Gpa2 Binding Partners Are Not Required for Gpa2 Membrane Localization

In heterotrimeric G proteins, Gβγ subunits can promote membrane localization of their associated Gα subunits. Therefore, the localization of Gpa2 was examined in the absence of Gpb1/2 or when Gpb1/2 were overexpressed. As shown in Figure 3, A and B, Gpa2 membrane localization was unchanged under both conditions. Furthermore, deletion of other known Gpa2 associated proteins, namely the GPCR Gpr1 or the Gγ subunit mimic Gpg1, or even the elimination of multiple binding partners (Gpb1/2 and Gpr1 or Gpb1/2 and Gpg1), did not perturb Gpa2 plasma membrane localization, suggesting these binding partners are not required for membrane targeting (Figure 3A).

Because Gpa2 is a component of the glucose sensing cAMP signaling pathway and the agonist induced redistribution of Gαs has been reported in mammalian cells (Wedegaertner *et al.*, 1996; Thiyagarajan *et al.*, 2002), we examined if carbon source affects Gpa2 protein localization (Figure 3C). Glucose serves as a ligand for Gpr1 (Yun *et al.*, 1998; Kraakman *et al.*, 1999; Lorenz *et al.*, 2000; Rolland *et al.*, 2000; Lemaire *et al.*, 2004). Glucose, fructose, and galactose are structurally related hexoses, yet galactose is not a ligand for Gpr1 (Lorenz *et al.*, 2000; Lemaire *et al.*, 2004). Fructose is controversial, although fructose can induce cAMP production when added to glucose-starved cells (Yun *et al.*, 1998; Lemaire *et al.*, 2004). Maltose and galactose induce filamentous growth in a Gpr1-Gpa2-independent manner (Lorenz *et al.*, 2000). Ethanol and glycerol are structurally unrelated nonfermentable carbon sources. As shown in Figure 3C, Gpa2 was localized to the plasma membrane to the same extent under all conditions tested. Therefore, the carbon sources examined do not influence Gpa2 protein localization and Gpa2 is localized to the cell membrane irrespective of activity of the Gpr1-Gpa2 signaling pathway.

Kelch Gβ Mimic Gpb2 Is Recruited to the Plasma Membrane by Gpa2

If the kelch proteins Gpb1/2 function as Gβ mimics, we hypothesized that Gpb1/2 should also be membrane localized. To examine protein localization, a functional GFP-Gpb2 protein was expressed in *gpa2*Δ cells (Figure 4). When GFP-Gpb2 was expressed alone, Gpb2 was found to be

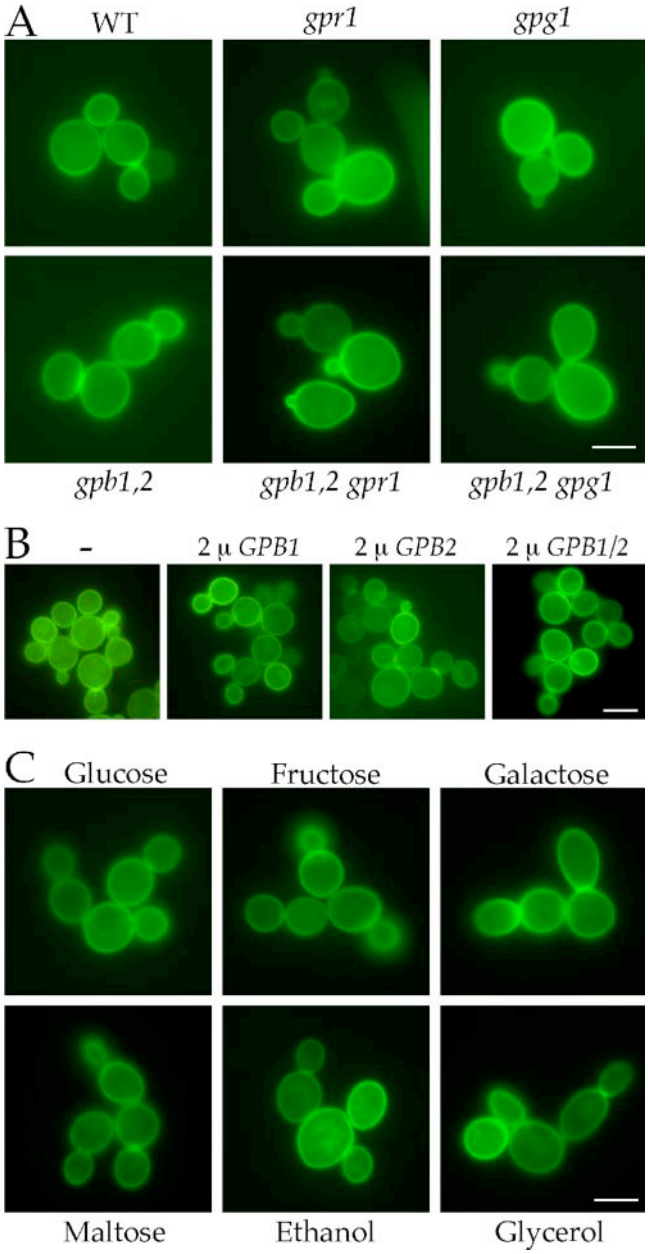

Figure 3. The Gα subunit Gpa2 is localized to the plasma membrane independent of its known binding partners. (A) Gpa2-GFP protein (pTH80) was expressed in *gpr1* (MLY232a/α), *gpg1* (THY224a/α), *gpb1,2* (THY212a/α), *gpb1,2 gpr1* (THY243a/α), and *gpb1,2 gpg1* (THY246a/α) mutant cells and protein localization was analyzed. (B) Overexpression of the kelch Gβ mimic proteins Gpb1/2 has no effect on Gpa2 membrane localization. The Gpa2-GFP protein was coexpressed with Gpb1 (pTH26), Gpb2 (pTH27), or both (pTH26 and pTH114) in wild-type cells (MLY97a/α). (C) Membrane localization of Gpa2 was not altered by carbon sources. *gpa2* mutant cells (MLY132a/α) expressing the Gpa2-GFP protein were grown in synthetic media containing different carbon sources and Gpa2 protein localization was assessed. Scale bars, 5 μm.

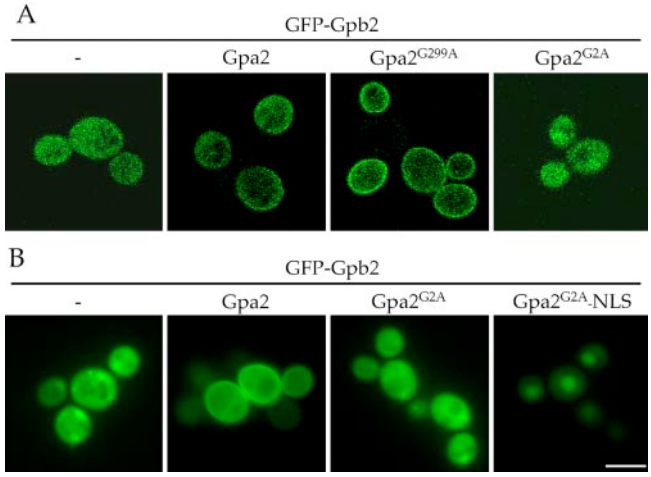

Figure 4. Gα subunit Gpa2 recruits the kelch Gβ subunit mimic Gpb2 to the plasma membrane. (A) A functional GFP-Gpb2 protein (pTH84) was coexpressed with Gpa2 (pTH47), $Gpa2^{G299A}$ (pTH49), $Gpa2^{G2A}$ (pTH62), or $Gpa2^{G2A}$-NLS (pTH149) proteins in *gpa2*Δ mutant cells (MLY212a/α), and protein localization was investigated by confocal (A) or direct fluorescence microscopy (B). The empty vector pTH19 (−) served as control. Nuclear localization was confirmed by DAPI staining (unpublished data). Scale bar, 5 μm.

cytoplasmic. However, when GFP-Gpb2 was coexpressed with either wild-type Gpa2 or a dominant negative Gpa2 ($Gpa2^{G299A}$), GFP-Gpb2 was directed to the plasma membrane (Figure 4). Confocal microscopic analysis revealed that Gpb2 was localized to the plasma membrane more extensively when coexpressed with the $Gpa2^{G299A}$ mutant protein that is unable to undergo the GTP-induced conformational change when compared with wild-type Gpa2 (Figure 4A). This finding is in accord with previous data showing that Gpb2 binds to Gpa2 in vivo and preferentially associates with Gpa2-GDP (Harashima and Heitman, 2002).

When GFP-Gpb2 was coexpressed with the nonfunctional $Gpa2^{G2A}$ mutant that is no longer directed to the plasma membrane, GFP-Gpb2 was no longer localized to the plasma membrane (Figure 4). To exclude the possibility that the observed Gpb2 membrane localization is an indirect secondary consequence due to overexpression of the functional wild-type Gpa2 protein, GFP-Gpb2 was coexpressed with a nuclear localization signal (NLS) containing $Gpa2^{G2A}$ mutant protein ($Gpa2^{G2A}$-NLS). Strikingly, $Gpa2^{G2A}$-NLS now misdirected Gpb2 to the nucleus (Figure 4B). Therefore, the Gα protein Gpa2 forms a stable complex with the kelch Gβ mimic protein Gpb2 and serves to recruit Gpb2 to the plasma membrane. That $Gpa2^{G2A}$-NLS directs Gpb2 to the nucleus also demonstrates that lipid modifications are not required for the Gpa2-Gpb2 interaction. This is consistent with findings regarding interaction of the yeast Gα subunit Gpa1 and the mammalian Gα subunit Gαi with their respective Gβ subunits (Jones *et al.*, 1990; Song *et al.*, 1996).

Kelch Gβ Mimic Gpb2 and the C-terminal Tail of the Gpr1 Receptor Bind to the N-terminal Region of Gpa2

In canonical Gα subunits, an N-terminal alpha helix called the αN domain provides a binding surface for the Gβ subunit and the coupled receptor (Lambright *et al.*, 1996; Wall *et al.*, 1998). Because the αN domain is less conserved among Gα subunits, we searched for any related alpha helical domain in the extended N-terminus of Gpa2 using the PHD secondary structure prediction method (Rost and Sander, 1993). A sequence spanning amino acid residues 49–57 was identified that is predicted to form an alpha helix, although this region does not share any significant identity with known αN domains (Figure 1).

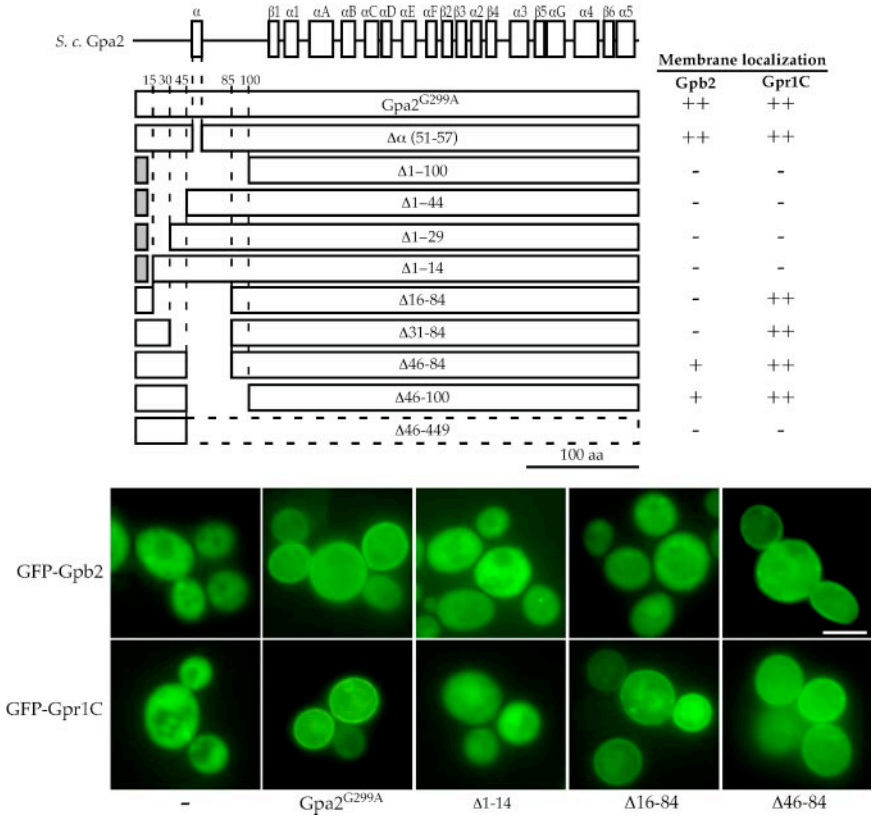

Figure 5. N-terminus of Gα Gpa2 is required for binding to the kelch protein Gpb2 and the GPCR Gpr1. A series of deletions was created in the N-terminal region of $Gpa2^{G299A}$, and these deletion constructs were coexpressed with the GFP-Gpb2 protein (pTH84) in *gpa2*Δ cells (MLY212a/α) or with GFP-Gpr1C (pTH170) in wild-type cells (S1338) to determine roles of the N-terminal region of Gpa2 on interaction with Gpb2 and the C-terminal tail of Gpr1. Deletion mutant $Gpa2^{G299A}$ proteins constructed and results are shown schematically. Δ1–14, Δ1–29, Δ1–44, and Δ1–100 mutant proteins were fused to the first 10 amino acids from the yeast Gα subunit Gpa1 to restore targeting to the plasma membrane and Gpa1 residues are depicted as a gray box. Scale bar, 5 μm.

To examine if this candidate alpha helical domain of Gpa2 is involved in the interaction with Gpb2, the domain was deleted in the dominant negative $Gpa2^{G299A}$ mutant ($Gpa2^{\Delta\alpha\ (51-57)}$) and the resulting mutant derivative was coexpressed with the GFP-Gpb2 protein to test for protein localization. As noted above, $Gpa2^{G299A}$ recruits GFP-Gpb2 to the plasma membrane (Figure 5). Similarly, $Gpa2^{\Delta\alpha\ (51-57)}$ also brought GFP-Gpb2 to the plasma membrane (Figure 5). Therefore, the sequence spanning amino acids 51–57, which is predicted to be an N-terminal alpha helical region, is not required for Gpa2-Gpb2 binding.

We next addressed whether other sequences in the Gpa2 N-terminal extension are required for Gpb2 interaction. For this purpose, deletions were introduced into the N-terminal region of the $GPA2^{G299A}$ allele to create Δ1–14, Δ1–29, Δ1–44, and Δ1–100 derivatives of $Gpa2^{G299A}$, which were also then fused to the first 10 amino acids from the *S. cerevisiae* Gα subunit Gpa1 that are sufficient for membrane localization (unpublished data; Gillen *et al.*, 1998). Internal deletions were also created (Δ16–84, Δ31–84, Δ46–84, and Δ46–100, Figure 5). This deletion mutant series was coexpressed with GFP-Gpb2 to examine which Gpa2 mutants are capable of recruiting GFP-Gpb2 to the plasma membrane (Figure 5). All deletions generated for this study (except for the Δ46–449 Gpa2 mutant) are predicted to have no significant impact on the secondary structure of Gpa2, based on PHD analysis, and the function and expression of these alleles of $GPA2^{G299A}$ were confirmed by introducing these alleles into wild-type diploid cells and examining pseudohyphal growth (unpublished data). All deletion constructs and representative results are shown in Figure 5.

GFP-Gpb2 did not associate with the plasma membrane when coexpressed with the Δ1–14, Δ1–29, Δ1–44, or Δ1–100 Gpa2 derivatives, indicating that the N-terminus of Gpa2 plays an important role in Gpb2 binding (Figure 5). However, the first 15 or 30 amino acids were not sufficient for Gpb2 binding because neither the Gpa2 Δ16–84 nor the Δ31–84 mutant was able to recruit Gpb2 to the plasma membrane. On the other hand, membrane localization of GFP-Gpb2 was observed when it was coexpressed with the Gpa2 Δ46–84 and Δ46–100 mutants. Taken together, these findings indicate that the first 45 amino acids are necessary for Gpb2 interaction. This N-terminal region alone (1–45 aa) was not sufficient because GFP-Gpb2 was cytoplasmic with the $Gpa2^{\Delta 46-449}$ variant. Structural analyses have revealed that Gβ binding interfaces are present not only in the N-terminus (the αN domain) but also in the central region (β2 to α2 domain) of conventional Gα molecules (Figure 1 and Lambright *et al.*, 1996; Wall *et al.*, 1998). Therefore, by analogy Gpa2 may also require the corresponding internal conserved region in conjunction with the N-terminal 1–45 aa to bind Gpb2, although we cannot exclude a possibility that the $Gpa2^{\Delta 46-449}$ variant failed to recruit Gpb2 to the plasma membrane because of instability. Note that the deletions examined were also introduced into a wild-type Gpa2 construct and tested for GFP-Gpb2 interaction as above, and results were essentially equivalent to the ones with the $Gpa2^{G299A}$ deletion variants with the minor difference that plasma membrane localization of GFP-Gpb2 was weaker when the wild-type Gpa2 deletion variant were coexpressed. This is consistent with the fact that $Gpa2^{G299A}$ binds to Gpb2 more strongly than does wild-type Gpa2 (Figure 4, Harashima and Heitman, 2002, 2004).

We next addressed regions of the Gpa2 molecule involved in association with the Gpr1 receptor. Previously, the Gpr1 C-terminal tail composed of 99 amino acids was isolated in a yeast two-hybrid screen that identified Gpa2 interacting proteins (Xue *et al.*, 1998). Because Gpr1 that is C-terminally

tagged with GFP is nonfunctional (unpublished data), likely because of interference with Gpr1-Gpa2 coupling, we fused GFP to the N-terminus of the 99 amino acid soluble C-terminal tail of Gpr1. The resulting GFP fusion protein (GFP-Gpr1C) was coexpressed with the $Gpa2^{G299A}$ variants to examine roles of the N-terminal extension on interactions with the coupled receptor Gpr1, as above (Figure 5, also see Figure 8).

As shown in Figure 5, any variant of Gpa2 lacking the first 15 amino acids failed to recruit GFP-Gpr1C to the plasma membrane ($Gpa2^{\Delta 1-14}$, $Gpa2^{\Delta 1-29}$, $Gpa2^{\Delta 1-44}$, and $Gpa2^{\Delta 1-100}$), whereas all of the variants containing amino acids 1–15 ($Gpa2^{\Delta 16-84}$, $Gpa2^{\Delta 31-84}$, $Gpa2^{\Delta 46-84}$, and $Gpa2^{\Delta 46-100}$) recruited GFP-Gpr1C, similar to full length $Gpa2^{G299A}$. The only exception was $Gpa2^{\Delta 46-449}$, which failed to recruit the GFP-Gpr1C to the plasma membrane. These observations indicate that the N-terminal region of Gpa2 participates in associating with the receptor C-terminal tail, but that C-terminal regions of Gpa2 likely also participate. Importantly, the C-terminal tail of other Gα subunits is known to be involved in receptor coupling (Slessareva *et al.*, 2003; Herrmann *et al.*, 2004). Consistent with this model, $Gpa2^{\Delta 1-100}$ still interacted with the C-terminal tail of Gpr1 in the yeast two-hybrid assay and Gpa2 function was perturbed by a C-terminal GFP tag (unpublished data). In summary, these data indicate that both the N-terminal and more C-terminal regions of the Gα protein Gpa2 are required for interactions with both Gpb2 and Gpr1.

Functional Roles of the Gpa2 N-terminus

To address roles of the Gpa2 amino terminus, N-terminal deletions were introduced into wild-type Gpa2. The resulting deletion alleles were expressed in diploid or haploid *gpa2* mutant cells to examine whether these mutants complement *gpa2* defects in pseudohyphal growth, invasive growth, and glucose-induced cAMP production (Figure 6). These mutant alleles were also introduced into diploid *gpr1 gpa2* mutant cells to examine whether they require Gpr1 for function or act as dominant alleles that bypass the receptor. Cells expressing $Gpa2^{\Delta 1-100}$ exhibited reduced pseudohyphal and invasive growth and reduced levels of basal and glucose-induced cAMP, indicating that the N-terminal region plays an important functional role or that deletion of the 1–100 amino acids might result in misfolding of Gpa2 (Figures 6). $Gpa2^{\Delta 46-84}$, $Gpa2^{\Delta 46-100}$, and $Gpa2^{\Delta\alpha\ (51-57)}$ all functioned as wild-type Gpa2, likely because Gpb2 and the C-terminal tail of Gpr1 still bind to these deletion proteins (Figure 6 and unpublished data). The Δ1–14, Δ1–29, Δ1–44, Δ16–84, or Δ31–84 *GPA2* mutant genes were largely able to complement *gpa2* mutant phenotypes. One interpretation of these results is that these deletion proteins still functionally interact with Gpr1 and Gpb2 via other Gpa2 domains and are capable of functioning, similar to wild-type Gpa2. Or expression of the deletion Gpa2 proteins from a multicopy plasmid might mask their reduced activity so that expression from a low copy plasmid could elicit altered mutant phenotypes. Alternatively, these results could be due to counterbalancing defects in Gpa2 interaction with Gpr1 and Gpb2 because Gpr1/Gpa2 and Gpb2 control the cAMP signaling pathway positively and negatively, respectively (see *Discussion*).

Kelch Gβ Mimic Proteins Gpb1/2 Function on the Plasma Membrane

Gpb2 is directed to the plasma membrane in a Gpa2 dependent manner, indicating that the kelch Gβ mimic proteins Gpb1/2 may function on the plasma membrane. To examine this hypothesis, the first 10 amino acids of Gpa2 (hereafter, the membrane localization sequence [MLS]) that suffice for membrane localization were fused to the N-terminus of the GFP-Gpb1 or GFP-Gpb2 protein. The resulting fusion proteins were tested for protein localization and complementation of the elevated filamentous phenotype of *gpb1,2* mutant cells (Figure 7). We also tested the effects of fusing a nuclear localization signal (NLS) from the SV40 T antigen to the N-terminus of the GFP-Gpb1 or GFP-Gpb2 protein (Figure 7).

The MLS- and NLS-fused GFP-Gpb1/2 proteins were predominantly localized to the plasma membrane and the nucleus, respectively (Figure 7A). Furthermore, the MLS-GFP-Gpb1/2 fusion proteins complemented the *gpb1,2* double mutant phenotype and restored wild-type pseudohyphal growth (Figure 7B). In contrast, the nuclear localized Gpb1/2 proteins (NLS-GFP-Gpb1/2) were nonfunctional (Figure 7B). These findings provide evidence that Gpb1/2 can function when heterologously targeted to the plasma membrane. These results also indicate that the as yet unidentified second target of Gpb1/2 might be membrane associated.

Kelch Gβ Mimic Proteins Gpb1/2 Inhibit Gpr1-Gpa2 Coupling

Gpa2 interacts with the C-terminal tail of the Gpr1 receptor and recruits the GFP-Gpr1 C-tail fusion protein to the plasma membrane. Here we used this assay to analyze Gpr1-Gpa2 coupling in further detail. GFP-Gpr1C is localized to the plasma membrane when coexpressed with the dominant negative $Gpa2^{G299A}$ allele. Additionally, membrane localization of GFP-Gpr1C was less pronounced when coexpressed with wild-type Gpa2, suggesting that the C-terminal tail of Gpr1 binds more strongly to $Gpa2^{G299A}$ compared to wild-type Gpa2 (Figure 8). On the other hand, interaction of Gpa2 with the C-terminal tail of Gpr1 was reduced even further with the dominant $Gpa2^{Q300L}$ allele (Figure 8). This is consistent with the widely accepted model in which the Gα-GDP complex binds to the cognate GPCR, whereas the Gα-GTP complex dissociates from the GPCR. To confirm the interaction between GFP-Gpr1C and Gpa2, the nonfunctional nuclear localized $Gpa2^{G2A}$-NLS was coexpressed with GFP-Gpr1C. In this case, GFP-Gpr1C was now misdirected to the nucleus (Figure 8).

Because Gpb2 is directed to the plasma membrane in a Gpa2-dependent manner and binds to the N-terminus of Gpa2 where the C-terminal tail of Gpr1 also binds, we hypothesized that Gpb1/2 could negatively regulate Gpa2 function by inhibiting the Gpr1-Gpa2 interaction. To address this hypothesis, the wild-type Gpb1/2 proteins were simultaneously coexpressed with the GFP-Gpr1C and $Gpa2^{G299A}$ proteins. As shown in Figure 8, the membrane localization of GFP-Gpr1 was significantly reduced by coexpression of Gpb1/2, indicating that Gpb1/2 compete with the C-terminal tail of Gpr1 for binding to the N-terminus of Gpa2. Gpb1/2 may thereby control Gpa2 function by impairing receptor coupling. This is in contrast to canonical Gβ subunits, which function to promote interactions of the Gα subunit with the associated GPCR.

DISCUSSION

The Roles of the N-terminal Region of Gpa2

The MG^2XXXS^6 sequence in open reading frames and the glycine residue of the consensus sequence are well defined as a myristoylation consensus sequence and the myristoyl-

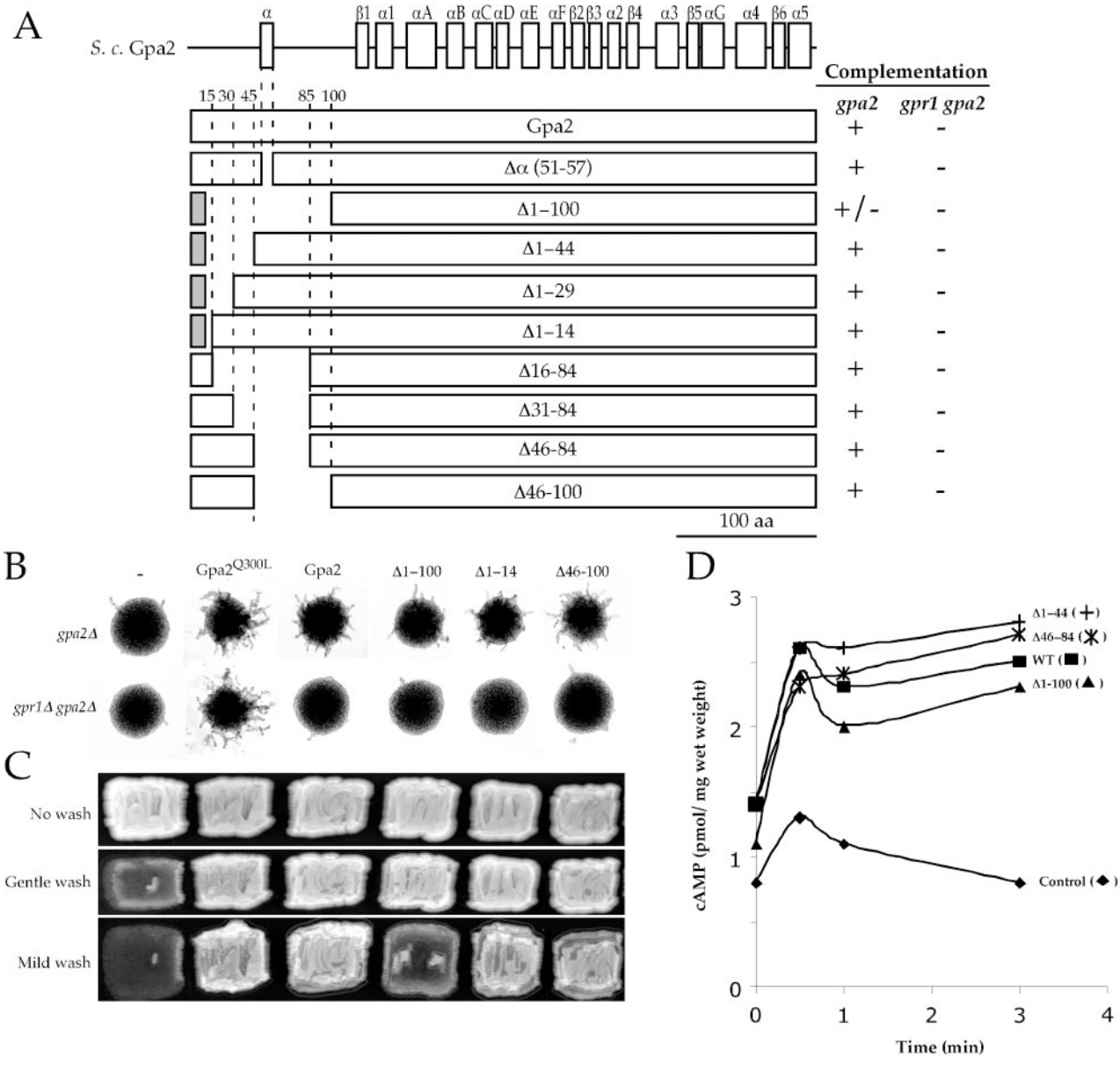

Figure 6. Function of the N-terminal deletion Gpa2 proteins in vivo. (A) Schematic of N-terminal deletion Gpa2 variants and complementation results in *gpa2* or *gpr1 gpa2* mutant cells. N-terminal deletions were created in the wild-type *GPA2* gene and introduced into *gpa2* (MLY132α for invasive growth assay and MLY132a/α for pseudohyphal growth assay) or *gpr1 gpa2* (MLY277a/α) mutant cells and ability to complement pseudohyphal and invasive growth defects was examined. Representative data are shown in B for pseudohyphal growth and in C for invasive growth. (D) Glucose-induced cAMP production in *gpa2* (MLY132α) mutant cells expressing the N-terminal deletion Gpa2 derivatives. The values shown are the mean of two independent experiments, except the control, which is representative of cells carrying the empty vector (pTH19).

ation site. On the other hand, no obvious consensus sequence is established for palmitoylation, yet palmitoylation mostly occurs in a cysteine residue(s) near the N-terminus. The Gα subunit Gpa2 contains the MG^{2}XXXS^6 myristoylation consensus sequence and a cysteine at the fourth position of its N-terminus. A cysteine after the N-terminal cysteine appears at the 189th position of the Gpa2 protein. Our biochemical studies revealed that Gpa2 is myristoylated and palmitoylated. Furthermore, the labeling and site-directed mutagenesis studies shown in Figure 2 provide evidence that Gpa2 is myristoylated at Gly^2 and, most likely, also palmitoylated at Cys^4.

Introduction of site-specific mutations (G2A, C4A, and S6Y) into the *GPA2* and *GPA2-GFP* fusion genes demonstrates that myristoylation and palmitoylation are critical for plasma membrane targeting and function of Gpa2. Although it still remains to be established why myristoylation is essential for Gα function, recent studies demonstrate that GPCR-Gα fusion proteins, in which Gα is localized to the plasma membrane yet no longer lipid modified, are functional in vivo (for review, see Seifert *et al.*, 1999). Furthermore, a nonmyristoylated Gαi2^{Q205L} protein is unable to signal and fails to transform rat fibroblasts (Gallego *et al.*, 1992). Consistently, we also found that a nonmyristoylated

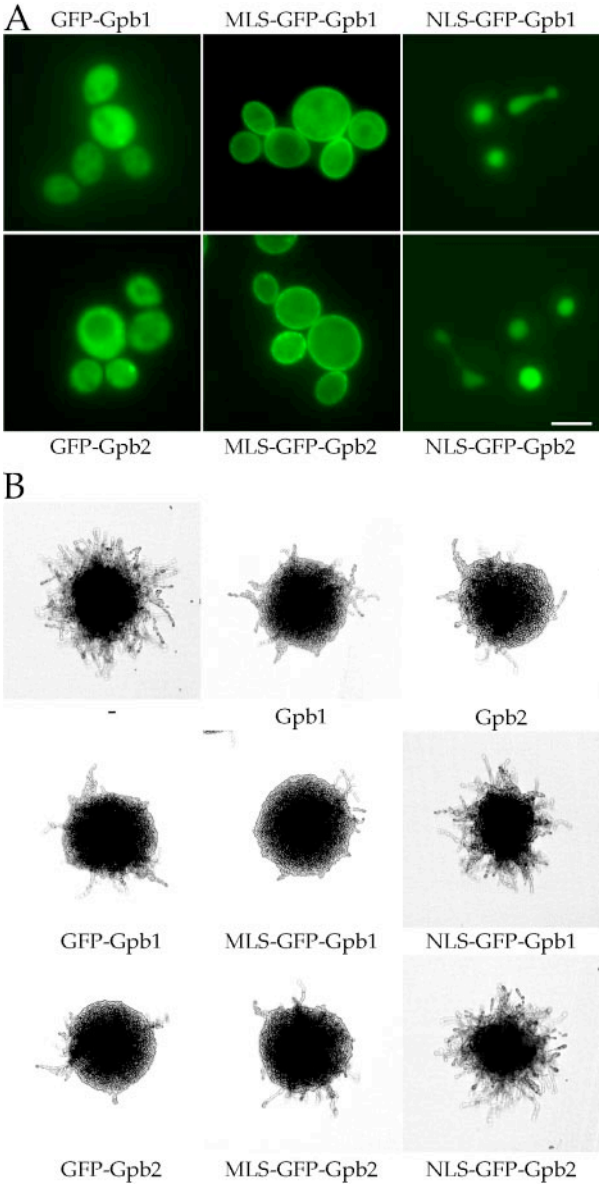

Figure 7. Kelch Gβ mimic proteins Gpb1/2 function on the plasma membrane. A membrane localization sequence (MLS) or nuclear localization signal (NLS) was fused to the N-terminus of the functional GFP-Gpb1/2 proteins (pTH106/pTH75) and the resulting fusion proteins (pTH163, pTH164, pTH166, or pTH167) were expressed in diploid *gpb1,2* double mutant cells (THY212a/α) to test for protein localization (A) and function (B). The MLS-GFP-Gpb1/2 fusion proteins were recruited to the plasma membrane and were as functional as the wild-type Gpb1/2 proteins, whereas the NLS-GFP-Gpb1/2 fusion proteins were directed to the nucleus and nonfunctional. Cells bearing the empty vector (pTH19) or the *GPB1* (pTH26) or *GPB2* (pTH27) plasmid served as controls. Scale bar, 5 μm.

dominant Gpa2^{Q300L} mutant (equivalent to Gαi2 Q205L) is incapable of enhancing filamentous growth in wild-type cells. These findings support a model in which lipid modifications are necessary for plasma membrane targeting that is a prerequisite for Gα function. Alternatively, myristoylation may play an important role in Gα structure that is required for receptor coupling (Preininger *et al.*, 2003).

In heterotrimeric G proteins, the N-terminus is also involved in interactions with G$\beta\gamma$ dimer, receptors, and effectors. Structural and biochemical studies implicate the N-terminal alpha helix (αN domain) in G$\beta\gamma$ dimer and receptor coupling (Lambright *et al.*, 1996; Wall *et al.*, 1998). Gpa2 contains an alpha helix in the extended N-terminus, yet the position of this helix is not conserved (Figure 1). More strikingly, the alpha helix is not involved in coupling to the kelch subunit Gpb2 or to the Gpr1 C-terminal tail. Studies using Gpa2 variants that carry a series of deletions in the Gpa2 N-terminus identified binding domains for the Gpr1 C-terminal tail and Gpb2 that map to amino acids 1–15 and 1–45 and are not predicted to form an alpha helix.

Lipid modifications alone are not sufficient to restore these interactions as the Gpa2 Δ1–14 mutant that is lipid modified on an appended Gpa1$^{1-10}$ peptide did not direct the binding partners to the plasma membrane. Rather, amino acid sequences that lie between residues 1–45 are important for the interactions. Interestingly, the non-alpha helical N-terminus (spanning amino acids 1–6) of Gαq is known to be involved in receptor selectivity (Kostenis *et al.*, 1997). Therefore, the N-terminus may play a direct role in receptor coupling by providing a binding interface or an indirect role by influencing overall structure. Either possibility is novel and further studies, especially structural studies, should address the role of the N-terminus of Gpa2.

The Role of the Gpr1 C-terminal Tail

Previous studies suggest the presence of preactivation complexes in which an unoccupied, inactive GPCR is coupled to the Gα subunit (Samama *et al.*, 1993; Stefan *et al.*, 1998; Dosil *et al.*, 2000). Such preactivation complexes are not necessarily required for formation of the activated ternary complex in which a ligand bound, activated receptor forms a complex with a G protein to stimulate GDP-GTP exchange on Gα, yet the preactivation complexes are involved in regulation of specificity and intensity of G-protein mediated signaling (Neubig, 1994; Shea and Linderman, 1997). In *S. cerevisiae*, the C-terminal tail of the α-factor receptor Ste2 is implicated in the formation of the preactivation complex with its associated Gα Gpa1 (Dosil *et al.*, 2000). Although no direct evidence has been reported for a preactivation complex between the Gpr1 receptor and Gpa2, our data support the existence of one. First, the cytoplasmic C-terminal tail of Gpr1 binds to wild-type Gpa2 and a nuclear localized Gpa2^{G2A}-NLS. Second, Gpr1 and Gpa2 are still functional in the absence of the Gβ mimic subunits Gpb1/2, suggesting a promiscuous coupling between Gpr1 and Gpa2.

These observations may be relevant to our finding that N-terminal deletion variants of Gpa2 (Δ1–14, Δ1–29, Δ1–44, and Δ1–100) that are unable to bind to the Gpr1 C-terminal tail are still functional and can respond to glucose to stimulate cAMP production. This interpretation may also explain why cells expressing these Gpa2 variants exhibited near wild-type phenotypes. It is conceivable that a reduced affinity of the Gpa2 variants with the Gpr1 receptor could result in a decrease in signaling leading to a low-PKA phenotype. However, these Gpa2 variants also show decreased binding to the kelch subunits Gpb1/2 that negatively control cAMP signaling, affecting Gpb1/2 function to activate the as yet unidentified second target that inhibits cAMP signaling.

Kelch Subunits Gpb1/2 Inhibit Gpr1-Gpa2 Coupling

G-protein activity is controlled at multiple steps including expression, protein localization, GDP-GTP exchange, and GTPase activity. GPCRs activate G proteins by stimulating GDP dissociation from Gα and acting as guanine nucleotide exchange factors, thereby leading to Gα in the active Gα-GTP form. On the other hand, the GoLoco family protein

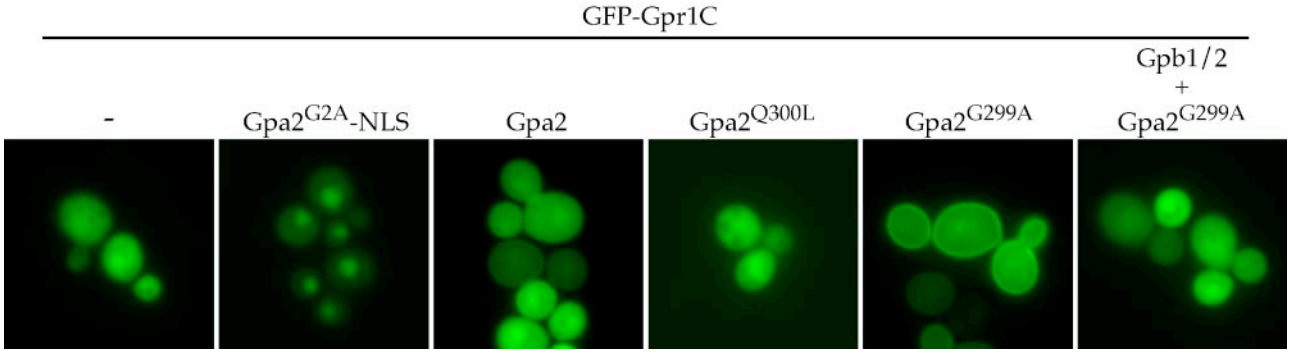

Figure 8. Kelch Gβ mimic proteins Gpb1/2 interfere with the interaction between Gpa2 and the C-terminal tail of Gpr1. (A) The GFP-Gpr1C fusion protein (pTH170) was expressed alone or coexpressed with Gpa2 variants, wild-type Gpa2 (pTH47), $Gpa2^{Q300L}$ (pTH48), $Gpa2^{G299A}$ (pTH49), or NLS-$Gpa2^{G2A}$ (pTH149) with or without Gpb1/2 (pTH174/pTH114) in wild-type cells (THY452). Empty vectors (pTH171 and pTH173) were used as controls for the Gpb1/2 plasmids, pTH174 and pTH114. The location of nuclei were confirmed by DAPI staining.

AGS3 functions as a guanine nucleotide dissociation inhibitor (GDI) by inhibiting GDP-GTP exchange (De Vries *et al.*, 2000). Although GoLoco homologues are conserved in multicellular eukaryotes, no such homolog is apparent in the yeast genome.

Our previous studies revealed that the kelch subunits Gpb1 and Gpb2 negatively control Gpa2 and preferentially associate with Gpa2-GDP (Harashima and Heitman, 2002). However, neither loss nor overexpression of Gpb1/2 perturbed Gpa2 membrane localization or expression. In addition, Gpb1/2 did not exhibit GDI activity under standard in vitro conditions (unpublished data). Here we show that Gpb1/2 inhibit Gpa2-Gpr1 coupling. A model governing how the kelch Gpb1/2 subunits control Gpa2 is that Gpb1/2 bind to the Gpa2 N-terminal region spanning amino acids 1–45 and occlude binding of the Gpr1 C-terminal tail to the first fifteen amino acids of Gpa2 (Figure 9).

In canonical heterotrimeric G proteins, Gβγ subunits are required for receptor-Gα coupling. In *S. cerevisiae*, the Gβγ dimer plays an essential role in pheromone receptor-Gα Gpa1 coupling (Blumer and Thorner, 1990). In mammalian systems, a role for the Gβγ subunits in coupling of β_2-adrenergic receptor-Gαs, M_2-muscarinic receptor-Gαo, A_1-adenosine and 5-HT_{1A} receptors-Gαi, and β_2-adrenergic re-

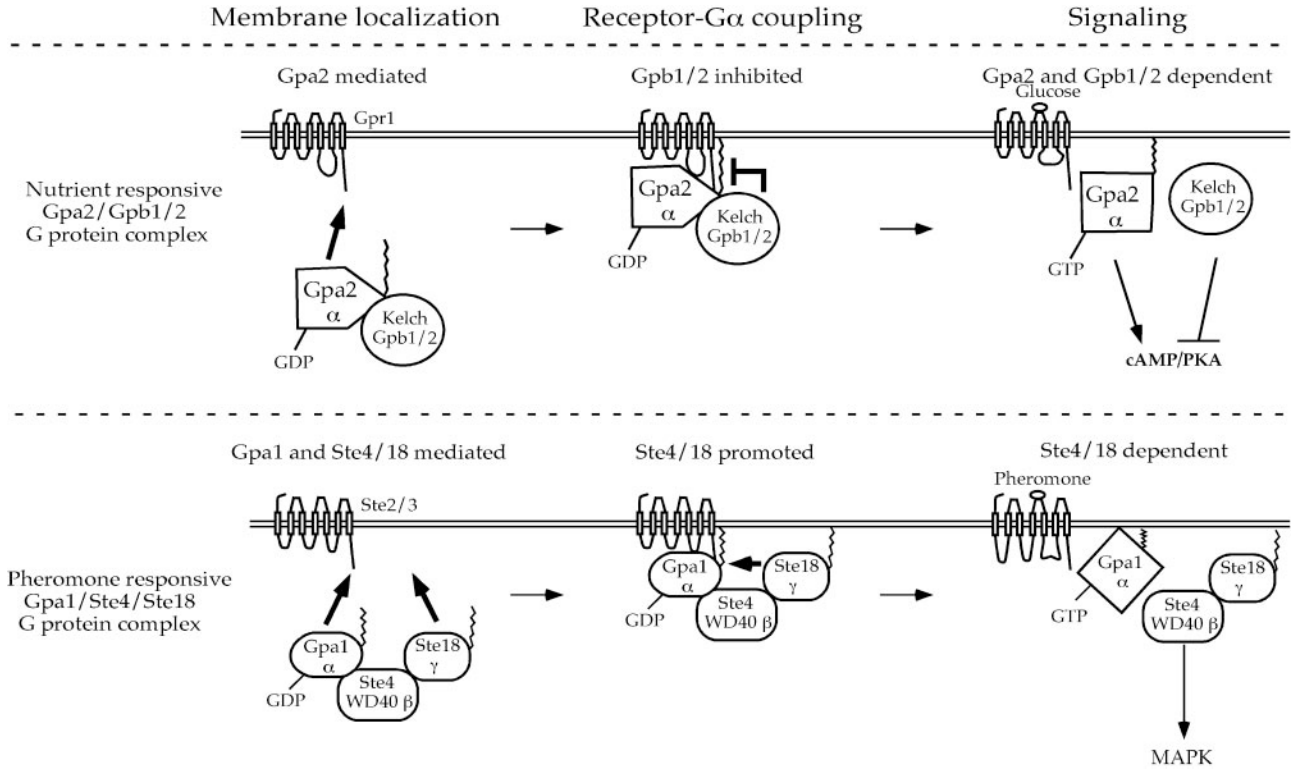

Figure 9. Model of canonical heterotrimeric and atypical G protein signaling in budding yeast. The canonical heterotrimeric G protein composed of the Gpa1/Ste4/Ste18 subunits regulates the pheromone responsive MAPK cascade, whereas the atypical heteromeric G protein consisting of the Gpa2/Gpb1/2 subunits controls the nutrient sensing cAMP-PKA signaling pathway. For details, see *Discussion*.

ceptor-Gαi has been established (Richardson and Robishaw, 1999; Hou *et al.*, 2001; Lim *et al.*, 2001; Kühn *et al.*, 2002). This function is opposite to the role of the kelch subunits, yet importantly, yeast and mammalian WD40 repeat Gβγ subunits and the kelch subunits all converge to modulate receptor-Gα coupling. That receptor-Gα coupling is oppositely regulated may depend on how tightly and specifically a given Gα binds to its associated receptor. In yeast, the pheromone receptor Ste2 is functionally coupled to the Gα protein Gpa1 and not to the Gpa2 Gα subunit (Blumer and Thorner, 1990). During diploid filamentation, the glucose receptor Gpr1 is associated with Gpa2 and not with the haploid specific Gα Gpa1. Importantly, the Gpa2 Gα subunit is still partially functional and able to signal in response to the agonist glucose via Gpr1 in the absence of Gpb1/2, suggesting that Gpa2 can functionally couple to its receptor in the absence of Gpb1/2 (Harashima and Heitman, 2002). Therefore, Gpa2 may normally be tightly associated with the Gpr1 receptor, and Gpb1/2 function to compete with this association to reduce signaling in the absence of glucose.

Generally, the intracellular third loop of GPCRs plays a crucial role in interactions with the Gα subunit. Although *S. cerevisiae* Gpa2 has been reported to interact with the intracellular third loop of Gpr1 in the yeast two-hybrid assay (Yun *et al.*, 1997), we were unable to recapitulate this result (unpublished data). This could be attributable to a weak interaction between Gpa2 and the third loop of Gpr1. In contrast, the Gpr1 C-terminal tail avidly binds to Gpa2 in two-hybrid assays (Yun *et al.*, 1997; Xue *et al.*, 1998; Kraakman *et al.*, 1999; Harashima and Heitman, 2002). We also showed that the Gpa2-Gpr1 C-terminal tail interaction can be detected using the GFP tagged C-terminal tail of Gpr1 in vivo (Figures 5 and 8). These data indicate that the Gpr1 C-terminus plays an important role in Gpa2 binding. This atypical feature of the Gpr1 receptor-Gpa2 Gα complex may mirror the unusual aspects by which the kelch subunits Gpb1/2 inhibit the signaling complex.

Is Gpa2 an Unusual Gα or an Ancestral Gα Subunit?

Our studies provide evidence that lipid modifications (myristoylation and palmitoylation) of Gα Gpa2 are necessary and sufficient for Gpa2 plasma membrane targeting but are not required for interaction with the kelch Gβ mimic subunit Gpb2. Instead, Gpa2 directs Gpb2 to the plasma membrane. Mammalian Gα subunits as well as the yeast canonical Gα subunit Gpa1 share similar features. Like Gpa2, lipid modifications but not the Gβγ dimer are required for plasma membrane localization of yeast Gpa1 and mammalian Gα (Song *et al.*, 1996; Gillen *et al.*, 1998; Galbiati *et al.*, 1999). It has also been reported that a nonlipidated Gα still binds to Gβγ subunits in yeast and mammals (Jones *et al.*, 1990; Degtyarev *et al.*, 1994; Song *et al.*, 1996). Studies also provide evidence that Gα, at least in part, directs Gβγ subunits to the plasma membrane in vivo (Song *et al.*, 1996; Takida and Wedegaertner, 2003). Although Gpa2 shares similar features with canonical Gα subunits, a striking contrast is the inability of Gpa2 to form a heterotrimeric G protein. The Gα subunit Gpa1 in the fission yeast *Schizosaccharomyces pombe*, which functions in pheromone-mediated signaling, also fails to form a heterotrimeric G protein with the known Gβγ subunits Git5/11. The kelch protein Ral2 has been proposed as a possible Gpa1-associated subunit based on genetic studies (Fukui *et al.*, 1989; Harashima and Heitman, 2002; Hoffman, 2005).

Another contrast between canonical Gα subunits and Gpa2 is that Gβγ subunits typically promote receptor-Gα coupling, whereas Gpb1/2 inhibit receptor-Gpa2 coupling (Figure 9). The receptor Gpr1 and Gα Gpa2 can still in part function and signal in response to glucose without the Gβ mimic subunits Gpb1/2, indicating a promiscuous and specific coupling between Gpr1 and Gpa2 even in the absence of Gpb1/2 (Harashima and Heitman, 2002). In *S. cerevisiae*, the cAMP-PKA signaling pathway is essential for cell growth and determines cell fates in response to extracellular nutrients (Harashima and Heitman, 2004). Therefore the cAMP-PKA signaling pathway should be strictly controlled, and for this reason, Gpb1/2 may interfere with promiscuous Gpr1-Gpa2 coupling to facilitate responses to extracellular nutrients. On the other hand, in canonical G proteins, the Gβγ dimer may control Gα function by increasing the specificity of receptor coupling (Richardson and Robishaw, 1999; Hou *et al.*, 2001; Lim *et al.*, 2001; Kühn *et al.*, 2002). Importantly, the kelch Gβ mimic subunits Gpb1/2 and canonical Gβγ dimer both regulate receptor-Gα coupling. Thus, the Gpa2/Gpb1/2 protein complex shares features with canonical heterotrimeric G proteins, and we propose Gpa2 is an ancestral subunit rather than an unusual Gα subunit. In this model, eukaryotic cells first acquired a GPCR and associated Gα subunit to sense and signal extracellular cues. Later, seven-bladed β-propeller-type subunits (kelch or WD40 based) were recruited to the GPCR-Gα signaling complex. Finally, farnesylated Gγ subunits were recruited to promote membrane localization. In this model, the atypical features of the nutrient and pheromone GPCR-Gα signaling modules in budding and fission yeasts might mirror features of their ancestral signaling modules from which they derive.

Alternatively, yeasts might uniquely have evolved an "alternative" Gα subunit and established a novel G protein signaling system to sense extracellular stimuli, in which an atypical Gα subunit forms a complex and functions with an unusual binding-partner kelch Gβ mimic protein. Further studies in both unicellular and multicellular organisms would distinguish these possibilities.

ACKNOWLEDGMENTS

We thank Sayoko Ito-Harashima for providing a yeast strain and Cristl Arndt and Emily Wenink for assistance. We also thank Yong-Sun Bahn, Alex Idnurm, Julian Rutherford, Chaoyang Xue, Andy Alspaugh, Pat Casey, Henrik Dohlman, and Bob Lefkowitz for critical reading. This study was supported by the Department of Defense Neurofibromatosis program (W81xwh-04-01-0208). T.H. was supported by a fellowship from the Children's Tumor Foundation and J.H. is an investigator of the Howard Hughes Medical Institute.

REFERENCES

Adams, J., Kelso, R., and Cooley, L. (2000). The kelch repeat superfamily of proteins: propellers of cell function. Trends Cell Biol. *10*, 17–24.

Arévalo-Rodríguez, M., and Heitman, J. (2005). Cyclophilin A is localized to the nucleus and controls meiosis in *Saccharomyces cerevisiae*. Eukaryot. Cell *4*, 17–29.

Ashrafi, K., Farazi, T. A., and Gordon, J. I. (1998). A role for *Saccharomyces cerevisiae* fatty acid activation protein 4 in regulating protein N-myristoylation during entry into stationary phase. J. Biol. Chem. *273*, 25864–25874.

Batlle, M., Lu, A. L., Green, D. A., Xue, Y., and Hirsch, J. P. (2003). Krh1p and Krh2p act downstream of the Gpa2p Gα subunit to negatively regulate haploid invasive growth. J. Cell Sci. *116*, 701–710.

Blumer, K. J., and Thorner, J. (1990). β and γ subunits of a yeast guanine nucleotide-binding protein are not essential for membrane association of the α subunit but are required for receptor coupling. Proc. Natl. Acad. Sci. USA *87*, 4363–4367.

Bourne, H. R. (1997). How receptors talk to trimeric G proteins. Curr. Opin. Cell Biol. *9*, 134–142.

Cabrera-Vera, T. M., Vanhauwe, J., Thomas, T. O., Medkova, M., Preininger, A., Mazzoni, M. R., and Hamm, H. E. (2003). Insights into G protein structure, function, and regulation. Endocr. Rev. *24*, 765–781.

Chen, C. A., and Manning, D. R. (2001). Regulation of G proteins by covalent modification. Oncogene *20*, 1643–1652.

Colombo, S. *et al.* (1998). Involvement of distinct G-proteins, Gpa2 and Ras, in glucose- and intracellular acidification-induced cAMP signalling in the yeast *Saccharomyces cerevisiae.* EMBO J. *17*, 3326–3341.

De Vries, L., Fischer, T., Tronchère, H., Brothers, G. M., Strockbine, B., Siderovski, D. P., and Farquhar, M. G. (2000). Activator of G protein signaling 3 is a guanine dissociation inhibitor for $G\alpha_i$ subunits. Proc. Natl. Acad. Sci. USA *97*, 14364–14369.

De Vries, L., and Gist Farquhar, M. (1999). RGS proteins: more than just GAPs for heterotrimeric G proteins. Trends Cell Biol. *9*, 138–144.

Degtyarev, M. Y., Spiegel, A. M., and Jones, T. L. (1994). Palmitoylation of a G protein α_i subunit requires membrane localization not myristoylation. J. Biol. Chem. *269*, 30898–30903.

Dohlman, H. G. (2002). G proteins and pheromone signaling. Annu. Rev. Physiol. *64*, 129–152.

Dohlman, H. G., and Thorner, J. W. (2001). Regulation of G protein-initiated signal transduction in yeast: paradigms and principles. Annu. Rev. Biochem. *70*, 703–754.

Dosil, M., Schandel, K. A., Gupta, E., Jenness, D. D., and Konopka, J. B. (2000). The C terminus of the *Saccharomyces cerevisiae* α-factor receptor contributes to the formation of preactivation complexes with its cognate G protein. Mol. Cell. Biol. *20*, 5321–5329.

Evanko, D. S., Thiyagarajan, M. M., and Wedegaertner, P. B. (2000). Interaction with $G\beta\gamma$ is required for membrane targeting and palmitoylation of $G\alpha_s$ and $G\alpha_q$. J. Biol. Chem. *275*, 1327–1336.

Farazi, T. A., Waksman, G., and Gordon, J. I. (2001). The biology and enzymology of protein *N*-myristoylation. J. Biol. Chem. *276*, 39501–39504.

Fishburn, C. S., Pollitt, S. K., and Bourne, H. R. (2000). Localization of a peripheral membrane protein: $G\beta\gamma$ targets $G\alpha_Z$. Proc. Natl. Acad. Sci. USA *97*, 1085–1090.

Fukui, Y., Miyake, S., Satoh, M., and Yamamoto, M. (1989). Characterization of the *Schizosaccharomyces pombe ral2* gene implicated in activation of the *ras1* gene product. Mol. Cell. Biol. *9*, 5617–5622.

Galbiati, F., Volonté, D., Meani, D., Milligan, G., Lublin, D. M., Lisanti, M. P., and Parenti, M. (1999). The dually acylated NH_2-terminal domain of $G_{i1\alpha}$ is sufficient to target a green fluorescent protein reporter to caveolin-enriched plasma membrane domains. Palmitoylation of caveolin-1 is required for the recognition of dually acylated G-protein α subunits *in vivo.* J. Biol. Chem. *274*, 5843–5850.

Gallego, C., Gupta, S. K., Winitz, S., Eisfelder, B. J., and Johnson, G. L. (1992). Myristoylation of the $G\alpha_{i2}$ polypeptide, a G protein α subunit, is required for its signaling and transformation functions. Proc. Natl. Acad. Sci. USA *89*, 9695–9699.

Gancedo, J. M. (2001). Control of pseudohyphae formation in *Saccharomyces cerevisiae.* Fems Microbiol. Rev. *25*, 107–123.

Gautam, N., Downes, G. B., Yan, K., and Kisselev, O. (1998). The G-protein $\beta\gamma$ complex. Cell Signal *10*, 447–455.

Gillen, K. M., Pausch, M., and Dohlman, H. G. (1998). N-terminal domain of Gpa1 (G protein α subunit) is sufficient for plasma membrane targeting in yeast *Saccharomyces cerevisiae.* J. Cell Sci. *111*, 3235–3244.

Gilman, A. G. (1987). G-Proteins: transducers of receptor-generated signals. Annu. Rev. Biochem. *56*, 615–649.

Guan, K. L., and Han, M. (1999). A G-protein signaling network mediated by an RGS protein. Genes Dev. *13*, 1763–1767.

Hamm, H. E., Deretic, D., Arendt, A., Hargrave, P. A., Koenig, B., and Hofmann, K. P. (1988). Site of G protein binding to rhodopsin mapped with synthetic peptides from the α subunit. Science *241*, 832–835.

Harashima, T., and Heitman, J. (2002). The Gα protein Gpa2 controls yeast differentiation by interacting with kelch repeat proteins that mimic Gβ subunits. Mol. Cell *10*, 163–173.

Harashima, T., and Heitman, J. (2004). Nutrient control of dimorphic growth in *Saccharomyces cerevisiae.* In: Topics in Current Genetics, Vol. 7, ed. J Winderickx and P. M. Taylor, Heidelberg: Springer-Verlag, 131–169.

Herrmann, R., Heck, M., Henklein, P., Henklein, P., Kleuss, C., Hofmann, K. P., and Ernst, O. P. (2004). Sequence of interactions in receptor-G protein coupling. J. Biol. Chem. *279*, 24283–24290.

Hoffman, C. S. (2005). Except in every detail: comparing and contrasting G-protein signaling in *Saccharomyces cerevisiae* and *Schizosaccharomyces pombe.* Eukaryot. Cell *4*, 495–503.

Hou, Y., Chang, V., Capper, A. B., Taussig, R., and Gautam, N. (2001). G Protein β subunit types differentially interact with a muscarinic receptor but not adenylyl cyclase type II or phospholipase C-β2/3. J. Biol. Chem. *276*, 19982–19988.

Ito, N., Phillips, S. E., Stevens, C., Ogel, Z. B., McPherson, M. J., Keen, J. N., Yadav, K. D., and Knowles, P. F. (1991). Novel thioether bond revealed by a 1.7 Å crystal structure of galactose oxidase. Nature *350*, 87–90.

Ito, N., Phillips, S.E.V., Yadav, K.D.S., and Knowles, P. F. (1994). Crystal structure of a free radical enzyme, galactose oxidase. J. Mol. Biol. *238*, 794–814.

Jeansonne, N. E. (1994). Yeast as a model system for mammalian seven-transmembrane segment receptors. Proc. Soc. Exp. Biol. Med. *206*, 35–44.

Johnson, D. R., Bhatnagar, R. S., Knoll, L. J., and Gordon, J. I. (1994). Genetic and biochemical studies of protein N-myristoylation. Annu. Rev. Biochem. *63*, 869–914.

Jones, T. L., Simonds, W. F., Merendino, J. J., Jr., Brann, M. R., and Spiegel, A. M. (1990). Myristoylation of an inhibitory GTP-binding protein α subunit is essential for its membrane attachment. Proc. Natl. Acad. Sci. USA *87*, 568–572.

Journot, L., Pantaloni, C., Bockaert, J., and Audigier, Y. (1991). Deletion within the amino-terminal region of $G_s\alpha$ impairs its ability to interact with $\beta\gamma$ subunits and to activate adenylate cyclase. J. Biol. Chem. *266*, 9009–9015.

Kostenis, E., Degtyarev, M. Y., Conklin, B. R., and Wess, J. (1997). The N-terminal extension of $G\alpha_q$ is critical for constraining the selectivity of receptor coupling. J. Biol. Chem. *272*, 19107–19110.

Kraakman, L., Lemaire, K., Ma, P. S., Teunissen, A.W.R.H., Donaton, M.C.V., Van Dijck, P., Winderickx, J., de Winde, J. H., and Thevelein, J. M. (1999). A *Saccharomyces cerevisiae* G-protein coupled receptor, Gpr1, is specifically required for glucose activation of the cAMP pathway during the transition to growth on glucose. Mol. Microbiol. *32*, 1002–1012.

Kübler, E., Mösch, H. U., Rupp, S., and Lisanti, M. P. (1997). Gpa2p, a G-protein α-subunit, regulates growth and pseudohyphal development in *Saccharomyces cerevisiae* via a cAMP-dependent mechanism. J. Biol. Chem. *272*, 20321–20323.

Kühn, B., Christel, C., Wieland, T., Schultz, G., and Gudermann, T. (2002). G-protein $\beta\gamma$-subunits contribute to the coupling specificity of the β_2-adrenergic receptor to G_s. Naunyn Schmiedebergs Arch. Pharmacol. *365*, 231–241.

Lambright, D. G., Sondek, J., Bohm, A., Skiba, N. P., Hamm, H. E., and Sigler, P. B. (1996). The 2.0 Å crystal structure of a heterotrimeric G protein. Nature *379*, 311–319.

Lefkowitz, R. J. (2000). The superfamily of heptahelical receptors. Nat. Cell Biol. *2*, E133–E136.

Lemaire, K., Van de Velde, S., Van Dijck, P., and Thevelein, J. M. (2004). Glucose and sucrose act as agonist and mannose as antagonist ligands of the G protein-coupled receptor Gpr1 in the yeast *Saccharomyces cerevisiae.* Mol. Cell *16*, 293–299.

Lengeler, K. B., Davidson, R. C., D'Souza, C., Harashima, T., Shen, W. C., Wang, P., Pan, X. W., Waugh, M., and Heitman, J. (2000). Signal transduction cascades regulating fungal development and virulence. Microbiol. Mol. Biol. Rev. *64*, 746–785.

Lim, W. K., Myung, C. S., Garrison, J. C., and Neubig, R. R. (2001). Receptor-G protein γ specificity: γ11 shows unique potency for A_1 adenosine and 5-HT_{1A} receptors. Biochemistry *40*, 10532–10541.

Linder, M. E., Pang, I. H., Duronio, R. J., Gordon, J. I., Sternweis, P. C., and Gilman, A. G. (1991). Lipid modifications of G protein subunits. Myristoylation of $G_{o\alpha}$ increases its affinity for $\beta\gamma$. J. Biol. Chem. *266*, 4654–4659.

Longtine, M. S., McKenzie III, A., Demarini, D. J., Shah, N. G., Wach, A., Brachat, A., Philippsen, P., and Pringle, J. R. (1998). Additional modules for versatile and economical PCR-based gene deletion and modification in *Saccharomyces cerevisiae.* Yeast *14*, 953–961.

Lorenz, M. C., and Heitman, J. (1997). Yeast pseudohyphal growth is regulated by GPA2, a G protein α homolog. EMBO J. *16*, 7008–7018.

Lorenz, M. C., Pan, X. W., Harashima, T., Cardenas, M. E., Xue, Y., Hirsch, J. P., and Heitman, J. (2000). The G protein-coupled receptor Gpr1 is a nutrient sensor that regulates pseudohyphal differentiation in *Saccharomyces cerevisiae.* Genetics *154*, 609–622.

Mombaerts, P. (2004). Genes and ligands for odorant, vomeronasal and taste receptors. Nat. Rev. Neurosci. *5*, 263–278.

Morales, J., Fishburn, C. S., Wilson, P. T., and Bourne, H. R. (1998). Plasma membrane localization of $G\alpha_z$ requires two signals. Mol. Biol. Cell *9*, 1–14.

Navon, S. E., and Fung, B. K. (1987). Characterization of transducin from bovine retinal rod outer segments. Participation of the amino-terminal region of T_α in subunit interaction. J. Biol. Chem. *262*, 15746–15751.

Neubig, R. R. (1994). Membrane organization in G-protein mechanisms. FASEB J. *8*, 939–946.

Pan, X., Harashima, T., and Heitman, J. (2000). Signal transduction cascades regulating pseudohyphal differentiation of *Saccharomyces cerevisiae.* Curr. Opin. Microbiol. *3*, 567–572.

Preininger, A. M., Van Eps, N., Yu, N. J., Medkova, M., Hubbell, W. L., and Hamm, H. E. (2003). The myristoylated amino terminus of $G\alpha_{i1}$ plays a critical role in the structure and function of $G\alpha_{i1}$ subunits in solution. Biochemistry *42*, 7931–7941.

Richardson, M., and Robishaw, J. D. (1999). The α_{2A}-adrenergic receptor discriminates between G_i heterotrimers of different $\beta\gamma$ subunit composition in Sf9 insect cell membranes. J. Biol. Chem. *274*, 13525–13533.

Rolland, F., de Winde, J. H., Lemaire, K., Boles, E., Thevelein, J. M., and Winderickx, J. (2000). Glucose-induced cAMP signalling in yeast requires both a G-protein coupled receptor system for extracellular glucose detection and a separable hexose kinase-dependent sensing process. Mol. Microbiol. *38*, 348–358.

Ross, E. M., and Wilkie, T. M. (2000). GTPase-activating proteins for heterotrimeric G proteins: Regulators of G protein signaling (RGS) and RGS-like proteins. Annu. Rev. Biochem. *69*, 795–827.

Rost, B., and Sander, C. (1993). Prediction of protein secondary structure at better than 70% accuracy. J. Mol. Biol. *232*, 584–599.

Samama, P., Cotecchia, S., Costa, T., and Lefkowitz, R. J. (1993). A mutation-induced activated state of the β_2-adrenergic receptor. Extending the ternary complex model. J. Biol. Chem. *268*, 4625–4636.

Schwartz, M. A., and Madhani, H. D. (2004). Principles of MAP kinase signaling specificity in *Saccharomyces cerevisiae.* Annu. Rev. Genet. *38*, 725–748.

Schwindinger, W. F., and Robishaw, J. D. (2001). Heterotrimeric G-protein $\beta\gamma$-dimers in growth and differentiation. Oncogene *20*, 1653–1660.

Seifert, R., Wenzel-Seifert, K., and Kobilka, B. K. (1999). GPCR-Gα fusion proteins: molecular analysis of receptor-G-protein coupling. Trends Pharmacol. Sci. *20*, 383–389.

Shea, L., and Linderman, J. J. (1997). Mechanistic model of G-protein signal transduction. Determinants of efficacy and effect of precoupled receptors. Biochem. Pharmacol. *53*, 519–530.

Sherman, F. (1991). Getting started with yeast. Methods Enzymol. *194*, 3–21.

Slessareva, J. E., Ma, H., Depree, K. M., Flood, L. A., Bae, H., Cabrera-Vera, T. M., Hamm, H. E., and Graber, S. G. (2003). Closely related G-protein-coupled receptors use multiple and distinct domains on G-protein α-subunits for selective coupling. J. Biol. Chem. *278*, 50530–50536.

Sondek, J., Bohm, A., Lambright, D. G., Hamm, H. E., and Sigler, P. B. (1996). Crystal structure of a G_A protein $\beta\gamma$ dimer at 2.1 Å resolution. Nature *379*, 369–374.

Song, J., and Dohlman, H. G. (1996). Partial constitutive activation of pheromone responses by a palmitoylation-site mutant of a G protein α subunit in yeast. Biochemistry *35*, 14806–14817.

Song, J., Hirschman, J., Gunn, K., and Dohlman, H. G. (1996). Regulation of membrane and subunit interactions by N-myristoylation of a G protein α subunit in yeast. J. Biol. Chem. *271*, 20273–20283.

Sprang, S. R. (1997). G protein mechanisms: Insights from structural analysis. Annu. Rev. Biochem. *66*, 639–678.

Stefan, C. J., Overton, M. C., and Blumer, K. J. (1998). Mechanisms governing the activation and trafficking of yeast G protein-coupled receptors. Mol. Biol. Cell *9*, 885–899.

Strader, C. D., Fong, T. M., Tota, M. R., Underwood, D., and Dixon, R. A. (1994). Structure and function of G protein-coupled receptors. Annu. Rev. Biochem. *63*, 101–132.

Takida, S., and Wedegaertner, P. B. (2003). Heterotrimer formation, together with isoprenylation, is required for plasma membrane targeting of G$\beta\gamma$. J. Biol. Chem. *278*, 17284–17290.

Tamaki, H., Miwa, T., Shinozaki, M., Saito, M., Yun, C. W., Yamamoto, K., and Kumagai, H. (2000). GPR1 regulates filamentous growth through *FLO11* in yeast *Saccharomyces cerevisiae.* Biochem. Biophys. Res. Commun. *267*, 164–168.

Thiyagarajan, M. M., Bigras, E., Van Tol, H. H., Hébert, T. E., Evanko, D. S., and Wedegaertner, P. B. (2002). Activation-induced subcellular redistribution of $G\alpha_s$ is dependent upon its unique N-terminus. Biochemistry *41*, 9470–9484.

Thompson, J. D., Higgins, D. G., and Gibson, T. J. (1994). CLUSTAL W: improving the sensitivity of progressive multiple sequence alignment through sequence weighting, position-specific gap penalties and weight matrix choice. Nucleic Acids Res. *22*, 4673–4680.

Wall, M. A., Coleman, D. E., Lee, E., Iñiguez-Lluhi, J. A., Posner, B. A., Gilman, A. G., and Sprang, S. R. (1995). The structure of the G protein heterotrimer $G_{i\alpha1\beta1\gamma2}$. Cell *83*, 1047–1058.

Wall, M. A., Posner, B. A., and Sprang, S. R. (1998). Structural basis of activity and subunit recognition in G protein heterotrimers. Structure *6*, 1169–1183.

Wedegaertner, P. B., Bourne, H. R., and von Zastrow, M. (1996). Activation-induced subcellular redistribution of $G_{s\alpha}$. Mol. Biol. Cell *7*, 1225–1233.

Wedegaertner, P. B., Chu, D. H., Wilson, P. T., Levis, M. J., and Bourne, H. R. (1993). Palmitoylation is required for signaling functions and membrane attachment of $G_q\alpha$ and $G_s\alpha$. J. Biol. Chem. *268*, 25001–25008.

Wilson, P. T., and Bourne, H. R. (1995). Fatty acylation of a_z. Effects of palmitoylation and myristoylation on α_z signaling. J. Biol. Chem. *270*, 9667–9675.

Wise, A., Grassie, M. A., Parenti, M., Lee, M., Rees, S., and Milligan, G. (1997). A cysteine-3 to serine mutation of the G-protein $G_{i1}\alpha$ abrogates functional activation by the α_{2A}-adrenoceptor but not interactions with the $\beta\gamma$ complex. Biochemistry *36*, 10620–10629.

Xue, Y., Batlle, M., and Hirsch, J. P. (1998). GPR1 encodes a putative G protein-coupled receptor that associates with the Gpa2p G_α subunit and functions in a Ras-independent pathway. EMBO J. *17*, 1996–2007.

Yamaguchi, Y., Katoh, H., and Negishi, M. (2003). N-terminal short sequences of α subunits of the G_{12} family determine selective coupling to receptors. J. Biol. Chem. *278*, 14936–14939.

Yun, C. W., Tamaki, H., Nakayama, R., Yamamoto, K., and Kumagai, H. (1997). G-protein coupled receptor from yeast *Saccharomyces cerevisiae.* Biochem. Biophys. Res. Commun. *240*, 287–292.

Yun, C. W., Tamaki, H., Nakayama, R., Yamamoto, K., and Kumagai, H. (1998). Gpr1p, a putative G-protein coupled receptor, regulates glucose-dependent cellular cAMP level in yeast *Saccharomyces cerevisiae.* Biochem. Biophys. Res. Commun. *252*, 29–33.

The kelch proteins Gpb1 and Gpb2 inhibit Ras activity via association with the *Saccharomyces cerevisiae* RasGAP neurofibromin homologs Ira1 and Ira2

Toshiaki Harashima[1, 3], Scott Anderson[2], John R. Yates III[2],

and Joseph Heitman[1, 4]

Department of Molecular Genetics and Microbiology[1]

Duke University Medical Center

Durham, NC 27710

The Scripps Research Institute[2]

La Jolla, CA 92037

[3]Present address, Division of Molecular Cell Biology,

National Institute for Basic Biology,

Nishigonaka 38, Myodaiji, Okazaki 444-8585 Aichi, Japan

[4]Corresponding author, 322 CARL Building, Research Drive

Phone: 919-684-2824

FAX: 919-684-5458

email: heitm001@duke.edu

Summary

The G protein coupled receptor (GPCR) Gpr1 and associated Gα subunit Gpa2 govern dimorphic transitions in response to extracellular nutrients by signaling coordinately with Ras to activate adenylyl cyclase in the yeast *Saccharomyces cerevisiae*. Gpa2 forms a protein complex with the kelch Gβ mimic subunits Gpb1/2, and previous studies demonstrate that Gpb1/2 negatively control cAMP-PKA signaling via Gpa2 and an unknown second target. Here we define these targets of Gpb1/2 as the yeast neurofibromin homologs, Ira1 and Ira2, which function as GTPase activating proteins of Ras. Gpb1/2 bind to a conserved C-terminal domain of Ira1/2, and loss of Gpb1/2 results in a destabilization of Ira1 and Ira2, leading to elevated levels of Ras2-GTP and unbridled cAMP-PKA signaling. Because the Gpb1/2 binding domain on Ira1/2 is conserved in the human neurofibromin protein, an analogous signaling network may contribute to the neoplastic development of neurofibromatosis type 1 (NF1).

Running Title, Stabilization of the RasGAP by kelch proteins

Introduction

Molecular switches composed of G-protein coupled receptors (GPCRs) and associated heterotrimeric G proteins transduce extracellular stimuli to intracellular signaling molecules including the ubiquitous second messenger cAMP. Canonical heterotrimeric G proteins consist of α, β, and γ subunits. Ligand binding induces conformational changes in the receptor, stimulating GDP to GTP exchange on the associated Gα subunits, leading to dissociation of the receptor-Gα subunit complex and release of the Gβγ dimer. Liberated Gα, Gβγ, or both signal via downstream effectors. Signal transduction is attenuated by either intrinsic or RGS stimulated GTP hydrolysis followed by reassociation of Gα-GDP with the Gβγ dimer (Cabrera-Vera et al., 2003; Dohlman et al., 1991; Gautam et al., 1998; Gilman, 1987; Ross and Wilkie, 2000).

The budding yeast *Saccharomyces cerevisiae* deploys two distinct GPCR-G protein signaling modules to sense pheromones and nutrients, respectively (Harashima and Heitman, 2004). One is haploid and mating-type specific and involves the pheromone receptors Ste2/3 coupled to the Gα subunit Gpa1 in a canonical heterotrimeric complex with the Gβγ subunits Ste4/18. In response to pheromone, the Gβγ Ste4/18 dimer dissociates from Gα Gpa1 and activates the pheromone responsive MAP kinase pathway to enable mating (Dohlman, 2002).

The second yeast GPCR signaling cascade involves the GPCR Gpr1, which is expressed in both haploid and diploid cells and activates the associated Gα subunit Gpa2 in response to glucose and structurally related sugars (Kraakman et al., 1999; Lemaire et al., 2004; Lorenz et al., 2000; Xue et al., 1998; Yun et al., 1998). Activated Gpa2 stimulates cAMP production by adenylyl cyclase and

engages the PKA signaling pathway (Colombo et al., 1998; Ivey and Hoffman, 2005; Lorenz and Heitman, 1997). In contrast to canonical Gα subunits, Gpa2 is unable to form a heterotrimeric G protein with the known Gβγ subunits Ste4/18. Instead, Gpa2 associates with two novel proteins, Gpb1 and Gpb2, which are functionally redundant, share ~35% sequence identity, and each contain seven kelch repeat motifs (Harashima and Heitman, 2002). In a striking example of convergent evolution, both the WD-40 repeat based Gβ subunits and the kelch repeat enzyme galactose oxidase are known to fold into seven bladed beta propeller structures that are essentially superimposable (Ito et al., 1991; Ito et al., 1994; Lambright et al., 1996; Sondek et al., 1996).

Mutants lacking the Gpr1 receptor or the coupled Gα subunit Gpa2 are defective in glucose induced cAMP production and filamentous growth, whereas *gpb1,2* double mutants exhibit increased PKA phenotypes, including enhanced filamentous growth, sensitivity to nitrogen starvation and heat shock, and impaired glycogen accumulation and sporulation (Batlle et al., 2003; Harashima and Heitman, 2002). Introduction of *gpa2* mutations only partially attenuates these *gpb1,2* mutant phenotypes, providing evidence that Gpb1/2 negatively regulate cAMP signaling by inhibiting Gpa2 and an as yet unidentified second target. Mutation of the gene encoding one of the three PKA catalytic subunits, Tpk2, largely suppresses the elevated PKA phenotypes of *gpb1,2* mutants, indicating that this second target may be a component of the cAMP signaling pathway itself (Harashima and Heitman, 2002). Our recent studies provide evidence that Gpb1/2 are recruited to and function at the plasma membrane in a

Gpa2-dependent manner, suggesting that the unidentified second target may be membrane-associated (Harashima and Heitman, 2005).

In *S. cerevisiae*, the cAMP-PKA signaling cascade is essential for cell viability. Loss of either adenylyl cyclase (Cyr1) or all three PKA catalytic subunits (Tpk1,2,3) is lethal (Toda et al., 1988; Toda et al., 1987b). On the other hand, elevated PKA activity as a consequence of mutations in the PKA regulatory subunit Bcy1 results in a growth defect (Toda et al., 1987a). Therefore, cAMP signaling must be strictly controlled in response to extracellular cues. Previous studies have defined two distinct pathways that converge on adenylyl cyclase, namely the Gpr1-Gpa2 and Ras mediated pathways. Notably, *ras2* mutants fail to produce cAMP in response to glucose, similar to *gpr1* and *gpa2* mutants, and *gpr1 ras2* and *gpa2 ras2* mutants exhibit a synthetic growth defect, suggesting that Gpr1-Gpa2 and Ras2 play a shared role in glucose-induced cAMP production (Bhattacharya et al., 1995; Colombo et al., 2004, Kübler et al., 1997; Jiang et al., 1998; Xue et al., 1998).

S. cerevisiae expresses two Ras proteins: Ras1 and Ras2 (Kataoka et al., 1984; Powers et al., 1984). Although Ras1 and Ras2 are functionally redundant for cell growth, Ras2 plays the predominant role in cAMP signaling in response to glucose. Ras activity is controlled positively by the guanine nucleotide exchange factors Cdc25 and Sdc25 (GEFs) and negatively by the GTPase activating proteins Ira1 and Ira2 (GAPs) (Chevallier-Multon et al., 1993; Crechet et al., 1990; Lai et al., 1993; Munder and Furst, 1992; Tanaka et al., 1991; Tanaka et al., 1990a). Ras2 is known to bind to and activate adenylyl cyclase, yet how Ras2 regulates adenylyl cyclase in response to glucose is not understood at a molecular level (Crechet et al., 2000; Field et al., 1988; Mintzer and Field, 1994;

Mintzer and Field, 1999; Shima et al., 2000). Previous studies have implicated Cdc25 in responses to glucose (Gross et al., 1999; Munder and Kuntzel, 1989; Portillo and Mazon, 1986). On the other hand, Ira1 has been shown to interact with adenylyl cyclase and may promote its membrane localization (Mitts et al., 1991). *ira1,2* double mutant cells exhibit constitutively elevated cAMP levels and are unable to further mount a cAMP increase in response to glucose (Colombo et al., 2004). Therefore, both Cdc25 and Ira1/2 may coordinately activate Ras2 and adenylyl cyclase in response to glucose.

The RasGAP Ira1/2 proteins are large (~350 kD) GTPase-activating proteins that are conserved from yeast to humans (Tanaka et al., 1989; Tanaka et al., 1990b). In humans, the RasGAP activity of the Ira1/2 homolog neurofibromin is implicated in one of the most common genetic diseases, neurofibromatosis type I (NF1) (Ballester et al., 1990; Cawthon et al., 1990; Viskochil et al., 1990; Wallace et al., 1990; Xu et al., 1990a). Although the *IRA1*, *IRA2*, and *NF1* genes were cloned more than a decade ago, how the RasGAP activity of these proteins is controlled is largely unknown. Here we identified the yeast neurofibromin homologs Ira1/2 as targets of the kelch Gβ mimic subunits Gpb1/2. Gpb1/2 bind to a conserved C-terminal domain, stabilize Ira1/2, and thereby serve to govern cAMP-PKA signaling by constraining Ras2-GTP excursions. These findings have profound potential implications for our understanding of NF1 functions in normal cell growth control and its dysregulation in individuals with NF1.

Results

Kelch Gβ mimic proteins act upstream of the PKA pathway

Our previous studies support models in which the kelch Gβ mimic subunits Gpb1/2 act as negative regulatory elements early in the PKA pathway in conjunction with the Gα protein Gpa2 and a second target (Harashima and Heitman, 2002). Gpb1/2 physically and functionally interact with Gpa2, which functions early in the PKA pathway, and we considered that the second target might be either an early or a later component of the cascade. Here epistasis analysis was used to pinpoint the site of Gpb1/2 action. *gpa2* mutations exhibit a slow growth phenotype in combination with *ras2* mutations, and this growth defect can be mitigated by provision of cAMP, providing evidence that the two play a shared role in regulating adenylyl cyclase (Kübler et al., 1997; Lorenz and Heitman, 1997; Xue et al., 1998). In models in which Gpb1/2 function downstream of adenylyl cyclase, *gpb1,2* mutations would be predicted to rescue the growth defect of *ras2 gpa2* double mutant cells. To test this hypothesis, two diploid mutant strains (*gpa2*/*gpa2 ras2*/*RAS2* and *gpb1,2*/*gpb1,2 gpa2*/*GPA2 ras2*/*ras2*) were constructed, sporulated, and dissected. As shown in Figure 1A, *gpb1,2 ras2 gpa2* cells were as growth impaired as *ras2 gpa2* cells, providing evidence that Gpb1/2 instead act early in the pathway via adenylyl cyclase or one of its regulatory elements such as Ras1/2, Cdc25, or Ira1/2.

To examine genetic interactions between *gpb1,2* and *ras2* mutations, the *RAS2* gene was deleted in *gpb1,2* double mutant cells and the resulting *gpb1,2 ras2* cells were tested for filamentous growth, *FLO11* expression, sensitivity to nitrogen starvation, and glycogen accumulation (Figure 1B-F). Consistent with

our previous findings, *gpb1,2* mutants exhibited elevated pseudohyphal and invasive growth, increased *FLO11* expression, sensitivity to nitrogen starvation, and reduced glycogen accumulation. Introduction of a *gpa2* mutation partially suppressed these *gpb1,2* mutant phenotypes (Figure 1 and (Harashima and Heitman, 2002). On the other hand, introduction of a *ras2* mutation more completely suppressed these *gpb1,2* mutant phenotypes. Steady state and glucose-induced cAMP levels were also determined (Figure 1G). As shown previously (Harashima and Heitman, 2002), an increased basal level of cAMP was observed in *gpb1,2* mutant cells, and this elevated cAMP level was restored to the wild-type level by a *ras2* mutation (Figure 1G). Introduction of a *ras1* mutation was unable to suppress any of the *gpb1,2* mutant phenotypes (data not shown). Taken together, these genetic studies support the hypothesis that Gpb1/2 act directly on Ras2 or one of its regulators such as the RasGEF Cdc25 or the RasGAP Ira1/2 proteins.

RasGAP proteins Ira1/2 interact with the kelch Gβ mimic subunits Gpb1/2

Possible targets of Gpb1/2 were identified by mass spectrometry analysis of the Gpb1/2 native protein complex. For this purpose, the FLAG epitope tag was fused to the carboxy terminus of Gpb1 and to the amino terminus of Gpb2. These FLAG tagged Gpb1/2 proteins were expressed from an attenuated *ADH1* promoter on a 2 μm plasmid (see Materials and Methods). Expression of the FLAG tagged proteins restored wild-type filamentous growth of the *gpb1,2* double mutant strain, indicating that both fusion proteins are functional (data not shown). Because endogenous Gpa2 and Gpb1/2 may compete for Gpb1/2

with other targets, the FLAG-tagged Gpb1/2 proteins were expressed in *gpa2 gpb1,2* triple mutant cells. Crude cellular extracts were prepared, and Gpb1/2 and interacting proteins were co-immunoprecipitated using an anti-FLAG affinity matrix. The native protein complexes were eluted with FLAG peptide and the eluted proteins were analyzed by mass spectrometry (see Materials and Methods).

This analysis revealed a number of candidate Gpb1/2 interacting proteins. Importantly, the list of Gpb2 interacting proteins included the RasGAP proteins Ira1 and Ira2 and no other components of the cAMP-PKA signaling cascade (including Cdc25, Ras1, Ras2, Cyr1, Pde1, Pde2, Bcy1, Tpk1, Tpk2, Tpk3, Flo8, or Sfl1) were identified (data not shown). Because Gpb1 and Gpb2, and also Ira1 and Ira2, represent partially redundant protein pairs, we hypothesized that Gpb1 and Gpb2 might bind to both Ira1 and Ira2. To address this possibility, Gpb1 was N-terminally tagged, expressed, and Gpb1/2-Ira1/2 interactions were examined in cells that also expressed a functional version of the Ira1 or Ira2 protein fused with three copies of the hemagglutinin epitope tag (3HA) (Figure 2). Importantly, this co-immunoprecipitation analysis revealed that Gpb1 and Gpb2 both interact with both Ira1 and Ira2 (Figures 2A and B).

The Gpb1 and Gpb2 proteins contain a unique N-terminal domain and a C-terminal domain containing seven kelch repeats. Our previous studies revealed that the kelch domains of Gpb2 bind to Gpa2 but the unique N-terminal domain does not (Harashima and Heitman, 2002). To examine which domain(s) is required for the Gpb1/2-Ira1/2 interaction, the FLAG tag was fused to either the N-terminus of the N-terminal unique domain (FLAG-Gpb2N) or to the C-terminal kelch domain (FLAG-Gpb2C), and the resulting fusion proteins and the

FLAG tagged full-length Gpb2 fusion protein (FLAG-Gpb2) were co-expressed with the Ira1-3HA protein in vivo (Figure 2C). In contrast to the Gpa2-Gpb1/2 interaction, neither the Gpb2 N-terminal nor the C-terminal domain alone was sufficient to bind to Ira1. Therefore, both Gpb2 domains are required for interaction with Ira1. We note that the unique N-terminal and the C-terminal kelch domains are both essential for Gpb1/2 function in vivo (Harashima and Heitman, 2002).

Because the *gpb1,2* mutant phenotypes were suppressed by *ras2* mutations and Gpb1/2 bind to the RasGAP proteins Ira1/2, Gpb1/2 could associate with Ira1/2 and function via Ras2. However, Gpb1/2 interacted with Ira1/2 in the absence of Ras2 as strongly as in the presence of Ras2 (Figure 2D). Therefore, Ras2 is dispensable for the Gpb1/2-Ira1/2 interactions and Gpb1/2 may control Ras activity through direct interaction with Ira1/2.

GPB1,2 genetically interact with IRA1,2, RAS2, and GPA2

ras2 mutants are defective in filamentous growth whereas wild-type cells expressing a dominant active $RAS2^{G19V}$ allele that lacks intrinsic GTPase activity exhibit elevated filamentous growth. Consistent with these findings was the observation that cells lacking the RasGAP Ira1, Ira2, or both Ira1 and Ira2 were also hyperfilamentous (Figure 3A). Importantly, *ira1,2* double mutant cells expressing Gpb1/2 and *ira1,2 gpb1,2* quadruple mutant cells lacking Gpb1/2 were morphologically indistinguishable from each other. These findings support models in which the hyperfilamentous phenotype conferred by the *gpb1,2* mutations may be exerted via Ira1/2.

Expression of the dominant active *GPA2*^{Q300L} and *RAS2*^{G19V} alleles dramatically enhances filamentous growth of wild-type cells (Figure 3B). In contrast, little if any further effect was observed when these dominant active mutant alleles were expressed in the hyperfilamentous *gpb1,2* double mutant, supporting models in which Gpa2 and Ras2 are activated by the *gpb1,2* mutations and Gpb1/2 function to negatively control the activity of both (Figure 3B).

If Gpb1/2 regulate the Ira1/2 RasGAP proteins, and the hyperfilamentous phenotype of the *gpb1,2* mutant is due to reduced Ira1/2 activity, increased expression of the *IRA2* gene should suppress the *gpb1,2* mutant phenotype. In fact, overexpression of the *IRA2* gene attenuated pseudohyphal differentiation of the *gpb1,2* mutant (Figure 3C).

Consistently, neither loss of the *IRA1/2* genes nor introduction of the *RAS2*^{G19V} gene exaggerated mutant phenotypes (including hyperinvasion, nitrogen starvation sensitivity, and decreased glycogen) associated with an elevated PKA activity in *gpb1,2* mutant cells (Figures 3D-F). On the other hand, overproduction of Ira2 was able to alleviate these *gpb1,2* mutant phenotypes (Figure 3D-F). In addition, the increased basal and glucose induced cAMP levels in *gpb1,2* mutant cells were significantly attenuated by Ira2 overproduction (Figure 3G).

In summary, these genetic data provide evidence that the Gpb1/2 kelch proteins negatively control cAMP signaling via the RasGAP proteins Ira1/2.

Gpb1/2 control Ira1/2 RasGAP activity

Biochemical and genetic data indicate that the RasGAP Ira1/2 proteins represent secondary targets of the kelch Gβ mimic proteins and that Gpb1/2

function to enhance Ira1/2 activity. To investigate this at a mechanistic level, we quantified Ras2-GTP levels by measuring Ras2 protein binding to the Raf1 kinase that specifically interacts with Ras-GTP (Colombo et al., 2004; de Rooij and Bos, 1997). In this assay, the Ras binding domain (RBD) from Raf1 is fused to gluthathione-S-transferase, allowing capture of Ras-GTP and detection following immunoprecipitation (see Materials and Methods). A low copy number plasmid carrying the wild-type *RAS2* or dominant active $RAS2^{G19V}$ gene was introduced into wild-type, *gpb1,2*, *ira1*, *ira2*, and *ira1,2* mutant strains. Transformants were grown in synthetic medium to mid-logarithmic growth phase and crude cell extracts were prepared to assess the steady state levels of Ras2-GTP.

As shown previously, the Ras-GTP level was increased ~5-fold in *ira1* and *ira2* single mutant cells, (Figure 4A and Tanaka et al., 1990a). Similarly, *gpb1,2* mutant cells also exhibited an ~5 fold increase in Ras2-GTP levels, indicative of reduced RasGAP activity (Figure 4A). The Ras-GTP level in *ira1,2* double mutant cells were further increased and comparable to that in wild-type and *gpb1,2* mutant cells expressing the $RAS2^{G19V}$ gene, in which an approximately 25-fold increase in Ras-GTP was observed (Figure 4A). These observations are in accord with the previous finding documenting that Ras2-GTP levels were indistinguishable between wild-type and *ira1,2* double mutant cells when the $RAS2^{G19V}$ gene was expressed (Tanaka et al., 1990a). In summary, loss of Gpb1/2 results in an elevation of Ras2-GTP, possibly by reducing but not eliminating the RasGAP activity of Ira1/2.

Kelch subunits control levels of the RasGAP Ira1/2 proteins

To elucidate how the kelch Gβ subunits Gpb1/2 control Ira1/2 RasGAP activity, we investigated the levels of the Ira1/2 proteins as well as Ira1/2-Ras2 interactions in the presence and absence of Gpb1/2. To examine protein levels, the functional 3HA epitope tagged Ira1 and Ira2 proteins were expressed. Neither Ira1 nor Ira2 was detectable by western blot analysis using crude cell extracts because of low expression levels (data not shown). The 3HA tagged Ira1/2 proteins were therefore enriched by immunoprecipitation using anti-HA conjugated agarose beads, which also enabled an examination of the levels of the Ras2 protein bound to the Ira1/2-3HA affinity captured proteins (Figure 4B).

As shown in Figure 4B, loss of Gpb1/2 resulted in a marked decrease in the levels of both Ira1 and Ira2 and a concomitant loss of Ras2 as an Ira1/2 interacting protein. Reintroduction of the wild-type *GPB1* and *GPB2* genes complemented this defect and restored the levels of Ira1/2 to the wild-type levels, indicating that the Gβ mimic kelch subunits Gpb1/2 govern the stability of the RasGAP Ira1/2 proteins.

To confirm this model, protein stability of Ira1/2 was examined in the presence and absence of Gpb1/2 by a pulse-chase analysis (Figure 4C and D). The protein synthesis inhibitor cycloheximide was added to logarithmically growing cells that express the 3HA-tagged Ira1 or Ira2 at a final concentration of 50 μg/ml. In wild-type cells, Ira1/2 and Fpr1 proteins were stable over time and the half life ($t_{1/2}$) of these proteins was more than 4 hr ($t_{1/2}$>4 hr, Figure 4C and D and data not shown). Similarly, the Fpr1 protein in *gpb1,2* double mutant cells was as stable as in wild-type cells (Figure 4C and D and data not shown).

However, levels of the Ira1/2 proteins decreased rapidly, and the half life of Ira1 and Ira2 was reduced to approximately 30 and 20 min, respectively (Figure 4C and D). Therefore, we conclude that Gpb1/2 bind to and stabilize Ira1/2 and that loss of Gpb1/2 leads to reduced Ira1/2 protein levels.

Gpb1/2 stabilize Ira1/2 by binding to a C-terminal domain

To establish how Gpb1/2 control stability of the Ira1/2 proteins, the Gpb1/2 binding domain on Ira1/2 was identified. For this purpose, deletions were created in the endogenous Ira1 C-terminus by inserting a 3HA epitope tagged form of Ira1 and expressing these deletion derivatives in an otherwise wild-type background (Figure 5, Δ2926~3092, Δ2715~3092, Δ2433~3092, and Δ1258~3092). Plasmids expressing the FLAG-Gpb1/2 proteins were then introduced into the resulting Ira1 deletion mutant cells and Gpb1/2-Ira1 interactions were examined by FLAG mediated co-immunoprecipitation (Figure 5A and B). As mentioned above, the endogenous low abundance Ira1/2 proteins were first captured using anti-HA conjugated agarose beads and protein levels were then determined by subsequent western blot with anti-HA antibody (indicated as "Input" in Figure 5B).

By western blot analysis the level of the C-terminally truncated 1~2925 aa Ira1 protein was significantly reduced and the shorter 1~2714 aa and 1~2432 aa Ira1 variant proteins were undetectable in this assay (Figure 5A and "Input" panel in Figure 5B). Because Gpb1/2 control the stability of the Ira1/2 proteins, deletion of a Gpb1/2 binding site should result in a decrease in Ira1/2 protein levels. Thus, we hypothesized that the Gpb1/2 binding site might be present in

the C-terminal region of Ira1 necessary for Ira1 stability. In fact, Gpb1/2 bound to the Ira1 deletion protein retaining residues 1-2925 but not to the derivative containing only residues 1~1257 (Figure 5A and "Co-IP" panel in Figure 5B). Furthermore, two N-terminal deletion derivatives that retain amino acid residues 2433~3092 and 2715~3092 were stably expressed and both associated with Gpb1/2 (Figure 5C). A C-terminal region spanning amino acids 2715~2925 of Ira1 also bound to Gpb1/2 (Figure 5D), and loss of this region resulted in instability of this Ira1 deletion derivative (Figure 5A, data not shown). Taken together, these results reveal that the Gpb1/2 binding domain (GBD) maps between amino acids 2715~2925 of Ira1. Significantly, this region is conserved in homologs of Ira1, including the human neurofibromin protein NF1 (see discussion).

Equivalent deletions were also introduced into Ira2 (Supplemental Figure 1). The level of the Ira2 C-terminal deletion protein retaining amino acids 1~2922 was reduced, and this Ira2 deletion derivative was still able to interact with Gpb1/2 (Supplemental Figures 1A and B). An Ira2 variant that preserves amino acids 1~2702 but not the GBD was now undetectable (Supplemental Figure 1B). These findings are similar to the equivalent Ira1 deletion proteins (1~2925 aa and 1~2702 aa) (Figure 5). Both Gpb1 and Gpb2 bind to Ira2 deletion derivatives retaining amino acids 2703~3079 and 2703~2922 that are homologous to the regions spanning the corresponding amino acids 2715~3092 and 2715-2925 of Ira1 (Supplemental Figure 1C and D). These results provide evidence that the GBD maps to the corresponding regions of both Ira1 and Ira2.

The C-terminus of Ira1/2 is required for function

Biochemical studies reveal that deletion of the C-terminal 167 amino acids and deletion of the C-terminal 378 amino acids or the GBD in the Ira1 protein reduce and abolish protein stability, respectively. To test for a physiological relevance of these results, homozygous diploid cells that express these Ira1 C-terminal deletions (Δ2926~3092, Δ2715~3092, and ΔGBD) were constructed and assessed for pseudohyphal differentiation (Figure 6A). Haploid cells that carry these Ira1 C-terminal deletions were also tested for invasive growth, nitrogen starvation sensitivity, and glycogen accumulation (Figures 6B-D). Cells expressing the truncated Ira1 derivative that contains amino acids 1~2925 and also includes the GBD exhibited significantly increased filamentous growth, sensitivity to nitrogen starvation, and decreased glycogen (Figure 6). Cells expressing the shorter Ira1 derivatives that lack the GBD (1~2714 aa or ΔGBD) were markedly hyperfilamentous and phenotypically indistinguishable from *gpb1,2* or *ira1* null mutant cells (Figure 6). Therefore, the GBD and the extreme C-terminal region are both involved in protein stability and physiological functions of the Ira1 protein.

Discussion

Kelch Gpb1/2 proteins stabilize the RasGAP proteins Ira1/2

The central finding of our study is the discovery that the activity of the yeast RasGAP neurofibromin homologs Ira1/2 is controlled by two novel components of the GPCR-Gα signaling module, the kelch Gβ mimic proteins Gpb1 and Gpb2. Our studies provide the first evidence that Gpb1/2 bind to and control the stability of the neurofibromin homologs Ira1 and Ira2 and thereby affect intracellular Ras-GTP levels. In conjunction with their role in binding the Gpa2-GDP complex and inhibiting receptor-Gα coupling, Gpb1/2 serve as potent molecular brakes to constrain signaling via the PKA signaling pathway during both vegetative growth and dimorphic transitions (Figure 7).

Deletion analysis enabled the definition of two C-terminal domains involved in the protein stability of Ira1/2. Namely, the Gpb1/2 binding domain (GBD) spanning amino acids 2715~2925 in Ira1 and the corresponding region in Ira2 (amino acids 2703~2922 aa) and the more extreme C-terminal region of Ira1/2 that is unique to the yeast proteins (Figure 5 and Supplemental Figure 1). The two domains have an additive effect, because the Ira1/2 C-terminally truncated proteins lacking the yeast specific domain were still detectable, yet deletions eliminating both domains or the GBD alone resulted in undetectable levels of the Ira1/2 C-terminal deletion variants (1~2714 aa Ira1 and 1~2702 aa Ira2). Consistent with this, Ira1/2 protein levels were significantly reduced in *gpb1,2* double mutants compared with those in wild-type cells (Figures 4B and 5 and Supplemental Figure 1). Therefore, two distinct mechanisms appear to govern the stability of Ira1/2. Importantly, Ira1 was found to be ubiquitinated in

a proteomic analysis of membrane-associated proteins (Hitchcock et al., 2003). This finding indicates that Ira1/2 protein stability might be controlled by a ubiquitin/proteasome dependent mechanism as neurofibromin (see below), and Gbp1/2 could inhibit Ira1/2 ubiquitination or interactions with the proteasome and thereby stabilize Ira1/2. Further studies will be required to elucidate in further detail the molecular mechanisms by which the yeast neurofibromin homologs Ira1/2 are stabilized. These would also shed light on how RasGAP activity of neurofibromin is controlled in response to extracellular stimuli (see below).

Interestingly, in previous studies a transversion mutation resulting in a premature nonsense codon at the 2700th amino acid was identified in Ira2, truncating the penultimate 222 amino acids including the Gpb1/2 binding domain and resulting in a loss of Ira2 function (Halme et al., 2004). These studies provide complementary support for our finding that the C-terminal domain of Ira1/2 is critical for biological function. Importantly, the role of the GBD is also likely to be conserved in the human neurofibromin because the GBD is conserved among the yeast and mammalian neurofibromin homologs. Therefore, our findings should shed light on how the GAP activity of the neurofibromin homologs is controlled and its dysregulation in the ontogeny of neurofibromatosis type 1 (see below).

The RasGAP proteins Ira1 and Ira2 share ~45% sequence similarity and are functionary redundant, yet each may also play specific roles in Ras regulation. First, *ira1,2* double mutants exhibit more severe phenotypes compared to each single mutant. For instance, *ira1,2* double mutants exhibit an increased sensitivity to heat shock, enhanced filamentous growth, and increased Ras-GTP

levels compared to *ira1* or *ira2* single mutants (Figure 3, Tanaka et al., 1990b; Tanaka et al., 1990a). Second, overproduction of the *IRA2* gene is able to suppress the heat shock sensitivity of the *ira1,2* double mutants but overexpression of the *IRA1* gene does not (Tanaka et al., 1990b). Similarly, we note that overexpression of *IRA2* suppresses the *gpb1,2* double mutant phenotype, whereas overexpression of *IRA1* does not (data not shown, Figure3). Third, *ira1* mutations suppress the lethality of *cdc25* mutations more efficiently than *ira2* mutations (Tanaka et al., 1990b). Therefore, Ira1 and Ira2 may be controlled by both common and specific regulators. Indeed, Tfs1, which is a member of the phosphatidylethanolamine-binding protein family and known as a cytoplasmic inhibitor CPY, specifically binds to and inhibits Ira2, although the mechanisms by which Tfs1 controls RasGAP activity of Ira2 remain unclear (Chautard et al., 2004). Further studies will be required to elucidate a regulatory role for Tfs1 in Ira2 RasGAP activity.

Gpb1/2 link signaling from the Gα subunit Gpa2 to Ras

Our studies demonstrate that a central molecular link between the GPCR Gpr1-Gα Gpa2 signaling module and Ras is exerted via the RasGAP Ira1/2. Our recent studies demonstrate that Gpb1/2 preferentially bind to the GDP bound form of Gpa2 (Harashima and Heitman, 2002, Figure 7). More recently, we found that Gpb1/2 are recruited to the plasma membrane in a Gpa2 dependent manner and function to inhibit coupling between the Gpr1 receptor and Gpa2 (Figure 7, Harashima and Heitman 2005). We hypothesize that the following molecular events transpire when the ligand glucose binds to the Gpr1 receptor

(Figure 7). First, GDP-GTP exchange occurs on Gpa2 and Gpb1/2 dissociate from Gpa2-GTP. Next, Gpa2-GTP stimulates cAMP production via adenylyl cyclase and the liberated Gpb1/2 subunits then interact with and stabilize the Ira1/2 proteins. On the other hand, Ras is also activated in response to glucose by Cdc25 mediated GDP-GTP exchange reaction. The Gpb1/2-bound and stabilized RasGAP proteins Ira1/2 now bind to Ras-GTP and stimulate GTP hydrolysis, attenuating Ras mediated activation of adenylyl cyclase. These mechanisms provide the cell with an elaborate and balanced regulatory network that constrains cAMP signaling within a tightly controlled physiological range. In this model, the kelch proteins Gpb1/2 play a dual inhibitory role to inhibit receptor-Gα coupling and to extinguish signaling by Ras-GTP via their action to stabilize and thereby promote the activity of the RasGAP proteins Ira1/2.

A recent report has suggested that Gpb1/2 might act late in the PKA pathway to regulate signaling, possibly via direct actions on the protein kinase A catalytic or regulatory subunit or on a protein phosphatase that impinges on PKA (Lu and Hirsch, 2005). While such a model is conceivable, no direct evidence linking Gpb1 or Gpb2 to either PKA subunits or candidate regulators was presented, and the sole evidence upon which the model is based is a very modest shift in the concentration at which cellular growth of *gpb1,2 cyr1 pde2* mutant cells is rescued by exogenous cAMP (from 1.5 to 0.75 mM cAMP); *cyr1 pde2* mutant cells are able to grow in the presence of exogenous cAMP at a final concentration of 1.5 mM but not at 0.75 mM. This evidence would appear to be insufficient to conclude that the actions of Gpb1/2 must be exerted in an adenylyl cyclase independent fashion. Instead, our genetic and physical evidence presented here support a model in which Gpb1 and Gpb2 instead

directly impinge upon an early component in the PKA signaling pathway, namely the neurofibromin homologs Ira1 and Ira2. In addition, simultaneous loss of Gpb1 and Gpb2 was unable to suppress the growth defect of *gpa2 ras2* double mutant cells (Figure 1A). However, given the complex nature of the PKA signaling cascade, one idea in which these two apparently conflicting models might be reconciled would be to consider that the signaling cascade might exist as a supramolecular complex, in which it might be difficult to assign a strictly linear signaling pathway. Given the size of the Ira1/2 proteins, it would not be surprising if these were to act as scaffolds for PKA signaling via interactions with Ras, Gpb1/2, and other signaling components. In such a model, Gpb1/2 might exert regulatory roles at multiple steps in the cascade. Further studies will be required to elucidate the potent inhibitory action of the kelch proteins Gpb1 and Gpb2 on the PKA signaling pathway.

A yeast model for neurofibromatosis type 1

Neurofibromatosis type 1 (NF1) is an autosomal dominant disorder that occurs in approximately one in every 3,500 newborn infants and is one of the most common genetic disorders afflicting humans. Mutations in the *NF1* gene result in pleiotropic manifestations that include learning disabilities, small stature, bony abnormalities, and benign neurofibromas involving peripheral nerves. In some cases, NF1 patients present with malignant tumors involving peripheral nerve sheath tumors, optic gliomas, or the hematopoietic system (for reviews, see Dasgupta and Gutmann, 2003; Parada, 2000; Zhu and Parada, 2002).

The human Ira1/2 homolog neurofibromin is a large protein (~ 300 kD) that shares sequence identity with members of the RasGAP family, including

p120GAP, and *Drosophila* NF1 (Buchberg et al., 1990; Cawthon et al., 1990; Marchuk et al., 1991; Wallace et al., 1990; Xu et al., 1990b). The RasGAP activity of neurofibromin has a pivotal role in Ras-dependent NF1 development because expression of the GAP related domain (GRD) of neurofibromin can alleviate these *NF1*$^{-/-}$-deficient phenotypes (DeClue et al., 1992; Hiatt et al., 2001).
In addition to regulating Ras activity, neurofibromin also governs G protein-mediated adenylyl cyclase activity in the fruit fly *Drosophila melanogaster* to control learning and memory, neuropeptide responses, and regulation of body size (Guo et al., 1997; Guo et al., 2000; Hannan et al., 2006; The et al., 1997; Tong et al., 2002). Expression of a human *NF1* transgene complements the phenotypes in *NF1*$^{-/-}$ flies associated with an adenylyl cyclase defect (Tong et al., 2002). Similarly, neurofibromin controls adenylyl cyclase activity in response to the neuropeptide PACAP in mammals (Dasgupta et al., 2003; Tong et al., 2002). Therefore, neurofibromin governs adenylyl cyclase activity not only in yeast but also in flies and in mammals. Importantly, the yeast RasGAP protein Ira1 binds to adenylyl cyclase and this interaction plays a crucial role in adenylyl cyclase activation (Mitts et al., 1991). Because heterologous expression of the GAP related domain (GRD) from mammalian neurofibromin rescues yeast *ira1* and *ira2* mutant phenotypes (Ballester et al. 1989; Ballester et al. 1990; Martin et al. 1990; Tanaka et al. 1990a; Xu et al. 1990a), the yeast RasGAPs Ira1 and Ira2 are structural and functional counterparts of mammalian neurofibromin and play key conserved roles in regulating both Ras and adenylyl cyclase.

Our studies identified the GBD in the C-terminal region of the yeast Ira1/2 proteins; importantly this region is conserved in the fly and mammalian neurofibromin homologs (2247~2417 aa in human NF1, Figure 7)). Analysis of

the mutational spectra in the *NF1* gene from NF1 patients reveals that many mutations lie downstream of the GRD and many missense, frameshift, nonsense, and splice site mutations map near or even within the GBD homologous region (Ars et al., 2003; Fahsold et al., 2000; Origone et al., 2002). These downstream mutations presumably leave the GRD functional but may affect protein stability of neurofibromin and lead to the development of NF1. Importantly, recent studies provide evidence that neurofibromin stability is controlled via proteolysis by a ubiquitin/proteasome system (Cichowski et al., 2003). Mammalian cells express a myriad of kelch repeat proteins and most of these remain to be characterized at a functional level. In many previous examples, signaling precedents established first in yeast were later found to also operate in multicellular eukaryotes. Our studies suggest that kelch repeat proteins related to Gpb1/2 may play an analogous role in controlling neurofibromin stability and signaling in flies and humans and might therefore provide clues to understand how NF1 develops and stimulate the development of novel therapeutic interventions.

Materials and Methods

Strains, Media, and Plasmids

Media and standard yeast experimental procedures were as described (Sherman, 1991). A heterozygous diploid *gpb1,2::loxP/gpb1,2::loxP gpa2::loxP-G418/GPA2 ras2::nat/ras2::nat* strain was isolated following a cross between stains THY387a and THY389α. Plasmids pTH109 (*3HA-loxP-nat*, C-terminal tag), pMA-FLAG-kanMX (*FLAG-G418*, C-terminal tag, Arevalo-Rodriguez and Heitman, 2005), and pFA6a-3HA-kanMX6 (3HA-G418, C-terminal tag, Longtine et al., 1998) and pTH153 (*loxP-hph-3HA*, N-terminal tag) were used as substrates for PCR to introduce C-terminal and N-terminal epitope tags, respectively. Plasmids pTH110 (*loxP-nat*), pUG6 (*loxP-G418*, Güldener et al., 1996), pFA6-kanMX2 (*G418*, Wach et al., 1994), pAG25 (*nat*, Goldstein and McCusker, 1999), and pAG32 (*hph*, Goldstein and McCusker, 1999) served as substrates to amplify gene deletion cassettes. The Cre-loxP system was employed to eliminate the dominant drug cassettes from loxP cassettes (Güldener et al., 1996). Yeast strains and plasmids used in this study are summarized in Supplemental Tables 1 and 2.

Phenotypic analysis

Pseudohyphal and invasive growth assays, sensitivity to nitrogen starvation, glycogen accumulation, northern analysis, and cAMP assay were conducted as described previously (Harashima and Heitman, 2002).

Preparation of crude cell extracts

Total cell extracts from yeast cells that were grown to mid-log phase (OD600 ≅ 0.8) in YPD or synthetic drop-out media were prepared in lysis buffer (50 mM HEPES (pH 7.6), 120 mM NaCl, 0.3% CHAPS, 1 mM EDTA, 20 mM NaF, 20 mM β-glycerophosphate, 0.1 mM Na-orthovanadate, 0.5 mM DTT, protease inhibitors (Calbiochem, cocktail IV), and 0.5 mM PMSF) using a bead-beater. After centrifugation (25,000 Xg, 20 min), protein concentrations of crude extracts were determined by the Bradford or BCA method. Equal amounts of crude extracts were subjected to immunoprecipitation or SDS-PAGE and western analysis.

Immunoprecipitation

HA tagged Ira1/2 proteins were captured using anti-HA agarose beads (F-7, Santa Cruz Biotechnology). The beads were then washed three times with lysis buffer, once with PBS, and once with elution buffer (50 mM HEPES (pH 7.6), 100 mM KCl, 1 mM EDTA, 20 mM β-glycerophosphate, 0.5 mM DTT, protease inhibitors (Calbiochem, cocktail IV), and 0.5 mM PMSF) for 5 min each. After washing, the immunoprecipitated proteins were eluted by the addition of HA peptide (Roche) at a final concentration of ~800 μg/ml in elution buffer with incubation for 30 min at 30°C. FLAG tagged proteins were immunoprecipitated using anti-FLAG M2 affinity gel (SIGMA), the beads were washed, and protein complexes were then eluted by incubating for 30 min at room temperature with FLAG peptide at a final concentration of ~500 μg/ml in elution buffer. The eluted proteins were denatured in SDS sample buffer and run in a 3-8% Tris-acetate or 4-20% Tris-glycine gradient gel (Invitrogen) and subjected to western

analysis using anti-HA (F-7 or Y-11, Santa Cruz Biotechnology) and anti-FLAG M2 antibodies (SIGMA). Endogenous Ras2 protein levels were analyzed using an anti-Ras2 antibody (yC-19, Santa Cruz Biotechnology). The Fpr1 protein served as a loading control and was examined using a polyclonal anti-Fpr1 antibody (Harashima and Heitman, 2002).

Mass spectrometry

The eluted protein samples were TCA precipitated, washed with acetone, resuspended in Tris buffer, 8 M urea, pH 8.6, reduced with 100 mM TCEP, and alkylated with 55 mM iodoacetamide. Trypsin digestion was performed in the presence of 1 mM $CaCl_2$ to enhance specificity. Peptide mixtures were separated by strong cation exchange (SCX) and reversed-phase chromatography (RP) by using a triphasic (RP/SCX/RP) column made from 15 cm of fused silica (360 microns (OD) x 100 micron (ID)). Peptides were eluted from the initial reversed-phase material using a 60 minute 0-80% gradient of 80% acetonitrile in 0.1% formic acid. Peptides were eluted with the following steps of 500 mM ammonium acetate bumps: 25%, 35%, 50%, 80%, and 100% from the SCX phase. Each salt elution was followed by a 90 minute gradient of 0-80% of 80% acetonitrile in 0.1% formic acid. Tandem mass spectra were collected using an LCQ Deca tandem mass spectrometer (ThermoElectron, Inc, San Jose CA) following the method of Washburn *et al*. (2001). Tandem mass spectra of peptides were searched through the *S. cerevisiae* database NCBI using the algorithm SEQUEST™ (Eng et al., 1994). Database searching results were analyzed using the program DTA Select and with the following filtering parameters for cross correlation scores 1.8 (+1), 2.8 (+2), and 3.5 (+3) (Tabb et al.,

2002; Washburn et al., 2001). Identities of specific bands were confirmed by visual inspection of tandem mass spectra to confirm and verify sequence assignment. Sequence assignments to specific spectra are checked by visual inspection of the quality of the match between tandem mass spectrum and sequence. A FLAG tagged GFP protein (pTH100) served as a mock control.

Ras-GTP detection

Total cellular extracts were prepared as above and employed for co-immunoprecipitation using a GST fused Ras binding domain (RBD) from the Raf1 kinase that preferentially binds to Ras-GTP (EZ-DETECT Ras activation kit, PIERCE Biotechnology). Experimental procedures were followed as manufacturer's instructions. Briefly, cellular extracts were mixed with the GST-Raf1-RBD and an immobilized glutathione disk (resin) to capture Ras2-GTP and incubated at 4°C. After 1 hr, the Ras2-GTP captured resin was washed, and bound Ras2-GTP was eluted by boiling in SDS sample buffer. Eluted samples that were prepared from *ira1,2* mutant cells expressing the wild-type Ras protein and wild-type and *gpb1,2* mutant cells expressing the dominant active Ras2 ($Ras2^{G19V}$) protein were 5-fold diluted and subjected to western analysis. Ras2-GTP and cellular Ras2 levels were determined densitometrically. The amount of Ras2-GTP was normalized to the amount of input Ras protein and compared to the levels present in wild-type cells.

Cycloheximide-chase assay

Cycloheximide (CHX) was added to exponentially growing cells at a final concentration of 50 μg/ml to inhibit de novo protein synthesis. At the time

points indicated, cells were collected and washed. Total cell extracts were prepared and subjected to immunoprecipitation for Ira1/2 or SDS-PAGE for Fpr1 as above.

Acknowledgments

We thank Akio Toh-e for providing a plasmid and Cristl Arndt and Emily Wenink for assistance. We also thank Julian Rutherford, Chaoyang Xue, and Yong-Sun Bahn for critical reading and Andy Alspaugh, Henrik Dohlman, Bob Lefkowitz, and Pat Casey for encouragement. We are indebted to Yoshinori Ohsumi for his tremendous support during the revision of this manuscript. This study was supported by Neurofibromatosis program of the Department of Defense (W81xwh-04-01-0208). Toshiaki Harashima was supported by a fellowship from the Children's Tumor Foundation and Joseph Heitman was an investigator of the Howard Hughes Medical Institute. Funding from the National Institute of Health (P41 RR11823-10) to JRY is gratefully acknowledged.

References

Arevalo-Rodriguez, M., and Heitman, J. (2005). Cyclophilin A is localized to the nucleus and controls meiosis in *Saccharomyces cerevisiae*. Eukaryot Cell *4*, 17-29.

Ars, E., Kruyer, H., Morell, M., Pros, E., Serra, E., Ravella, A., Estivill, X., and Lázaro, C. (2003). Recurrent mutations in the *NF1* gene are common among neurofibromatosis type 1 patients. J Med Genet *40*, e82.

Ballester, R., Marchuk, D., Boguski, M., Saulino, A., Letcher, R., Wigler, M., and Collins, F. (1990). The *NF1* locus encodes a protein functionally related to mammalian GAP and yeast *IRA* proteins. Cell *63*, 851-859.

Ballester, R., Michaeli, T., Ferguson, K., Xu, H. P., McCormick, F., and Wigler, M. (1989). Genetic analysis of mammalian GAP expressed in yeast. Cell *59*, 681-686.

Batlle, M., Lu, A. L., Green, D. A., Xue, Y., and Hirsch, J. P. (2003). Krh1p and Krh2p act downstream of the Gpa2p Gα subunit to negatively regulate haploid invasive growth. J Cell Sci *116*, 701-710.

Bhattacharya, S., Chen, L., Broach, J. R., and Powers, S. (1995). Ras membrane targeting is essential for glucose signaling but not for viability in yeast. Proc Natl Acad Sci U S A *92*, 2984-2988.

Buchberg, A. M., Cleveland, L. S., Jenkins, N. A., and Copeland, N. G. (1990). Sequence homology shared by neurofibromatosis type-1 gene and *IRA-1* and *IRA-2* negative regulators of the *RAS* cyclic AMP pathway. Nature *347*, 291-294.

Cabrera-Vera, T. M., Vanhauwe, J., Thomas, T. O., Medkova, M., Preininger, A., Mazzoni, M. R., and Hamm, H. E. (2003). Insights into G protein structure, function, and regulation. Endocr Rev *24*, 765-781.

Cawthon, R. M., Weiss, R., Xu, G. F., Viskochil, D., Culver, M., Stevens, J., Robertson, M., Dunn, D., Gesteland, R., O'Connell, P., and et al. (1990). A major segment of the neurofibromatosis type 1 gene: cDNA sequence, genomic structure, and point mutations. Cell *62*, 193-201.

Chautard, H., Jacquet, M., Schoentgen, F., Bureaud, N., and Bénédetti, H. (2004). Tfs1p, a member of the PEBP family, inhibits the Ira2p but not the Ira1p Ras GTPase-activating protein in *Saccharomyces cerevisiae*. Eukaryot Cell *3*, 459-470.

Chevallier-Multon, M. C., Schweighoffer, F., Barlat, I., Baudouy, N., Fath, I., Duchesne, M., and Tocque, B. (1993). *Saccharomyces cerevisiae* Cdc25 (1028-1589) is a guanine nucleotide releasing factor for mammalian ras proteins and is oncogenic in NIH3T3 cells. J Biol Chem *268*, 11113-11118.

Cichowski, K., Santiago, S., Jardim, M., Johnson, B. W., and Jacks, T. (2003). Dynamic regulation of the Ras pathway via proteolysis of the NF1 tumor suppressor. Genes Dev *17*, 449-454.

Colombo, S., Ma, P. S., Cauwenberg, L., Winderickx, J., Crauwels, M., Teunissen, A., Nauwelaers, D., de Winde, J. H., Gorwa, M. F., Colavizza, D., and Thevelein, J. M. (1998). Involvement of distinct G-proteins, Gpa2 and Ras, in glucose- and intracellular acidification-induced cAMP signalling in the yeast *Saccharomyces cerevisiae*. EMBO J *17*, 3326-3341.

Colombo, S., Ronchetti, D., Thevelein, J. M., Winderickx, J., and Martegani, E. (2004). Activation state of the Ras2 protein and glucose-induced signaling in *Saccharomyces cerevisiae*. J Biol Chem *279*, 46715-46722.

Crechet, J. B., Jacquet, E., Bernardi, A., and Parmeggiani, A. (2000). Analysis of the role of the hypervariable region of yeast Ras2p and its farnesylation in the interaction with exchange factors and adenylyl cyclase. J Biol Chem *275*, 17754-17761.

Crechet, J. B., Poullet, P., Mistou, M. Y., Parmeggiani, A., Camonis, J., Boy-Marcotte, E., Damak, F., and Jacquet, M. (1990). Enhancement of the GDP-GTP exchange of Ras proteins by the carboxyl-terminal domain of Scd25. Science *248*, 866-868.

Dasgupta, B., Dugan, L. L., and Gutmann, D. H. (2003). The neurofibromatosis 1 gene product neurofibromin regulates pituitary adenylate cyclase-activating polypeptide-mediated signaling in astrocytes. J Neurosci *23*, 8949-8954.

Dasgupta, B., and Gutmann, D. H. (2003). Neurofibromatosis 1: closing the GAP between mice and men. Curr Opin Genet Dev *13*, 20-27.

de Rooij, J., and Bos, J. L. (1997). Minimal Ras-binding domain of Raf1 can be used as an activation-specific probe for Ras. Oncogene *14*, 623-625.

DeClue, J. E., Papageorge, A. G., Fletcher, J. A., Diehl, S. R., Ratner, N., Vass, W. C., and Lowy, D. R. (1992). Abnormal regulation of mammalian $p21^{ras}$ contributes to malignant tumor growth in von Recklinghausen (type 1) neurofibromatosis. Cell *69*, 265-273.

Dohlman, H. G. (2002). G proteins and pheromone signaling. Annu Rev Physiol *64*, 129-152.

Dohlman, H. G., Thorner, J., Caron, M. G., and Lefkowitz, R. J. (1991). Model systems for the study of seven-transmembrane-segment receptors. Annu Rev Biochem *60*, 653-688.

Eng, J., McCormack, L., and Yates, R. (1994). An approach to correlate tandem mass spectral data of peptides with amino acid sequences in a protein database. Am Soc Mass Spectrom *5*, 976-989.

Fahsold, R., Hoffmeyer, S., Mischung, C., Gille, C., Ehlers, C., Kücükceylan, N., Abdel-Nour, M., Gewies, A., Peters, H., Kaufmann, D., *et al.* (2000). Minor lesion mutational spectrum of the entire *NF1* gene does not explain its high mutability but points to a functional domain upstream of the GAP-related domain. Am J Hum Genet *66*, 790-818.

Field, J., Nikawa, J., Broek, D., MacDonald, B., Rodgers, L., Wilson, I. A., Lerner, R. A., and Wigler, M. (1988). Purification of a *RAS*-responsive adenylyl cyclase complex from *Saccharomyces cerevisiae* by use of an epitope addition method. Mol Cell Biol *8*, 2159-2165.

Gautam, N., Downes, G. B., Yan, K., and Kisselev, O. (1998). The G-protein βγ complex. Cell Signal *10*, 447-455.

Gilman, A. G. (1987). G-Proteins: transducers of receptor-generated signals. Annual Review of Biochemistry *56*, 615-649.

Goldstein, A. L., and McCusker, J. H. (1999). Three new dominant drug resistance cassettes for gene disruption in *Saccharomyces cerevisiae*. Yeast *15*, 1541-1553.

Gross, A., Winograd, S., Marbach, I., and Levitzki, A. (1999). The N-terminal half of Cdc25 is essential for processing glucose signaling in *Saccharomyces cerevisiae*. Biochemistry *38*, 13252-13262.

Guo, H. F., The, I., Hannan, F., Bernards, A., and Zhong, Y. (1997). Requirement of *Drosophila* NF1 for activation of adenylyl cyclase by PACAP38-like neuropeptides. Science *276*, 795-798.

Guo, H. F., Tong, J., Hannan, F., Luo, L., and Zhong, Y. (2000). A neurofibromatosis-1-regulated pathway is required for learning in *Drosophila*. Nature *403*, 895-898.

Güldener, U., Heck, S., Fielder, T., Beinhauer, J., and Hegemann, J. H. (1996). A new efficient gene disruption cassette for repeated use in budding yeast. Nucleic Acids Res *24*, 2519-2524.

Halme, A., Bumgarner, S., Styles, C., and Fink, G. R. (2004). Genetic and epigenetic regulation of the *FLO* gene family generates cell-surface variation in yeast. Cell *116*, 405-415.

Hannan, F., Ho, I., Tong, J., Zhu, Y., Nurnberg, P., and Zhong, Y. (2006). Effect of neurofibromatosis type I mutations on a novel pathway for adenylyl cyclase activation requiring neurofibromin and Ras. Hum Mol Genet, published online March 2, 2006.

Harashima, T., and Heitman, J. (2002). The Gα protein Gpa2 controls yeast differentiation by interacting with kelch repeat proteins that mimic Gβ subunits. Mol Cell *10*, 163-173.

Harashima, T., and Heitman, J. (2004). Nutrient control of dimorphic growth in *Saccharomyces cerevisiae*. Topics in Current Genetics *Vol.7*, 131-169.

Harashima, T., and Heitman, J. (2005). Gα subunit Gpa2 recruits kelch repeat subunits that inhibit receptor-G protein coupling during cAMP-induced

dimorphic transitions in *Saccharomyces cerevisiae*. Mol Biol Cell *16*, 4557-4571.

Hiatt, K. K., Ingram, D. A., Zhang, Y., Bollag, G., and Clapp, D. W. (2001). Neurofibromin GTPase-activating protein-related domains restore normal growth in *Nf1*-/- cells. J Biol Chem *276*, 7240-7245.

Hitchcock, A. L., Auld, K., Gygi, S. P., and Silver, P. A. (2003). A subset of membrane-associated proteins is ubiquitinated in response to mutations in the endoplasmic reticulum degradation machinery. Proc Natl Acad Sci U S A *100*, 12735-12740.

Ito, N., Phillips, S. E., Stevens, C., Ogel, Z. B., McPherson, M. J., Keen, J. N., Yadav, K. D., and Knowles, P. F. (1991). Novel thioether bond revealed by a 1.7 Å crystal structure of galactose oxidase. Nature *350*, 87-90.

Ito, N., Phillips, S. E. V., Yadav, K. D. S., and Knowles, P. F. (1994). Crystal structure of a free radical enzyme, galactose oxidase. J Mol Biol *238*, 794-814.

Ivey, F. D., and Hoffman, C. S. (2005). Direct activation of fission yeast adenylate cyclase by the Gpa2 Gα of the glucose signaling pathway. Proc Natl Acad Sci U S A *102*, 6108-6113.

Jiang, Y., Davis, C., and Broach, J. R. (1998). Efficient transition to growth on fermentable carbon sources in *Saccharomyces cerevisiae* requires signaling through the Ras pathway. EMBO J *17*, 6942-6951.

Kataoka, T., Powers, S., McGill, C., Fasano, O., Strathern, J., Broach, J., and Wigler, M. (1984). Genetic analysis of yeast *RAS1* and *RAS2* genes. Cell *37*, 437-445.

Kraakman, L., Lemaire, K., Ma, P. S., Teunissen, A. W. R. H., Donaton, M. C. V., Van Dijck, P., Winderickx, J., de Winde, J. H., and Thevelein, J. M. (1999). A *Saccharomyces cerevisiae* G-protein coupled receptor, Gpr1, is specifically required for glucose activation of the cAMP pathway during the transition to growth on glucose. Mol Microbiol *32*, 1002-1012.

Kübler, E., Mösch, H. U., Rupp, S., and Lisanti, M. P. (1997). Gpa2p, a G-protein α-subunit, regulates growth and pseudohyphal development in *Saccharomyces cerevisiae* via a cAMP-dependent mechanism. J Biol Chem *272*, 20321-20323.

Lai, C. C., Boguski, M., Broek, D., and Powers, S. (1993). Influence of guanine nucleotides on complex formation between Ras and Cdc25 proteins. Mol Cell Biol *13*, 1345-1352.

Lambright, D. G., Sondek, J., Bohm, A., Skiba, N. P., Hamm, H. E., and Sigler, P. B. (1996). The 2.0 Å crystal structure of a heterotrimeric G protein. Nature *379*, 311-319.

Lemaire, K., Van de Velde, S., Van Dijck, P., and Thevelein, J. M. (2004). Glucose and sucrose act as agonist and mannose as antagonist ligands of the G protein-coupled receptor Gpr1 in the yeast *Saccharomyces cerevisiae*. Mol Cell *16*, 293-299.

Longtine, M. S., McKenzie III, A., Demarini, D. J., Shah, N. G., Wach, A., Brachat, A., Philippsen, P., and Pringle, J. R. (1998). Additional modules for versatile and economical PCR-based gene deletion and modification in *Saccharomyces cerevisiae*. Yeast *14*, 953-961.

Lorenz, M. C., and Heitman, J. (1997). Yeast pseudohyphal growth is regulated by GPA2, a G protein α homolog. EMBO J *16*, 7008-7018.

Lorenz, M. C., Pan, X. W., Harashima, T., Cardenas, M. E., Xue, Y., Hirsch, J. P., and Heitman, J. (2000). The G protein-coupled receptor Gpr1 is a nutrient sensor that regulates pseudohyphal differentiation in *Saccharomyces cerevisiae*. Genetics *154*, 609-622.

Lu, A., and Hirsch, J. P. (2005). Cyclic AMP-independent regulation of protein kinase A substrate phosphorylation by Kelch repeat proteins. Eukaryot Cell *4*, 1794-1800.

Marchuk, D. A., Saulino, A. M., Tavakkol, R., Swaroop, M., Wallace, M. R., Andersen, L. B., Mitchell, A. L., Gutmann, D. H., Boguski, M., and Collins, F. S. (1991). cDNA cloning of the type 1 neurofibromatosis gene: complete sequence of the *NF1* gene product. Genomics *11*, 931-940.

Martin, G. A., Viskochil, D., Bollag, G., McCabe, P. C., Crosier, W. J., Haubruck, H., Conroy, L., Clark, R., O'Connell, P., Cawthon, R. M., and et al. (1990). The GAP-related domain of the neurofibromatosis type 1 gene product interacts with *ras* p21. Cell *63*, 843-849.

Mintzer, K. A., and Field, J. (1994). Interactions between adenylyl cyclase, CAP and RAS from *Saccharomyces cerevisiae*. Cell Signal *6*, 681-694.

Mintzer, K. A., and Field, J. (1999). The SH3 domain of the *S. cerevisiae* Cdc25p binds adenylyl cyclase and facilitates Ras regulation of cAMP signalling. Cell Signal *11*, 127-135.

Mitts, M. R., Bradshaw-Rouse, J., and Heideman, W. (1991). Interactions between adenylate cyclase and the yeast GTPase-activating protein Ira1. Mol Cell Biol *11*, 4591-4598.

Munder, T., and Furst, P. (1992). The *Saccharomyces cerevisiae CDC25* gene product binds specifically to catalytically inactive ras proteins in vivo. Mol Cell Biol *12*, 2091-2099.

Munder, T., and Kuntzel, H. (1989). Glucose-induced cAMP signaling in *Saccharomyces cerevisiae* is mediated by the Cdc25 protein. FEBS Lett *242*, 341-345.

Origone, P., De Luca, A., Bellini, C., Buccino, A., Mingarelli, R., Costabel, S., La Rosa, C., Garrè, C., Coviello, D. A., Ajmar, F., *et al.* (2002). Ten novel mutations in the human neurofibromatosis type 1 (NF1) gene in Italian patients. Hum Mutat *20*, 74-75.

Parada, L. F. (2000). Neurofibromatosis type 1. Biochim Biophys Acta *1471*, M13-19.

Portillo, F., and Mazon, M. J. (1986). The *Saccharomyces cerevisiae* start mutant carrying the *cdc25* mutation is defective in activation of plasma membrane ATPase by glucose. J Bacteriol *168*, 1254-1257.

Powers, S., Kataoka, T., Fasano, O., Goldfarb, M., Strathern, J., Broach, J., and Wigler, M. (1984). Genes in *S. cerevisiae* encoding proteins with domains homologous to the mammalian ras proteins. Cell *36*, 607-612.

Ross, E. M., and Wilkie, T. M. (2000). GTPase-activating proteins for heterotrimeric G proteins: Regulators of G protein signaling (RGS) and RGS-like proteins. Annual Review of Biochemistry *69*, 795-827.

Sherman, F. (1991). Getting started with yeast. Methods Enzymol *194*, 3-21.

Shima, F., Okada, T., Kido, M., Sen, H., Tanaka, Y., Tamada, M., Hu, C. D., Yamawaki-Kataoka, Y., Kariya, K., and Kataoka, T. (2000). Association of yeast adenylyl cyclase with cyclase-associated protein CAP forms a

second Ras-binding site which mediates its Ras-dependent activation. Mol Cell Biol *20*, 26-33.

Sondek, J., Bohm, A., Lambright, D. G., Hamm, H. E., and Sigler, P. B. (1996). Crystal structure of a G_A protein βγ dimer at 2.1 Å resolution. Nature *379*, 369-374.

Tabb, D. L., McDonald, W. H., and Yates, J. R., III (2002). DTASelect and Contrast: tools for assembling and comparing protein identifications from shotgun proteomics. J Proteome Res *1*, 21-36.

Tanaka, K., Lin, B. K., Wood, D. R., and Tamanoi, F. (1991). *IRA2*, an upstream negative regulator of RAS in yeast, is a RAS GTPase-activating protein. Proc Natl Acad Sci U S A *88*, 468-472.

Tanaka, K., Matsumoto, K., and Toh-e, A. (1989). *IRA1*, an inhibitory regulator of the *RAS*-cyclic AMP pathway in *Saccharomyces cerevisiae*. Mol Cell Biol *9*, 757-768.

Tanaka, K., Nakafuku, M., Satoh, T., Marshall, M. S., Gibbs, J. B., Matsumoto, K., Kaziro, Y., and Toh-e, A. (1990a). *S. cerevisiae* genes *IRA1* and *IRA2* encode proteins that may be functionally equivalent to mammalian *ras* GTPase activating protein. Cell *60*, 803-807.

Tanaka, K., Nakafuku, M., Tamanoi, F., Kaziro, Y., Matsumoto, K., and Toh-e, A. (1990b). *IRA2*, a second gene of *Saccharomyces cerevisiae* that encodes a protein with a domain homologous to mammalian *ras* GTPase-activating protein. Mol Cell Biol *10*, 4303-4313.

The, I., Hannigan, G. E., Cowley, G. S., Reginald, S., Zhong, Y., Gusella, J. F., Hariharan, I. K., and Bernards, A. (1997). Rescue of a *Drosophila NF1* mutant phenotype by protein kinase A. Science *276*, 791-794.

Toda, T., Cameron, S., Sass, P., and Wigler, M. (1988). *SCH9*, a gene of *Saccharomyces cerevisiae* that encodes a protein distinct from, but functionally and structurally related to, cAMP-dependent protein kinase catalytic subunits. Genes Dev *2*, 517-527.

Toda, T., Cameron, S., Sass, P., Zoller, M., Scott, J. D., Mcmullen, B., Hurwitz, M., Krebs, E. G., and Wigler, M. (1987a). Cloning and characterization of *BCY1*, a locus encoding a regulatory subunit of the cyclic AMP-dependent protein kinase in *Saccharomyces cerevisiae*. Mol Cell Biol *7*, 1371-1377.

Toda, T., Cameron, S., Sass, P., Zoller, M., and Wigler, M. (1987b). Three different genes in *S. cerevisiae* encode the catalytic subunits of the cAMP-dependent protein kinase. Cell *50*, 277-287.

Tong, J., Hannan, F., Zhu, Y., Bernards, A., and Zhong, Y. (2002). Neurofibromin regulates G protein-stimulated adenylyl cyclase activity. Nat Neurosci *5*, 95-96.

Viskochil, D., Buchberg, A. M., Xu, G., Cawthon, R. M., Stevens, J., Wolff, R. K., Culver, M., Carey, J. C., Copeland, N. G., Jenkins, N. A., and et al. (1990). Deletions and a translocation interrupt a cloned gene at the neurofibromatosis type 1 locus. Cell *62*, 187-192.

Wach, A., Brachat, A., Pohlmann, R., and Philippsen, P. (1994). New heterologous modules for classical or PCR-based gene disruptions in *Saccharomyces cerevisiae*. Yeast *10*, 1793-1808.

Wallace, M. R., Marchuk, D. A., Andersen, L. B., Letcher, R., Odeh, H. M., Saulino, A. M., Fountain, J. W., Brereton, A., Nicholson, J., Mitchell, A. L.,

and et al. (1990). Type 1 neurofibromatosis gene: identification of a large transcript disrupted in three NF1 patients. Science *249*, 181-186.

Washburn, M. P., Wolters, D., and Yates, J. R., 3rd (2001). Large-scale analysis of the yeast proteome by multidimensional protein identification technology. Nat Biotechnol *19*, 242-247.

Xu, G. F., Lin, B., Tanaka, K., Dunn, D., Wood, D., Gesteland, R., White, R., Weiss, R., and Tamanoi, F. (1990a). The catalytic domain of the neurofibromatosis type 1 gene product stimulates *ras* GTPase and complements *ira* mutants of *S. cerevisiae*. Cell *63*, 835-841.

Xu, G. F., O'Connell, P., Viskochil, D., Cawthon, R., Robertson, M., Culver, M., Dunn, D., Stevens, J., Gesteland, R., White, R., and et al. (1990b). The neurofibromatosis type 1 gene encodes a protein related to GAP. Cell *62*, 599-608.

Xue, Y., Batlle, M., and Hirsch, J. P. (1998). *GPR1* encodes a putative G protein-coupled receptor that associates with the Gpa2p G_{α} subunit and functions in a Ras-independent pathway. EMBO J *17*, 1996-2007.

Yun, C. W., Tamaki, H., Nakayama, R., Yamamoto, K., and Kumagai, H. (1998). Gpr1p, a putative G-protein coupled receptor, regulates glucose-dependent cellular cAMP level in yeast *Saccharomyces cerevisiae*. Biochem Biophys Res Commun *252*, 29-33.

Zhu, Y., and Parada, L. F. (2002). The molecular and genetic basis of neurological tumours. Nat Rev Cancer *2*, 616-626.

Figure legends

Figure 1. Genetic interactions between *gpb1,2* and *ras2* mutations. (A) *gpb1,2* mutations are unable to suppress the synthetic growth defect of *gpa2 ras2* mutant cells. Diploid *gpa2::G418/gpa2::hph ras2::nat/RAS2* (left, THY388a/α) and *gpb1,2::loxP/gpb1,2::loxP gpa2::loxP-G418/GPA2 ras2::nat/ras2::nat* (right, see "Materials and Discussion") cells were sporulated and dissected. Progeny genotypes were determined based on segregation of the dominant drug resistant markers (*G418*, *hph*, and *nat*). (B-F) *ras2* mutations alleviate increased PKA phenotypes associated with *gpb1,2* mutations, including enhanced pseudohyphal growth (B), hyperinvasive growth (C), increased *FLO11* expression (D), sensitivity to nitrogen starvation (E), and reduced glycogen accumulation (F). Diploid strains, MLY61a/α (WT), THY170a/α (*gpa2*), XPY5a/α (*tpk2*), MLY187a/α (*ras2*), THY212a/α (*gpb1,2*), THY242a/α (*gpb1,2 gpa2*), THY245a/α (*gpb1,2 tpk2*), and THY247a/α (*gpb1,2 ras2*) were employed to assay pseudohyphal growth, and isogenic haploid strains, MLY40α (WT), THY170α, XPY5α, MLY187α, THY212α, THY242α, THY245α, and THY247α to study invasive growth, *FLO11* expression, sensitivity to nitrogen starvation, and glycogen accumulation. (G) Glucose-induced cAMP production in WT (MLY40α), *ras2* (MLY187α), *gpb1,2* (THY212α), and *gpb1,2 ras2* (THY247α) mutant cells. Glucose was added to glucose starved cells, and at the indicated time points, cells were collected and cAMP levels were determined. The values shown are the mean of two independent experiments.

Figure 2. Kelch Gβ mimic subunits interact with RasGAP Ira1/2. (A and B) Ira1 (A) and Ira2 (B) physically bind to Gpb1/2 in vivo. The N-terminally FLAG-tagged Gpb1 (pTH111) and Gpb2 (pTH88) proteins were expressed in yeast cells that also express C-terminally 3HA tagged Ira1 (THY355a, panel A) or Ira2 (THY356a, panel B). (C) Gpb2 requires both the unique N-terminal and the C-terminal kelch domains to interact with Ira1. The N-terminally FLAG tagged Gpb2 N-terminal region (FLAG-Gpb2N, pTH190), C-terminal kelch domains (FLAG-Gpb2C, pTH188), or full length Gpb2 (FLAG-Gpb2, pTH88) were co-expressed with the Ira1-3HA protein in vivo (THY381a). Positions of molecular marker (128, 85, 41.7, and 32.1 k) are indicated to the right of the panel. (D) Ras2 is dispensable for the Gpb2-Ira1 interaction. Protein-protein interactions between Gpb2 and Ira1 were examined in the presence (THY355a) and absence (THY479α) of Ras2 using cells that express the FLAG tagged Gpb2 (pTH88). Crude cell extracts were prepared from exponentially growing cells and subjected to immunoprecipitations using anti-FLAG affinity gel. To verify expression levels of the 3HA tagged Ira1/2 proteins and because of low expression levels of Ira1/2, the Ira1/2-3HA proteins were immunoprecipitated using anti-HA agarose beads, eluted, and then analyzed by western analysis and indicated as "Input". Cells expressing both Ira1-3HA and Trp1-FLAG fusion proteins (THY450a) served as the control. Fpr1 was used as the loading control.

Figure 3. Genetic interactions between *gpb1,2* and *ira1,2* mutations. (A) Wild-type (MLY61a/α), *gpb1,2* (THY212a/α), *ira1,2* (THY345a/α), *ira1* (THY337a/α), *ira2* (THY336a/α), and *gpb1,2 ira1,2* (THY346a/α) mutant strains were assayed

for pseudohyphal growth. (B) The dominant active *GPA2*^{Q300L} (pTH48) and *RAS2*^{G19V} (pMW2) alleles were introduced into wild-type (MLY61a/α) and *gpb1,2* mutant cells (THY212a/α) and tested for effects on filamentous growth. (C) The *IRA2* gene (pKF56) suppressed the increased filamentous phenotype of *gpb1,2* mutant cells (THY212a/α). pTH27 (*GPB2*) and an empty vector pTH19 were introduced into wild-type (MLY61a/α) or *gpb1,2* mutant cells (THY212a/α) as controls. Cells were grown on SLAD agar medium at 30ºC for 5 days and photographed in panels A, B, and C. Haploid cells indicated were tested for invasive growth (D), nitrogen starvation sensitivity (E), glycogen accumulation (F), and glucose-induced cAMP production (G). (D) Cells were grown on YPD at 30ºC for 5 days and photographed after weak (W), mild (M) or strong (S) washing. (E) Cells were grown on YPD at 30ºC for 2 days, replica-plated onto nitrogen replete (+NH_4) and no nitrogen (-NH_4) media. After 6 (left panel) or 10 (right panel) days at 30 ºC, cells were replica-plated onto YPD again and incubated under the same conditions. (F) Glycogen levels of cells grown on YPD at 30ºC for 2 days were determined using iodine vapor. (G) cAMP levels were determined in response to glucose readdition as described in the legend of Figure 1.

Figure 4. Kelch subunits Gpb1/2 stabilize the RasGAP proteins Ira1/2. (A) The relative increase in Ras2-GTP was examined in isogenic wild-type (MLY41a) and *ras2* (MLY187α), *ira1* (THY337a), *ira2* (THY336a), *ira1,2* (THY345a), and *gpb1,2* (THY212a) mutant cells, expressing the wild-type (pMW1) or dominant active (G19V, pMW2) *RAS2* gene. Representative data are shown in the upper panel.

Note that purified Ras2-GTP from *ira1,2* double mutant cells expressing the wild-type Ras2 protein and wild-type and *gpb1,2* mutant cells that express the dominant active Ras2 ($Ras2^{G19V}$) protein was 5-fold diluted prior to western analysis, as the levels of Ras2-GTP in these cells were higher than those in the other cells. This permitted accurate measurement of the levels of Ras2-GTP by densitometry. After detection of levels of the GTP bound Ras2 and total cellular Ras protein ("Input") by western blot, signals were densitometrically quantified. Levels of Ras2-GTP were normalized to "Input" Ras2 levels and shown as a relative level to Ras2-GTP in wild-type cells in the lower panel. The values shown in the lower panel are the means of two or three independent experiments with the standard error of the mean. (B) The *GPB1* (pTH26) and *GPB2* (pTH114) genes were introduced into wild-type strains THY427a (*IRA1-3HA*) and THY428a *(IRA2-3HA*) and *gpb1,2* double mutant strains THY425a (*gpb1,2 IRA1-3HA*) and THY426a (*gpb1,2 IRA2-3HA*) to examine protein stability of Ira1/2 and the interactions between Ras2 and Ira1/2. The Ira1/2-Ras2 protein complex was co-immunoprecipitated using anti-HA conjugated agarose gels and eluted by the addition of HA peptide (shown as "Co-IP (HA)" in upper panel). A yeast strain THY475 (Trp1-3HA) carrying the empty vector pTH19 was employed as a control. Fpr1 served as a loading control. "NT" indicates the non-tagged, wild-type Ira1 or Ira2 protein. Based on densitometric analysis the steady state protein levels of Ira1 and Ira2 were reduced in *gpb1,2* double mutant cells by at least 2- to 10-fold compared to wild-type cells. Cells expressing a 3HA tagged Trp1 fusion protein served as a control. Note that the Ira1/2 proteins were undetectable in western blot using crude extracts because of low expression levels. (C and D) Gpb1/2 stabilize Ira1/2. Protein stability of Ira1 (C) and Ira2

(D) was investigated by cycloheximide-chase assay in the presence and absence of Gpb1/2. Cycloheximide (CHX) was added to exponentially growing cells at a final concentration of 50 μg/ml. At the indicated time points after CHX addition, cells expressing the 3HA tagged Ira1 protein (THY425 and THY427, panel C) or the 3HA tagged Ira2 protein (THY426 and THY428, panel D) were collected, washed, and cell extracts were prepared. The 3HA tagged Ira1/2 proteins were analyzed as above. After western blot (upper panel), signals were densitometorically quantified, and % protein abundance of Ira1 and Fpr1 at "Time 0" is shown in the lower panel.

Figure 5. Kelch Gpb1/2 subunits bind to the C-terminus of Ira1. The FLAG-Gpb1 (pTH111) and FLAG-Gpb2 (pTH88) fusion proteins were expressed in yeast cells that also express the 3HA tagged wild type Ira1 or Ira1 deletion variants, and protein complexes were immunoprecipitated. (A) Schematic of Ira1 deletion proteins created and summary of results obtained from assays of protein abundance (western blots) and Gpb1/2 binding (immunoprecipitation) as below. Positions of deletions created in Ira1 are shown and numbered. A conserved region between Ira1/2 and the human neurofibromin protein is shaded in grey. The RasGAP related domain (GRD) and the Gpb1/2 binding domain (GBD) are shown as a hatched and dark grey rectangle, respectively. (B) Protein interactions were investigated using crude cell extracts from cells expressing the 3HA tagged full length Ira1 (1~3092, THY355a) or Ira1 deletion variants (1~2925 (THY424a), 1~2714 (THY402a), 1~2432 (THY401a), and 1~1257 (THY404a)). Positions of full length wild-type Ira1 (1~3092 aa) and deletion variants (1~2925 and 1~1257 aa) are indicated to the left of the panel. Positions at which

molecular weight markers (250, 210, and 148 k) migrated are indicated to the right of the panels. The deletion of 167 amino acids from the Ira1 C-terminus leads to reduced protein levels of Ira1 from 3- to 7 fold in comparison of the full length Ira1 protein level and the further deletion (378 amino acids) results in undetectable levels ("Input" panel). Note that some smaller Ira1-3HA species were also detected via the C-terminal HA tag, indicating that these are proteolysis products lacking N-terminal regions. This further supports the assignment of the GBD to the C-terminal region of Ira1. (C) N-terminal deletion Ira1 variants (2433~3092 aa (THY438a) and 2715~3092 aa (THY440a)) were tested for interaction with Gpb1/2. Positions of the N-terminal deletion Ira1 variants (2432~3092 and 2715~3092 aa) are indicated to the left of the panel. (D) A putative GBD of Ira1 spanning amino acids 2715~2925 (THY468a) was examined for Gpb1/2 interactions. Note that a deletion Ira1 variant that lacks this domain (Ira1 Δ2715~2925 aa variant in panel A) was undetectable because of protein instability, consistent with the role of Gpb1/2 in Ira1 protein stability. Crude extracts were prepared from cells grown to mid-log phase in synthetic dropout medium. Protein complexes were immunoprecipitated using anti-FLAG affinity gel. Because the levels of the full length Ira1 and these Ira1 N- and C-terminal deletion variant proteins in crude extracts were too low to detect by western blot, the full length and deletion Ira1 proteins were immunoprecipitated using anti-HA agarose beads, eluted, subject to western analysis, and examined for protein stability and indicated as "Input" in panels B, C, and D. Yeast strains (THY450a, THY464a, and THY467a) that carry the empty vector pTH19 were used as a control. Fpr1 in crude cell extracts served as loading controls and were also shown as "Input".

Figure 6. The C-terminus of Ira1/2 is necessary for function. (A) Isogenic homozygous diploid cells were tested for filamentous growth: WT (MLY61a/α), *gpb1,2* (THY212a/α), *ira1* (THY337a/α), *IRA1-3HA* (1~3092 aa, THY355a/α), *IRA1-3HA* (1~2925 aa, THY424a/α), *IRA1-3HA* (1~2714 aa, THY402a/α), *IRA1-3HA* (ΔGBD (Δ2715~2925 aa), THY471a/α). Cells were grown at 30°C for 5 days on SLAD medium and photographed. Invasive growth (B), nitrogen starvation sensitivity (C), and glycogen accumulation (D) were examined using isogenic haploid cells. (B) Cells were grown on YPD 30°C for 5 days and washed off under a current of water. (C) After 7 days on nitrogen replete or depleted medium, cells were replica-plated onto YPD. (D) Glycogen accumulation was assessed using iodine vapor. Details were as described in the figure legend to Figure 1.

Figure 7. A dual role of the kelch proteins Gpb1/2 as molecular brakes on cAMP signaling. (A) A schematic of the yeast neurofibromin homolog Ira1 and human neurofibromin proteins. A conserved region including the GRD and the GBD is shown in grey. GRD; hatched rectangle, GBD; bold rectangle. (B) A model for how the kelch Gβ mimic proteins Gpb1/2 control cAMP signaling. See details in the text.

Supplemental Figure 1. The GBD in Ira2 maps to the equivalent C-terminal region of Ira1. (A) The protein structure of the Ira1/2 proteins is depicted schematically. Positions of deletions created in Ira1/2 are shown and numbered. The Gpb1/2 biding domain (GBD) on Ira2 was also determined by assessing

protein interactions between Gpb1/2 and C-terminal (1~2922 aa (THY 456a) and 1~2702 aa (THY 457a), panel B) and N-terminal (2703~3079 aa (THY 466a), panel C) Ira2 deletion variants and an Ira2 C-terminal domain (2703~2922 aa (THY473), panel B). The migration positions of full length wild-type Ira2 (3079 aa) and Ira2 deletion variants (1~2922 aa) are indicated to the left of the panel. Positions at which molecular weight markers (250, 210, and 148 k) migrated are also indicated to the right of the panels in B. Yeast strains (THY451a, THY466a,and THY474a) carrying the empty plasmid pTH19 were employed as a control. Details are essentially as described in the legend to Figure 5, unless otherwise specifically noted.

Figure 1. Harashima et al.

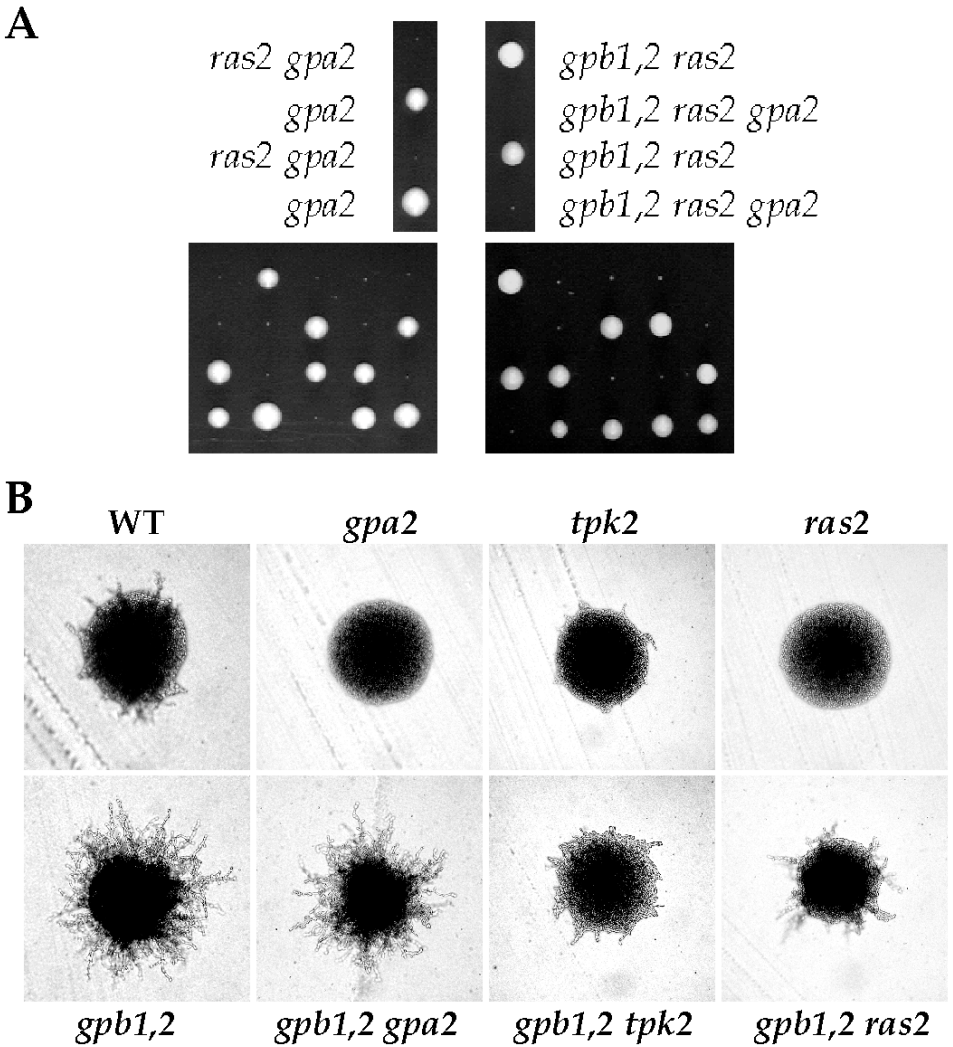

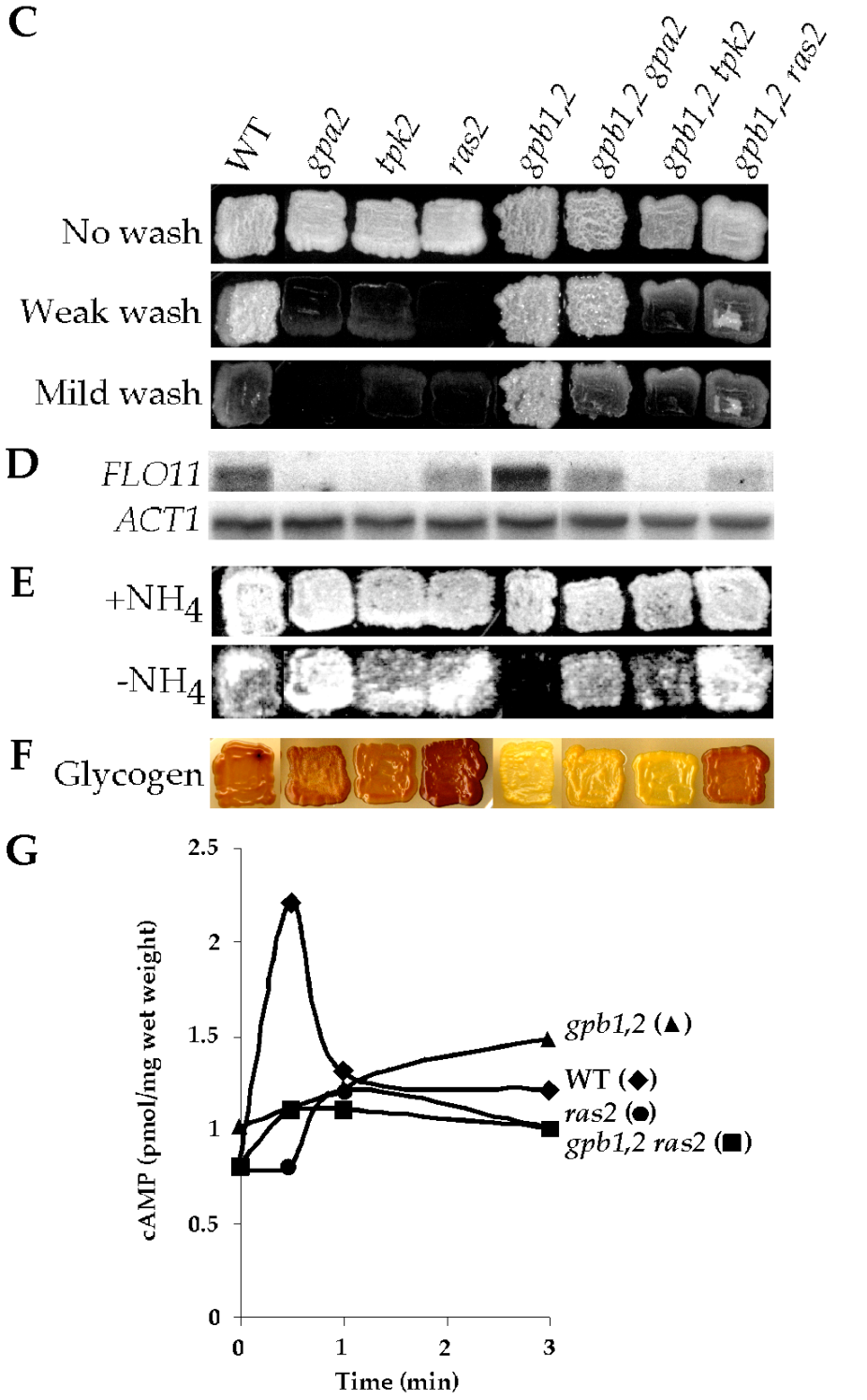

Figure 2. Harashima et al.

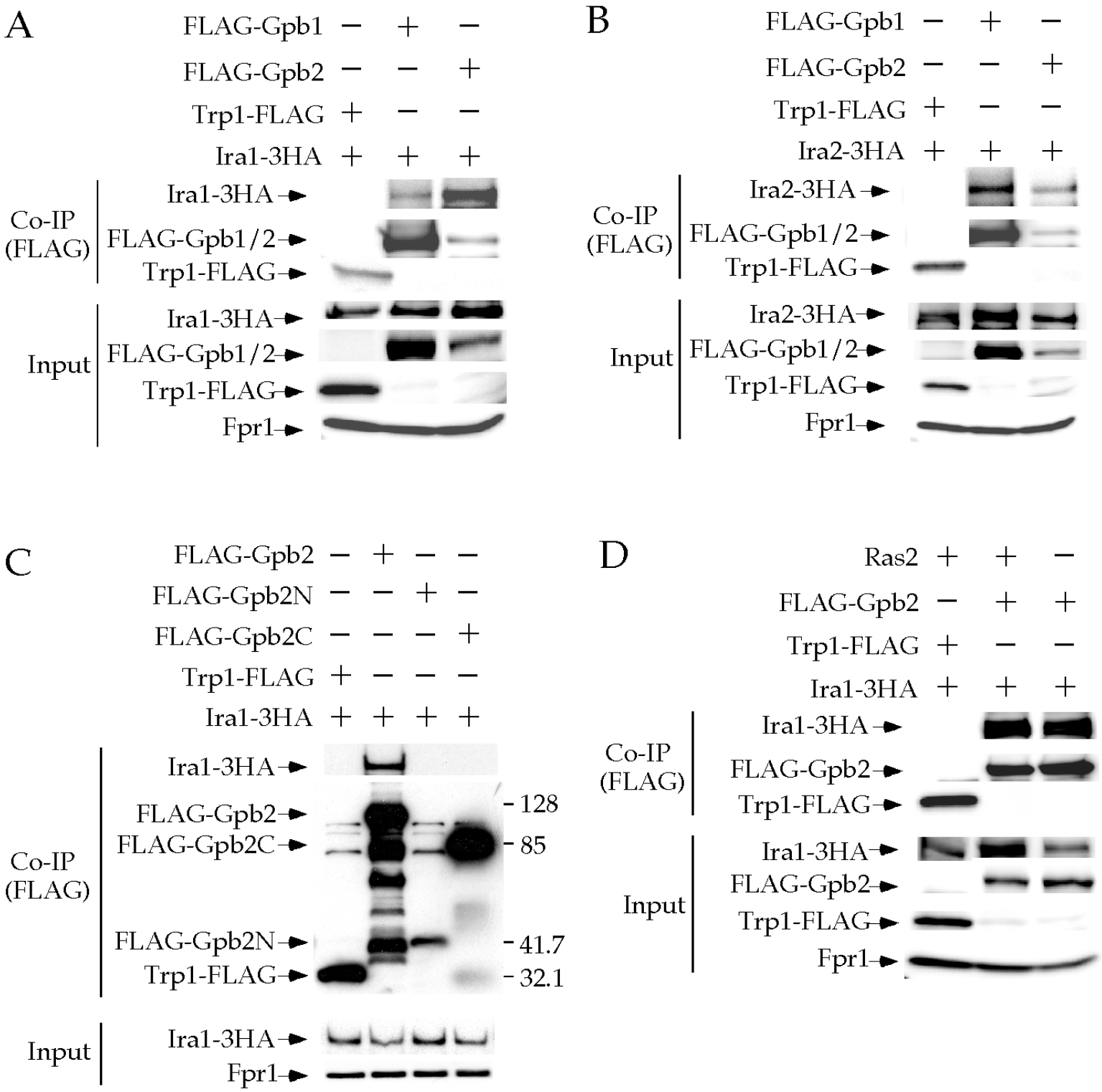

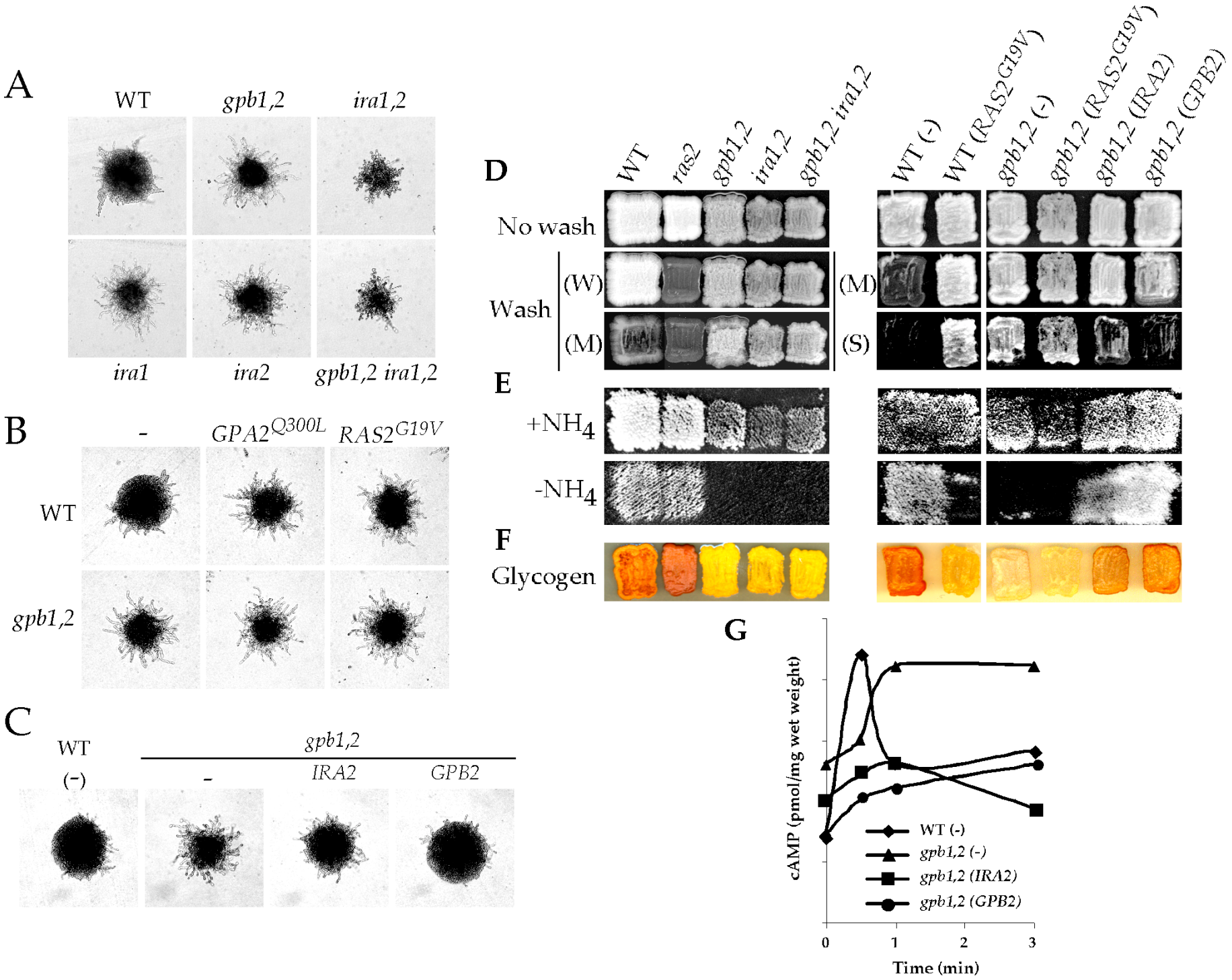
A
WT
gpb1,2
ira1,2
ira1
ira2
gpb1,2 ira1,2
B
-
GPA2Q300L
RAS2G19V
WT
gpb1,2
C
WT
(-)
gpb1,2
-
IRA2
GPB2
D
WT
ras2
gpb1,2
ira1,2
gpb1,2 ira1,2
WT (-)
WT (RAS2G19V)
gpb1,2 (-)
gpb1,2 (RAS2G19V)
gpb1,2 (IRA2)
gpb1,2 (GPB2)
No wash
Wash
(W)
(M)
(M)
(S)
E
+NH4
-NH4
F
Glycogen
G
cAMP (pmol/mg wet weight)
WT (-)
gpb1,2 (-)
gpb1,2 (IRA2)
gpb1,2 (GPB2)
0
1
2
3
Time (min)

Figure 4. Harashima et al.

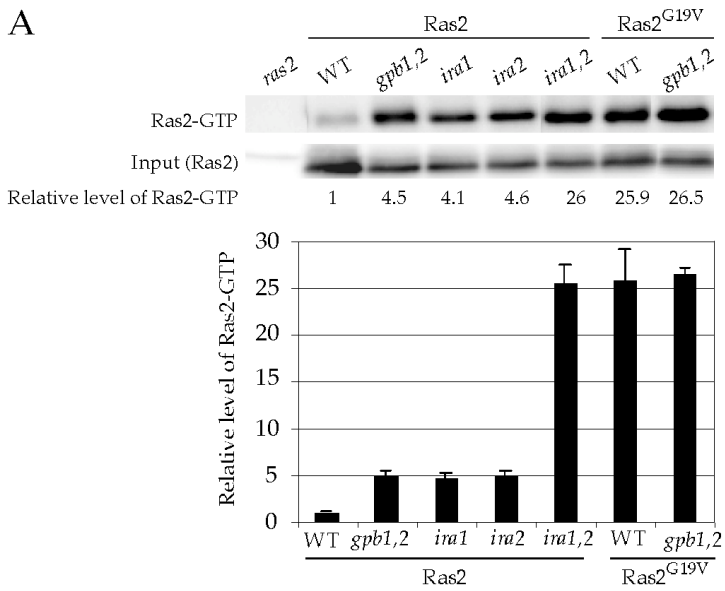

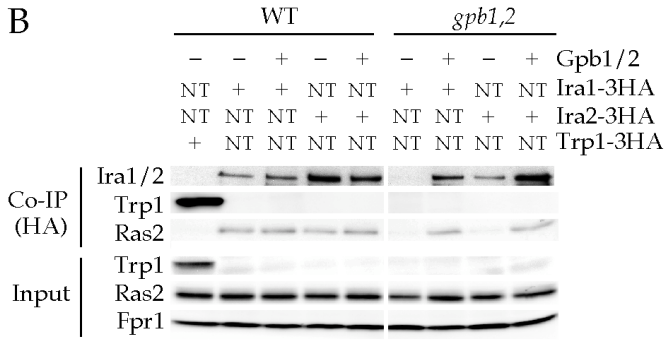

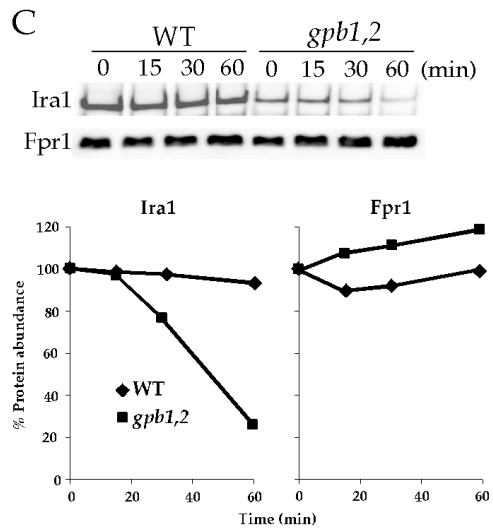

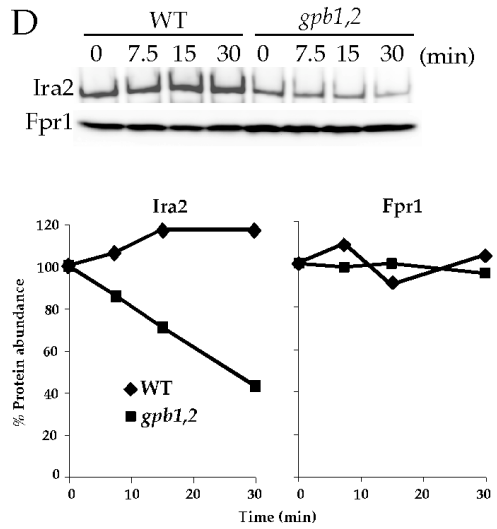

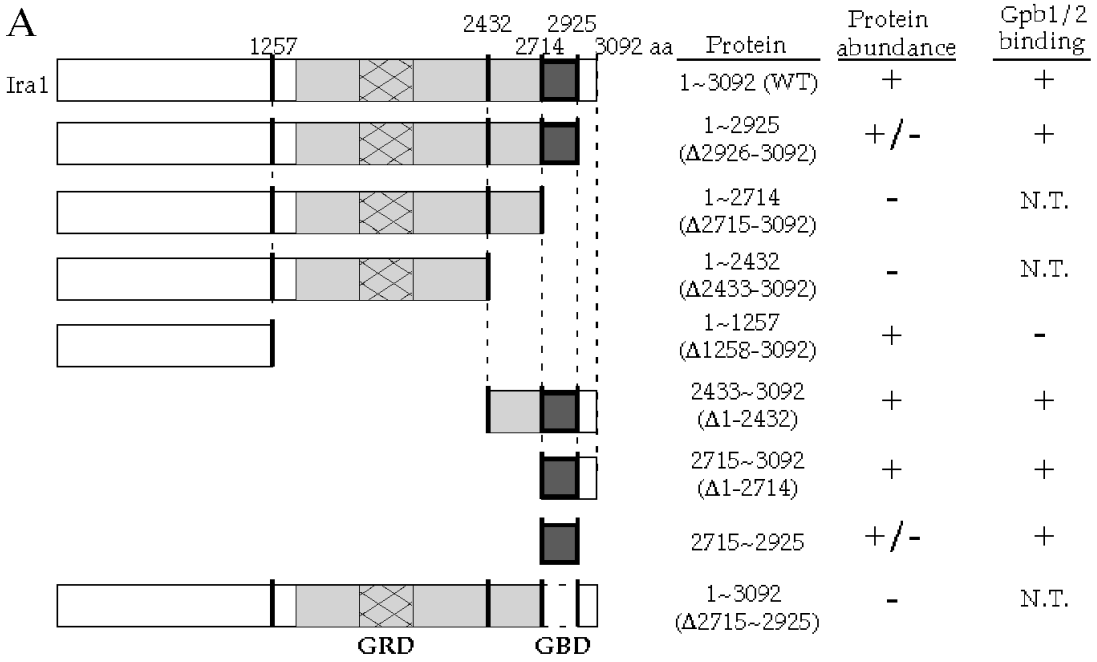
A
1257
2432
2714
2925
3092 aa
Ira1
GRD
GBD
Protein
Protein abundance
Gpb1/2 binding
1~3092 (WT) + +
1~2925 (Δ2926-3092) +/- +
1~2714 (Δ2715-3092) - N.T.
1~2432 (Δ2433-3092) - N.T.
1~1257 (Δ1258-3092) + -
2433~3092 (Δ1-2432) + +
2715~3092 (Δ1-2714) + +
2715~2925 +/- +
1~3092 (Δ2715~2925) - N.T.

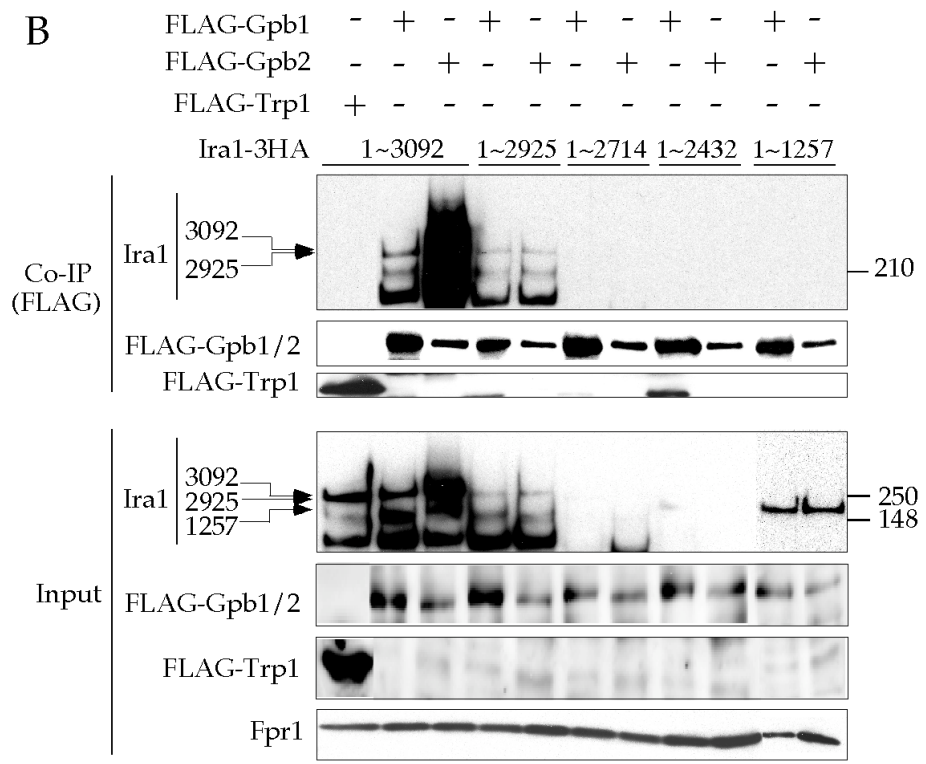
B
FLAG-Gpb1
FLAG-Gpb2
FLAG-Trp1
Ira1-3HA
1~3092
1~2925
1~2714
1~2432
1~1257
Co-IP (FLAG)
Ira1
3092
2925
210
FLAG-Gpb1/2
FLAG-Trp1
Input
Ira1
3092
2925
1257
250
148
FLAG-Gpb1/2
FLAG-Trp1
Fpr1

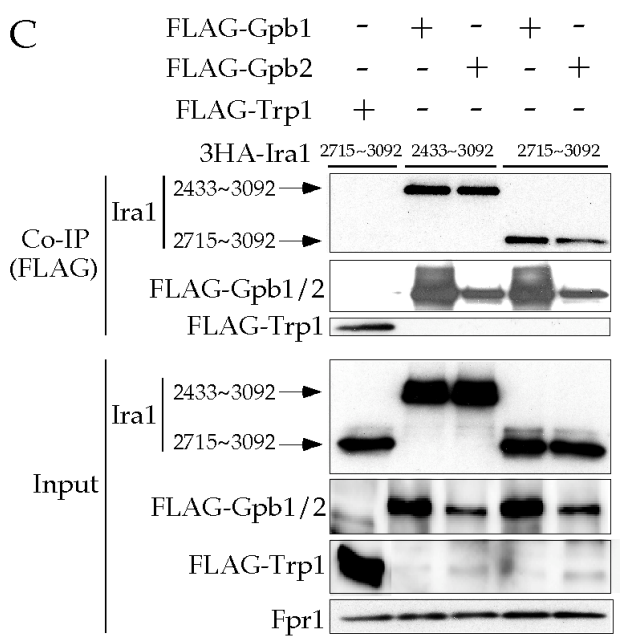
C
FLAG-Gpb1
FLAG-Gpb2
FLAG-Trp1
3HA-Ira1
2715~3092
2433~3092
2715~3092
Co-IP (FLAG)
Ira1
2433~3092
2715~3092
FLAG-Gpb1/2
FLAG-Trp1
Input
Ira1
2433~3092
2715~3092
FLAG-Gpb1/2
FLAG-Trp1
Fpr1

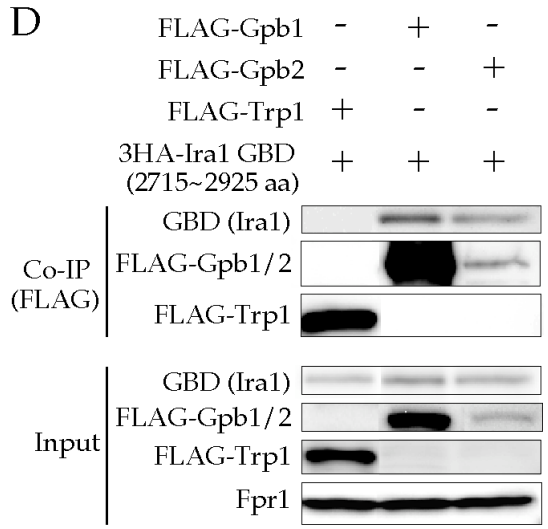
D
FLAG-Gpb1
FLAG-Gpb2
FLAG-Trp1
3HA-Ira1 GBD (2715~2925 aa)
Co-IP (FLAG)
GBD (Ira1)
FLAG-Gpb1/2
FLAG-Trp1
Input
GBD (Ira1)
FLAG-Gpb1/2
FLAG-Trp1
Fpr1

Figure 6. Harashima et al.

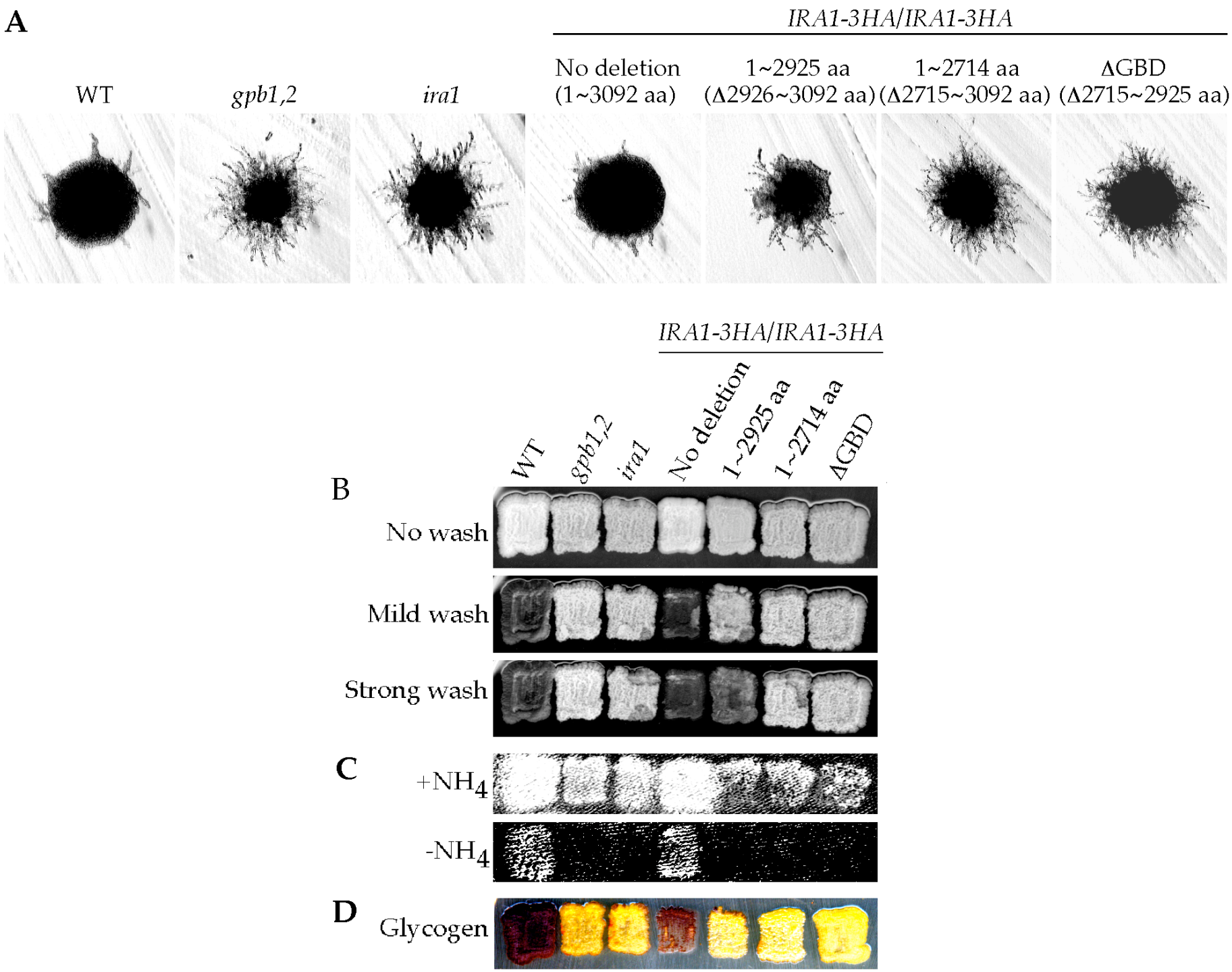

Figure 7. Harashima et al

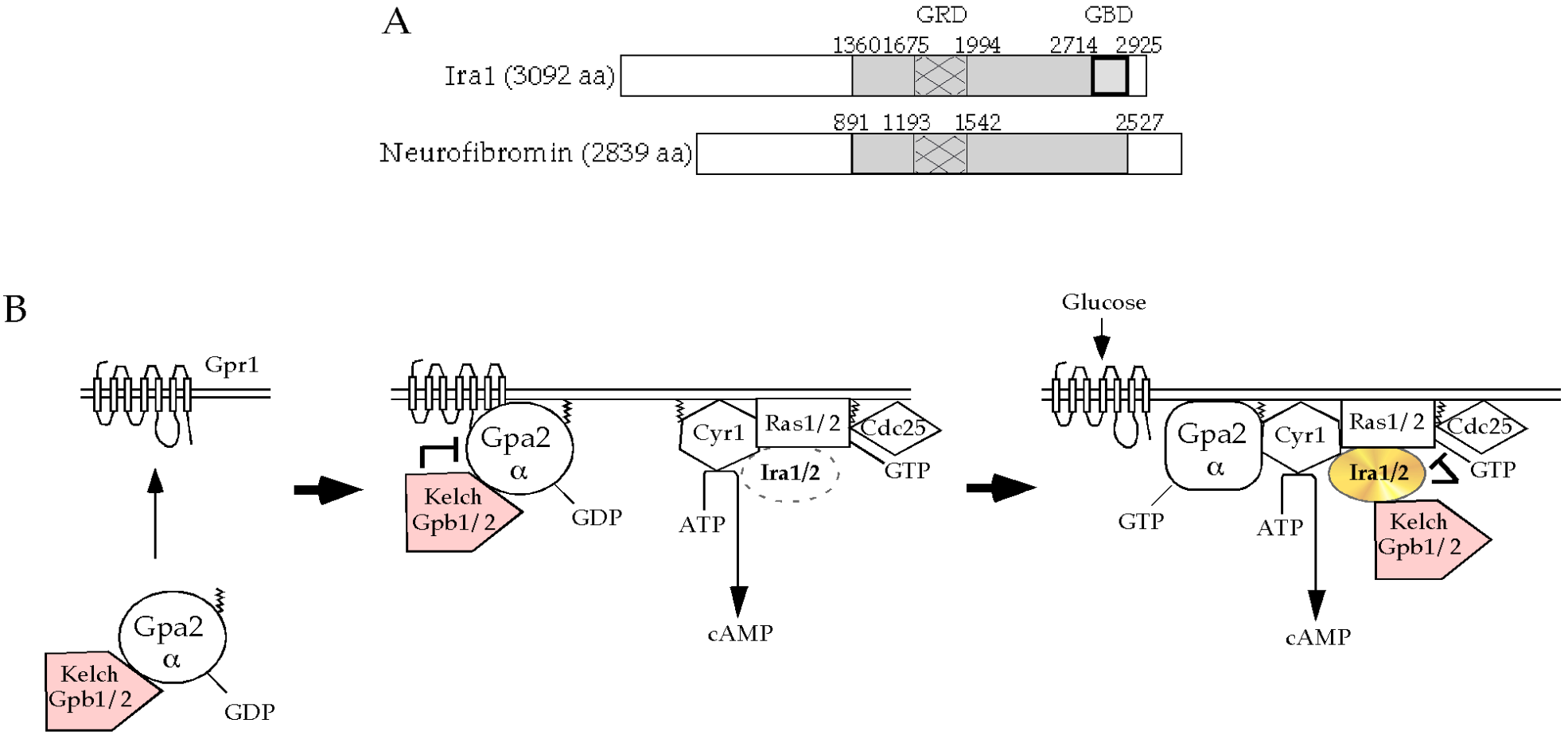

- Gpa2-dependent membrane localization
- Gpb1/2-dependent inhibition of Gpr1-Gpa2 coupling
- Ras-dependent adenylyl cyclase activation
- Gpa2-dependent adenylyl cyclase activation
- Gpb1/2-dependent Ira1/2 stabilization

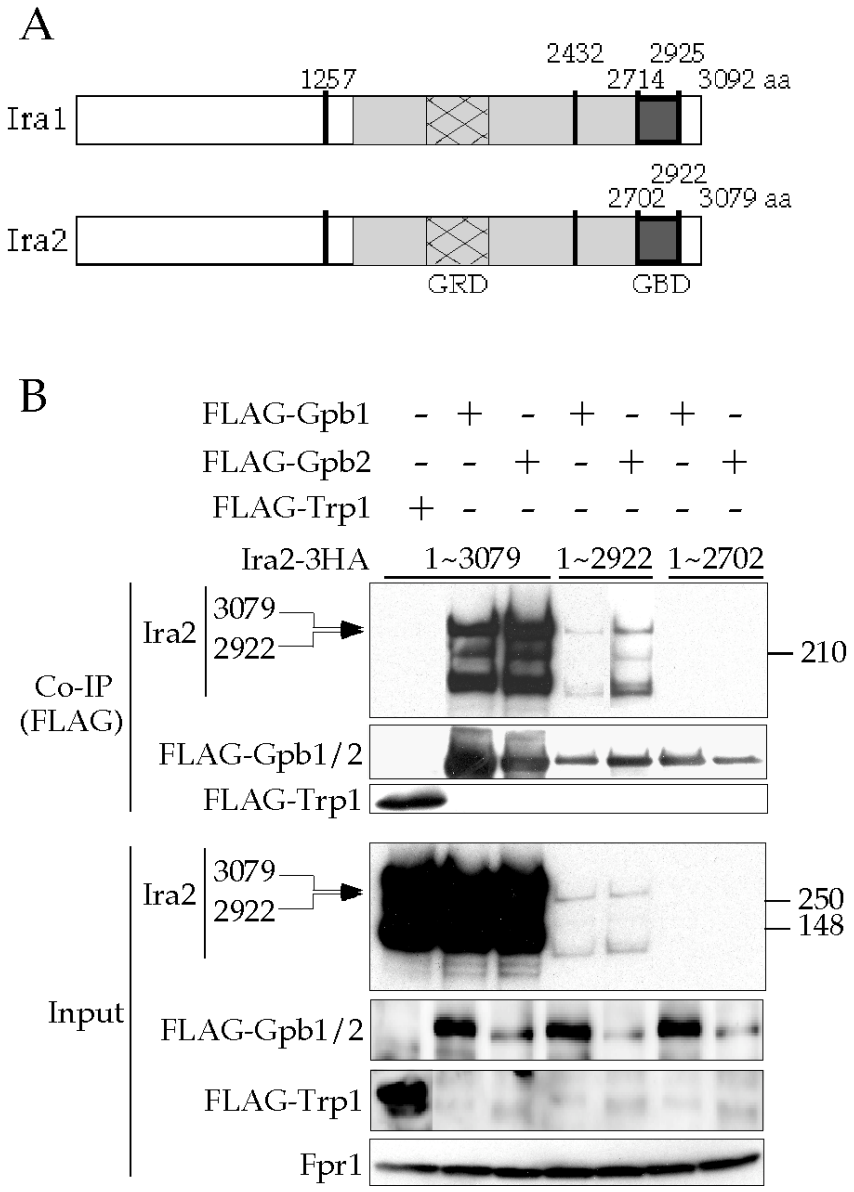
A
Ira1
1257
2432
2925
2714
3092 aa
Ira2
2922
2702
3079 aa
GRD
GBD
B
FLAG-Gpb1 - + - + - + -
FLAG-Gpb2 - - + - + - +
FLAG-Trp1 + - - - - - -
Ira2-3HA 1~3079 1~2922 1~2702
Co-IP (FLAG)
Ira2
3079
2922
210
FLAG-Gpb1/2
FLAG-Trp1
Input
Ira2
3079
2922
250
148
FLAG-Gpb1/2
FLAG-Trp1
Fpr1
C
FLAG-Gpb1 - + -
FLAG-Gpb2 - - +
FLAG-Trp1 + - -
Ira2-3HA 2703~3079
Co-IP (FLAG)
Ira2 (2703~3079)
FLAG-Gpb1/2
FLAG-Trp1
Input
Ira2 (2703~3079)
FLAG-Gpb1/2
FLAG-Trp1
Fpr1
D
FLAG-Gpb1 - + -
FLAG-Gpb2 - - +
FLAG-Trp1 + - -
Ira2-3HA 2703~2922
Co-IP (FLAG)
Ira2 (2703~2922)
FLAG-Gpb1/2
FLAG-Trp1
Input
Ira2 (2703~2922)
FLAG-Gpb1/2
FLAG-Trp1
Fpr1

Supplemental TABLE 1

***S. cerevisiae* strains**

Σ1278b congenic strains

Strain	Genotype	Source/Reference
MLY40α	*MAT*α *ura3-52*	Lorenz and Heitman (1997)
MLY41a	*MAT*a *ura3-52*	Lorenz and Heitman (1997)
MLY61a/α	*MAT*a/α *ura3-52/ura3-52*	Lorenz and Heitman (1997)
MLY187α	*MAT*α *ras2*Δ*::G418 ura3-52*	Laboratory stock
MLY187a/α	*MAT*a/α *ras2*Δ*::G418/ras2*Δ*::G418 ura3-52/ura3-52*	Laboratory stock
THY170α	*MAT*α *gpa2*Δ*::hph ura3-52*	Harashima and Heitman (2002)
THY170a/α	*MAT*a/α *gpa2*Δ*::hph/gpa2*Δ*::hph ura3-52/ura3-52*	Harashima and Heitman (2002)
THY212a	*MAT*a *gpb1*Δ*::hph gpb2*Δ*::G418 ura3-52*	Harashima and Heitman (2002)
THY212α	*MAT*α *gpb1*Δ*::hph gpb2*Δ*::G418 ura3-52*	Harashima and Heitman (2002)
THY212a/α	*MAT*a/α *gpb1*Δ*::hph/gpb1*Δ*::hph gpb2*Δ*::G418/gpb2*Δ*::G418 ura3-52/ura3-52*	Harashima and Heitman (2002)
THY242α	*MAT*α *gpb1*Δ*::hph gpb2*Δ*::G418 gpa2*Δ*::hph ura3-52*	Harashima and Heitman (2002)
THY242a/α	*MAT*a/α *gpb1*Δ*::hph/gpb1*Δ*::hph gpb2*Δ*::G418/gpb2*Δ*::G418*	Harashima and Heitman (2002)

	gpa2Δ::hph/gpa2Δ::hph ura3-52/ura3-52	
THY245α	*MATα gpb1Δ::hph gpb2Δ::G418 tpk2Δ::G418 ura3-52*	Harashima and Heitman (2002)
THY245a/α	*MAT*a/α *gpb1Δ::hph/gpb1Δ::hph gpb2Δ::G418/gpb2Δ::G418 tpk2Δ::G418/tpk2Δ::G418 ura3-52/ura3-52*	Harashima and Heitman (2002)
THY247α	*MATα gpb1Δ::hph gpb2Δ::G418 ras2Δ::nat ura3-52*	This study
THY247a/α	*MAT*a/α *gpb1Δ::hph/gpb1Δ::hph gpb2Δ::G418/gpb2Δ::G418 ras2Δ::nat/ras2Δ::nat ura3-52/ura3-52*	This study
THY336a	*MAT*a *ira2Δ::loxP-nat ura3-52*	This study
THY336a/α	*MAT*a/α *ira2Δ::loxP-nat/ira2Δ::loxP-nat ura3-52/ura3-52*	This study
THY337a	*MAT*a *ira1Δ::loxP-nat ura3-52*	This study
THY337α	*MATα ira1Δ::loxP-nat ura3-52*	This study
THY337a/α	*MAT*a/α *ira1Δ::loxP-nat/ira1Δ::loxP-nat ura3-52/ura3-52*	This study
THY345a	*MAT*a *ira1Δ::loxP ira2Δ::loxP-nat ura3-52*	This study
THY345a/α	*MAT*a/α *ira1Δ::loxP/ira1Δ::loxP ira2Δ::loxP-nat/ira2Δ::loxP-nat ura3-52/ura3-52*	This study
THY346a/α	*MAT*a/α *gpb1Δ::hph/gpb1Δ::hph gpb2Δ::G418/gpb2Δ::G418 ira1Δ::loxP/ira1Δ::loxP ira2Δ::loxP-nat/ira2Δ::loxP-nat*	This study

	ura3-52/*ura3-52*	
THY355a	*MAT*a *IRA1-3HA-loxP-nat ura3-52*	This study
THY355α	*MAT*α *IRA1-3HA-loxP-nat ura3-52*	This study
THY355a/α	*MAT*a/α *IRA1-3HA-loxP-nat/IRA1-3HA-loxP-nat ura3-52/ura3-52*	This study
THY356a	*MAT*a *IRA2-3HA-loxP-nat ura3-52*	This study
THY381a	*MAT*a *IRA1-3HA-loxP ura3-52*	This study
THY387a	*MAT*a *gpb1,2*Δ*::loxP gpa2*Δ*::loxP-G418 ras2*Δ*::nat ura3-52* (pMW1)	This study
THY388a/α	*MAT*a/α *gpa2*Δ*::G418/gpa2*Δ*::hph ras2*Δ*::nat/RAS2 ura3-52/ ura3-52*	This study
THY389α	*MAT*a *gpb1,2*Δ*::loxP ras2*Δ*::nat ura3-52*	This study
THY401a	*MAT*a *IRA1(1~2432 aa)-3HA-loxP-nat ura3-52*	This study
THY402a	*MAT*a *IRA1(1~2714 aa)-3HA-loxP-nat ura3-52*	This study
THY402a/α	*MAT*a/α *IRA1(1~2714 aa)-3HA-loxP-nat/IRA1(1~2714 aa)-3HA-loxP-nat ura3-52/ura3-52*	This study
THY404a	*MAT*a *IRA1(1~1257 aa)-3HA-loxP-nat ura3-52*	This study
THY424a	*MAT*a *IRA1(1~2925 aa)-3HA-loxP-nat ura3-52*	This study
THY424α	*MAT*α *IRA1(1~2925 aa)-3HA-loxP-nat ura3-52*	This study
THY424a/α	*MAT*a/α *IRA1(1~2925 aa)-3HA-loxP-nat/IRA1(1~2925 aa)-3HA-loxP-nat*	This study

	ura3-52/ura3-52	
THY425a	*MAT*a *gpb1*Δ*::nat gpb2*Δ*::loxP IRA1-3HA-G418 ura3-52 leu2*Δ*::hisG*	This study
THY426a	*MAT*a *gpb1*Δ*::nat gpb2*Δ*::loxP IRA2-3HA-G418 ura3-52 leu2*Δ*::hisG*	This study
THY427a	*MAT*a *IRA1-3HA-G418 ura3-52 leu2*Δ*::hisG*	This study
THY428a	*MAT*a *IRA2-3HA-G418 ura3-52 leu2*Δ*::hisG*	This study
THY438a	*MAT*a *IRA1(2433~3092 aa)-3HA-loxP-nat ura3-52*	This study
THY440a	*MAT*a *IRA1(2715~3092 aa)-3HA-loxP-nat ura3-52*	This study
THY450a	*MAT*a *IRA1-3HA-loxP TRP1-FLAG-G418 ura3-52*	This study
THY456a	*MAT*a *IRA2(1~2922 aa)-3HA-loxP-nat ura3-52*	This study
THY457a	*MAT*a *IRA2(1~2702 aa)-3HA-loxP-nat ura3-52*	This study
THY461a	*MAT*a *loxP-3HA-IRA2(2703~3079 aa) ura3-52*	This study
THY464a	*MAT*a *loxP-3HA-IRA1(2715~3092 aa) TRP1-FLAG-G418 ura3-52*	This study
THY466a	*MAT*a *loxP-3HA-IRA2(2703~3079 aa) TRP1-FLAG-G418 ura3-52*	This study
THY467a	*MAT*a *loxP-3HA-IRA1GBD(2715~2925 aa)-loxP-nat TRP1-FLAG-G418 ura3-52*	This study
THY468a	*MAT*a *loxP-3HA-IRA1GBD(2715~2925 aa))-G418 ura3-52*	This study
THY471a	*MAT*a *IRA1*(Δ*GBD*(*Δ2715~2925 aa*)::*loxP*)*-3HA-G418 ura3-52*	This study
THY471α	*MAT*α *IRA1*(Δ*GBD*(*Δ2715~2925 aa*)::*loxP*)*-3HA-G418 ura3-52*	This study

THY471a/α	*MAT*a/α *IRA1*(Δ*GBD*(*Δ2715~2925 aa*)::*loxP*)-*3HA-G418*/*IRA1*(Δ*GBD* (Δ*2715~2925 aa*)::loxP)-*3HA-G418 ura3-52*/*ura3-52*	This study
THY473a	*MAT*a *loxP-3HA-IRA2GBD*(*2703~2922 aa*)-*loxP-nat ura3-52*	This study
THY474a	*MAT*a *loxP-3HA-IRA2GBD*(*2703~2922 aa*)-*loxP-nat TRP1-FLAG-G418 ura3-52*	This study
THY475a	*MAT*a *TRP1-3HA-G418 ura3-52 leu2*Δ*::hisG*	This study
THY479α	*MAT*α *IRA1-3HA-G418 ras2::G418 ura3-52 leu2*Δ*::hisG*	This study
XPY5α	*MAT*α *tpk2*Δ*::G418 ura3-52*	Pan and Heitman (1999)
XPY5a/α	*MAT*a/α *tpk2*Δ*::G418*/*tpk2*Δ*::G418 ura3-52*/*ura3-52*	Pan and Heitman (1999)

Supplemental TABLE 2

Plasmids

Plasmid	Description	Source/Reference
pTH19	P_{ADH1} *URA3* 2μ	Harashima and Heitman (2005)
pTH26	P_{ADH1}-*GPB1 URA3* 2μ (pTH19)	Harashima and Heitman (2005)
pTH27	P_{ADH1}-*GPB2 URA3* 2μ (pTH19)	Harashima and Heitman (2005)
pTH48	P_{ADH1}-*GPA2*^{Q300L} *URA3* 2μ (pTH19)	Harashima and Heitman (2005)
pTH67	P_{ADH1}-*GPB1-FLAG URA3* 2μ (pTH19)	This study
pTH88	P_{ADH1}-*FLAG-GPB2 URA3* 2μ (pTH19)	This study
pTH100	P_{ADH1}-*GFP-FLAG URA3* 2μ (pTH19)	Harashima and Heitman (2005)
pTH109	*3HA-loxP-nat*	This study
pTH110	*loxP-nat*	This study
pTH111	P_{ADH1}-*FLAG-GPB1 URA3* 2μ (pTH19)	This study
pTH114	P_{ADH1}-*GPB2 LEU2* 2μ (pTH171)	Harashima and Heitman (2005)
pTH153	*loxP-hph-3HA*	This study
pTH171	P_{ADH1} *LEU2* 2μ (pTH19 derivative)	Harashima and Heitman (2005)

pTH188	P_{ADH1}-*FLAG-GPB2C URA3* 2μ (pTH19)	This study
pTH190	P_{ADH1}-*FLAG-GPB2N URA3* 2μ (pTH19)	This study
pMW1	*RAS2 URA3* CEN	M. Wiglar
pMW2	$RAS2^{G19V}$ *URA3* CEN	M. Wiglar
pKF56	*IRA2 URA3* 2μ	A. Toh-e